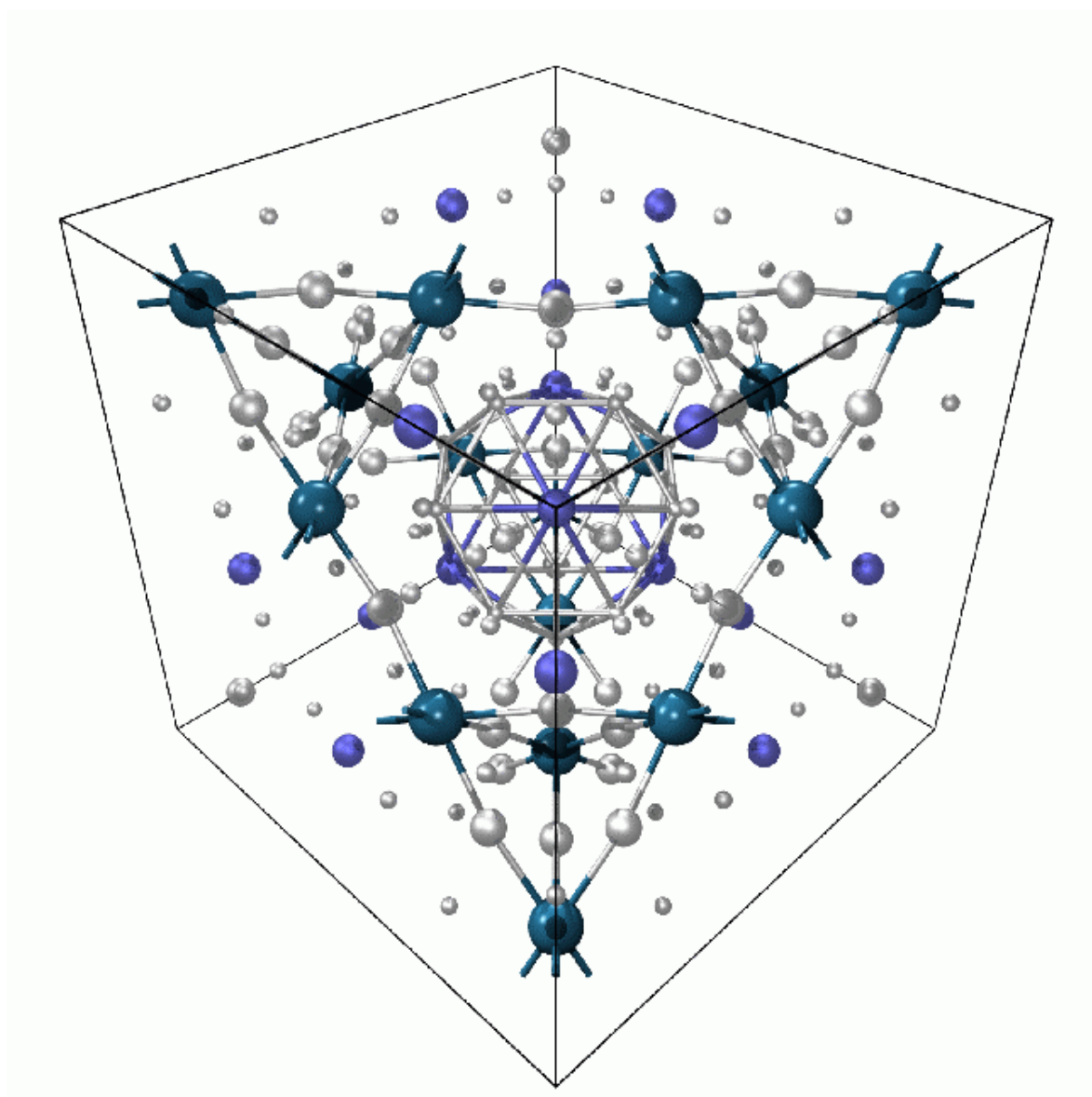


# NANOVED 2007

4th International Conference  
on Nanosciences and Nanotechnologies



**Program and Abstracts**

*Bratislava, Slovakia, November 11 – 14, 2007*

**NANOVED 2007**  
**4<sup>th</sup> International Conference**  
**on Nanosciences and Nanotechnologies**

**Bratislava, Slovakia, November 11 – 14, 2007**

**Organizers**

Institute of Physics, Slovak Academy of Sciences  
Bratislava, Slovakia

Institute of Electrical Engineering, Slovak Academy of Sciences  
Bratislava, Slovakia

Institute of Materials and Machine Mechanics, Slovak Academy of Sciences  
Bratislava, Slovakia

jointly with

Technical University of Vienna  
Vienna, Austria

Montanuniversitaet Leoben  
Leoben, Austria

co-organized with the help of Department of Intl. Cooperation SAS

**Sponsors**

Austrian Science and Research Liaison Office (ASO)  
NANOSMART, Center of Excellence SAS

**Organizing Committee**

P. Lobotka (Bratislava)  
F. Šimančík (Bratislava)  
P. Švec (Bratislava)  
I. Vávra (Bratislava)

G. Dehm (Leoben)  
R. Groessinger (Vienna)  
R. Pippan (Leoben)  
H. Sassik (Vienna)

# PROGRAMME

## Sunday, November 11, 2007

16.00 – 24.00

Registration

20.00

Welcome Party

## Monday, November 12, 2007

8:45 – 9.00

Opening

9.00 – 10.40

Ferrari, A. (Cambridge)

Nanotubes, nanowires and related structures; session chair: *H. Sassik*  
Nanotechnology with graphene, nanotubes and diamond-like carbon  
(invited)

Andzane, J. (Riga)

Structure dependent conductive, field emission and mechanical properties  
of carbon nanotubes grown by different methods

Erts, D. (Riga)

In situ characterization of bistable nanoelectromechanical devices based  
on semiconductor nanowires

Birjukovs, P. (Riga)

Conductive properties of semiconductor nanowire arrays

10.40 – 11.10

coffee break

11.10 – 12.50

Groessinger, R. (Vienna)

Nanocrystalline magnetic materials I; session chair: *O. Schneeweiss*  
Magnetic nanocrystalline materials (invited)

Mehmood, N. (Vienna)

Magnetostriction in Fe-Ga rapidly solidified alloys

Zeleňáková, A. (Košice)

Highly ordered superparamagnetic FeAu nanoparticles

Milkovič, O. (Košice)

Properties of Fe nanoparticles produced by isolation from Cu matrix

### 13.00 Lunch

14.00 – 15.40

Škorvánek, I. (Košice)

Nanocrystalline magnetic materials II; session chair: *R. Groessinger*  
Recent advances on soft magnetic nanocrystalline alloys (invited)

Sitek, J. (Bratislava)

Phase analysis of HITPERMs

Granitzer, P. (Graz)

Magnetism of Ni nanoarrays in porous silicon

Schneeweiss, O. (Brno)

Magnetic features of preparation of  $\alpha$ -iron nanoparticles from the natural  
ferrihydrite precursor

15.40 – 16.10

coffee break

16.10 – 18.10

Krtil, P. (Prague)

Nanostructured films and coatings; session chair: *J. Pištora*  
Nano-crystalline and nano-particulate electrocatalysts - new challenges in  
electrochemical energy and chemicals generation (invited)

Lančok, J. (Prague)

Novel hybrid physical vapor deposition systems for preparation of  
nanostructured thin films

Lofaj, F. (Košice)

Microstructure and properties of PVD WC-C coatings

Kunitsyna, E. V. (St. Petersburg)

Nanoscale surface modification of the III-V semiconductor materials  
through sulfur passivation

Vávra, I. (Bratislava)

Properties of nanocomposite films prepared by technology of  
discontinuous periodic multilayers

### 18.30 Dinner

19.30 – 20.30

Round-table discussion: Initiation of potential collaborations in FP7

20:30 - 22:00

Priority NMP

Poster session

**Tuesday, November 13, 2007**

9.00 – 10.40 <b>Balázsi, Cs. (Budapest)</b>  <b>Dusza, J. (Košice)</b> <b>Kašiarová, M. (Košice)</b>	Nanostructured ceramics; session chair: <b>P. Baláž</b> <b>Novel structural concepts of ceramic based nanocomposites: Towards enhanced functionality (invited)</b> <b>Ceramic nanocomposites (invited)</b> <b>Microstructure and creep deformation of Si<sub>3</sub>N<sub>4</sub>-SiC micro/nanocomposite</b>
10.40 – 11.10	coffee break
11.10 – 12.50 <b>Komadel, P. (Bratislava)</b> <b>Hrachová, J. (Bratislava)</b> <b>Baláž, P. (Košice)</b>  <b>Zeleňák, V. (Košice)</b>	Nanocomposites; session chair: <b>J. Dusza</b> <b>Clay minerals used in polymer-clay composites (invited)</b> <b>Properties of rubber/clay composites</b> <b>Kinetics of mechanochemical synthesis of Me/FeS nanoparticles (Me=Cu, Pb, Sb)</b> <b>Highly ordered nanoporous materials and their applications</b>
<b>13.00 Lunch</b>	
14.00 – 15.40 <b>Barák, I. (Bratislava)</b> <b>Hianik, T. (Bratislava)</b> <b>Cirák, J. (Bratislava)</b>  <b>Lefaix, H. (Paris)</b>	Nanostructures in biology and medicine; session chair: <b>Cs. Balázsi</b> <b>DNA biochips for microbial pathogen detection (invited)</b> <b>Properties of nanofabricated biosensors based on DNA aptamers</b> <b>Investigation of artificial receptor – target molecule interactions for the development of biosensors based on molecular recognition</b> <b>Synthesis, microstructures and cytocompatibility of new nanostructured amorphous Ti-based alloys for biomedical applications</b>
15.40 – 16.10	coffee break
16.10 – 18.10 <b>Kečkeš, J. (Leoben)</b> <b>Massl, S. (Leoben)</b>  <b>Matoy, K. (Leoben)</b>  <b>Hafok, M. (Leoben)</b>  <b>Huepf, T. (Graz)</b>	Mechanical properties of nanostructured materials; session chair: <b>F. Simančík</b> <b>Stress and strain in small-scale materials (invited)</b> <b>A cantilever technique to determine stress distributions in residually stressed surface near regions</b> <b>Stress measurement in small dimensions using micro-cantilever deflection technique</b> <b>Grain refinement of single crystals and alloys processed by high pressure torsion</b> <b>Thermophysical properties by different measurement techniques - the project High Temperature Metallic Melts</b>
<b>19.30 Banquet and Young Researchers Competition Evaluation; poster session (continued)</b>	

## Wednesday, November 14, 2007

9.00 – 10.40 Miglierini, M. (Bratislava) Pištora, J. (Ostrava) Illeková, E. (Bratislava)  Chikvaidze, G. (Riga)	Characterization methods of nanomaterials; session chair: <i>I. Vávra</i> <b>Structural transformations in Fe-based nanocrystalline alloys (invited)</b> <b>Application of evanescent waves to nanostructures characterization</b> <b>On the mechanism of thermally activated solid-state reaction and formation of intermetallic nanograins in Al/Ti nanoscaled multilayer foils</b> <b>Characterization of sulfonated poly(ether ether ketone) polymer electrolyte for fuel cells by FTIR spectroscopy</b>
10.40 – 11.10	coffee break
11.10 – 12.50 Štich, I. (Bratislava)  Crljen, Z. (Zagreb) Krupa, I. (Bratislava)  Medvid', A. (Riga)	Organic and semiconducting nanomaterials; session chair: <i>P. Krtil</i> <b>Organometallic nanojunctions probed by different chemistries: thermo-, photo- and mechanochemistry (invited)</b> <b>How good conductors pi-conjugated molecules are?</b> <b>Various aspects of immobilization of glucose sensitive proteins within hybrid silica gel matrices</b> <b>Laser induced self-assembling formation of semiconductors nanohills for nanoelectronic and optoelectronic applications</b>
12.50 – 13.00	<b>Concluding remarks and closing ceremony</b>
13.00 Lunch	

# List of Lectures

- L01. A. C. Ferrari  
*Nanotechnology with graphene, nanotubes and diamond-like carbon*
- L02 J. Andzane, J. Tobin, Z. Li, J. Prikulis, J.D. Holmes, D. Erts  
*Structure dependent conductive, field emission and mechanical properties of carbon nanotubes grown by different methods*
- L03. D. Erts, J. Andzane-, J. D. Holmes  
*In situ characterization of bistable nanoelectromechanical devices based on semiconductor nanowires*
- L04. P. Birjukovs, K. Didriksone, J. Svirkssts, N. Petkov, J. D. Holmes, D. Erts  
*Conductive properties of semiconductor nanowire arrays*
- L05. R.Grössinger, R.Sato Turtelli, H.Sassik  
*Magnetic nanocrystalline materials*
- L06. Nasir Mehmood, R.Sato Turtelli, F.Kubel, R. Grössinger  
*Magnetostriction in Fe-Ga rapidly solidified alloys*
- L07. A. Zeleňáková, J. Kováč, V. Zeleňák  
*Highly ordered superparamagnetic FeAu nanoparticles*
- L08. Ondrej Milkovič, Štefan Nižník, Ivan Škorvánek, Jozef Kováč  
*Properties of Fe nanoparticles produced by isolation from Cu matrix*
- L09. I. Škorvánek, J. Marcin, J. Turčanová, J. Kováč, P. Švec and D. Janičkovič  
*Recent advances on soft magnetic nanocrystalline alloys*
- L10. J.Sitek, P.Butvin, B.Butvinová, T.Kañuch  
*Phase analysis of HITPERMs*
- L11. P. Granitzer, K. Rumpf, M. Hofmayer, S. Ausserlechenr, P. Pölt, S. Simic, H. Krenn  
*Magnetism of Ni nanoarrays in porous silicon*
- L12. J. Filip, M. Hapla, R. Zbořil, M. Mašláň, O. Schneeweiss  
*Magnetic features of preparation of  $\alpha$ -iron nanoparticles from the natural ferrihydrite precursor*
- L13. Petr Krtíl  
*Nano-crystalline and nano-particulate electrocatalysts - new challenges in electrochemical energy and chemicals generation*
- L14. J. Lančok, J. Bulíř, P. Pokorný, M. Novotný, F Fendrych, C. Garapon  
*Novel hybrid physical vapor deposition systems for preparation of nanostructured thin films*
- L15. F. Lofaj, M. Ferdinandy  
*Microstructure and properties of PVD WC-C coatings*
- L16. E.V. Kunitsyna, T.V. L'vova, M.S. Dunaevskii, Y.V. Terent'ev, and Y.P. Yakovlev  
*Nanoscale surface modification of the III-V semiconductor materials through sulfur passivation*
- L17. I. Vávra, P. Lobotka, J. Sobota Š. Gaži, K. Sedláčková, P. Majchrák, J. Dérer  
*Properties of nanocomposite films prepared by technology of discontinuous periodic multilayers*
- L18. Cs. Balazsi  
*Novel structural concepts of ceramic based nanocomposites: Towards enhanced functionality*

- L19. J. Dusza, P. Šajgalík  
*Ceramic nanocomposites*
- L20. M. Kašiarová, F. Dorčáková, B. Shollock, A. Boccaccini, J. Dusza  
*Microstructure and creep deformation of Si<sub>3</sub>N<sub>4</sub>-SiC micro/nanocomposite*
- L21. Peter Komadel, Jana Hrachová  
*Clay minerals used in polymer-clay composites*
- L22. Jana Hrachová, Peter Komadel, Ivan Chodák  
*Properties of rubber/clay composites*
- L 23. P. Baláž, E. Dutková, I. Škorvánek, J. Kováč, A. Šatka, E. Gock  
*Kinetics of mechanochemical synthesis of Me/FeS nanoparticles (Me=Cu, Pb, Sb)*
- L24. V. Zelenák  
*Highly ordered nanoporous materials and their applications*
- L25. I. Barák, M. Barbaro, D. Blaškovič, D. Mullerová, A. Campo, L. Raffo  
*DNA biochips for microbial pathogen detection*
- L26. T. Hianik  
*Properties of nanofabricated biosensors based on DNA aptamers*
- L27. J. Cirák, M. Weis, R. Janiček, T. Hianik  
*Investigation of artificial receptor – target molecule interactions for the development of biosensors based on molecular recognition*
- L28. H. Lefaix, P. Vermaut, D. Janickovic, P. Svec, R. Portier, A. Asselin, J. M. Sautier, F. Prima  
*Synthesis, microstructures and cytocompatibility of new nanostructured amorphous Ti-based alloys for biomedical applications*
- L29. R. Pippan, J. Keckes, G. Dehm  
*Stress and strain in small-scale materials*
- L30. S. Massl, J. Keckes, R. Pippan  
*A cantilever technique to determine stress distributions in residually stressed surface near regions*
- L31. K. Matoy, H. Schönherr, T. Detzel, T. Schöberl, R. Pippan, C. Motz, G. Dehm  
*Stress measurement in small dimensions using micro-cantilever deflection technique*
- L32. M. Hafok, R. Pippan  
*Grain refinement of single crystals and alloys processed by high pressure torsion*
- L33. Thomas Huepf, Claus Cagran, Georg Lohöfer and Gernot Pottlacher  
*Thermophysical properties by different measurement techniques - the project High Temperature Metallic Melts*
- L34. M. Miglierini, T. Kaňuch, M. Pavúk, M. Pavlovič, P. Švec, D. Janičkovič, M. Mašláň, R. Zbořil, Y. Jirásková, G. Schumacher and I. Zizak  
*Structural transformations in Fe-based nanocrystalline alloys*
- L35. J. Pištora, J. Vlček, M. Lesňák  
*Application of evanescent waves to nanostructures characterization*
- L36. E. Illekova, J.C. Gachon, A. Rogachev, J.C. Schuster  
*On the mechanism of thermally activated solid-state reaction and formation of intermetallic nanograins in Al/Ti nanoscaled multilayer foils*

L37. G. Chikvaдзе, Xin Wang, Guntars Vaivars, Janis Kleperis  
*Characterization of sulfonated poly(ether ether ketone) polymer electrolyte for fuel cells by FTIR spectroscopy*

L38. I. Štich  
*Organometallic nanojunctions probed by different chemistries: thermo-, photo- and mechanochemistry*

L39. Z. Crljen  
*How good conductors pi-conjugated molecules are ?*

L40. Igor Krupa, Tomáš Nedelčev, Dušan Chorvát, Jr, Igor Lacík  
*Various aspects of immobilization of glucose sensitive proteins within hybrid silica gel matrices*

L41. A. Medvids, I.Dmitruk, P.Onufrijevs, I.Pundyk  
*Laser induced self-assembling formation of semiconductors nanohills for nanoelectronic and optoelectronic applications*

# List of Poster Contributions

- P1. Pavel Baláž, Denis Horváth, Martin Gmitra  
*The Dynamical Response to the Node Defect in Thermally Activated Magnetic Dot Arrays*
- P2. Pavel Baláž, Martin Gmitra, Józef Barnaś  
*Spin-polarized Current-pulse-induced Spin-switching in Spin-valves*
- P3. M. Balog, F. Simancik  
*ECAP as the technique for consolidation of rapidly solidified Al based particles*
- P4. P. Butvin, B. Butvinová, Y. Halahovets, P. Šiffalovič  
*Influence of surface properties on petermination of RQ ribbon's magnetic properties*
- P5. K. Csach, J. Miškuf, A. Juríková, V.A. Khonik, V.Z. Bengus, E.D. Tabachnikova, A.V. Podolskiy  
*Creep and fracture of amorphous and nanostructured alloys*
- P6. J. Dusza, L. Hegedúšová, Z. Bastl, J. Morgiel, P. Švec  
*Characterization of Hollow and Bamboo-Like Carbon Nanofibers*
- P7. V. Gajdoš, T. Hianik, H. Drahovská, J. Turňa, A. Kochman, W. Kutner, P. Vadgama  
*Detection of the DNA hybridization using a thickness shear mode method. Effect of the oligonucleotide chain length and position of complementary DNA sequence*
- P8. L. Hegedúšová, J. Dusza, M. Hnatko, P. Šajgalík  
*Contact strength of  $Si_3N_4/SiC$  nanoceramics*
- P9. M. Hnatko, Š. Lojanová, P. Šajgalík  
 *$Si_3N_4/SiC$  nanocomposite prepared by the addition of  $SiO_2 + C$  by hot pressing and gas pressure sintering methods*
- P10. T. Papaioannou, P. Svec, D. Janickovic, E. Illekova, E. Hristoforou  
*Phase transformations of Co-enhanced Finemet amorphous ribbons based on resistance-temperature correlation*
- P11. A. Kovalčíková, J. Dusza, M. Balog, P. Šajgalík  
*Microstructure and mechanical properties of silicon carbide based ceramics*
- P12. Matej Mičušík, Mária Omastová, Igor Krupa, Petra Pötschke, Jürgen Pionteck, Polycarpos Pissis, Fahad S al Mubaddel  
*Effect of various types of polypropylene matrices on properties of carbon nanotubes-containing nanocomposites*
- P13. J. Kuchta, M. Franko, M. Fulier, P. Švec, J. Bydžovský  
*Research and development of electrotechnical applications of nanocrystalline materials*
- P14. S. Longauer, O. Milkovič, G. Janák  
*Preparation of nanorods Fe by precipitation from solid solution*
- P15. J. Marcin, J. Turčanová, P. Švec, I. Škorvánek  
*Effect of field annealing on magnetic anisotropy and coercivity in nanocrystalline Fe-Co-M-B-(Cu) (M=Zr, Mo) alloys*
- P16. A. Zentko, M. Zentková, Z. Arnold, M. Cieslar, J. Kamarád, V. Kavečanský, S. Maťaš, M. Mihalik, Z. Mitróová and V. Zeleňák  
*Effect of pressure on magnetic properties of  $TM_3[Cr(CN)_6]_2 \cdot nH_2O$  nanoparticles*
- P17. M. Paluga, P. Švec, D. Janičkovič, P. Mrafko  
*Surface morphology in amorphous Fe-Mo-Cu-B ribbon system*

- P18. M. Pavúk, M. Miglierini, T. Kaňuch, P. Švec, D. Janičkovič, G. Schumacher and I. Zizak  
*Kinetics of crystallization in the  $Fe_{79}Mo_8Cu_1B_{12}$  amorphous alloy by synchrotron radiation*
- P19. Gabriela Popescu, Liana Vladutiu, , Mariana Lucaci, I. Badoi  
*Formation of nanostructures using different routes*
- P20. K. Sedláčková, R. Ionescu, Cs. Balázs  
*Carbon nanotubes added hexagonal  $WO_3$  films for sensing applications*
- P21. R.O. Grasin, K. Sedláčková, T. Ujvári, I. Bertóti, G. Radnóczy  
*Carbon-metal (Ni or Ti) nanocomposite thin films*
- P22. B. Škorić, D. Kakaš, G. Favaro and A. Miletić  
*Characterization of thin hard films using micro and nano analysis*
- P23. L. Svobodová, M. Šnejdárková, T. Hianik  
*The properties of affinity biosensors based on nanofabricated surfaces*
- P24. M. Šefčíková, D. Šuster, V. Kavečanský, P. Diko, H. Babu, D. Cardwell  
 *$Y_2Ba_4CuRuO_y$  nanoparticles in  $YBa_2Cu_3O_{7-d}$  bulk superconductors*
- P25. Petr Šmejkal, Jiří Pflieger, Blanka Vlčková  
*Fragmentation of Ag nanoparticles in aqueous ambient by nanosecond laser pulses*
- P26. J. Špaková, A. Duszová, L. Hegedúsová, J. Dusza  
*Indentation tests of CNT+ $ZrO_2$  composite*
- P27. P. Švec, J. Turčanová, D. M. Kepaptsoglou, D. Janičkovič, I. Škorvánek, P. Švec, Sr.  
*Formation of metastable phases in Ni-rich Fe-Ni-Nb-B rapidly quenched system*
- P28. Arvydas Tamulis, Vyintas Tamulis  
*Quantum Processes of Self-Assembly, Photosynthesis and Molecular Computing in Artificial Minimal Living Cells*
- P29. T. Tätté, M. Paalo, R. Talviste, J. Shulga, K. Saal, A. Lõhmus and I. Kink  
*Preparation of semi – 1D transition metal oxide structures*
- P30. T. Traussnig, S. Landgraf, I. Letofsky-Papst, G. Kothleitner, K. Rumpf, P. Granitzer, U. Brossmann, H. Krenn and R. Würschum  
*Synthesis and superparamagnetic properties of FePt-nanoparticles*
- P31. J. Turčanová, J. Marcin, J. Kováč, D. Janičkovič, P. Švec and I. Škorvánek  
*Structure and magnetic properties of FeNiNbB nanocrystalline alloys*
- P32. Mariana Lucaci, Violeta Tsakiris, Alexandru Biris, Radu Liviu Orban, Gabriela Popescu, Liana Maria Vladutiu  
*Processing of some hydrogen storage metallic materials*
- P33. G. Vlasák, C. F. Conde, D. Janičkovič, P. Švec  
*Magnetostriction measurements of (Fe-Co)-Mo-Cu-B alloys with varying atomic Fe/Co ratio*
- P34. M. Zentková, A. Zentko, M. Mihalik, S. Mat’áš, Z. Mitroóová, Z. Jagličić and V. Zelenák  
*Magnetic relaxations and memory effects in nickel-chromium cyanide nanoparticles*

## **Abstracts**

### **Invited and oral contributions**

## **Nanotechnology with graphene, nanotubes and diamond-like carbon**

Andrea C. Ferrari

Department of Engineering, University of Cambridge, Cambridge CB3 0FA, UK

Carbon based materials play a major role in today's science and technology. Carbon is a very versatile element, which can crystallise in the form of diamond or graphite. Great excitement has followed the discovery of new forms of carbon, including fullerenes, nanotubes and single layer graphene. This fuels the enormous amount of research in the ever-growing field of nanotechnology. In recent years, there have been continuous important advances in the science of carbon such as chemical vapour deposition of diamond, the discovery of fullerenes and carbon nanotubes, and the production of isolated single layer graphene. There are also many non-crystalline carbons, known as amorphous carbons and nanostructured carbons (mixture of amorphous and graphitic carbon, nanotubes and fullerenes). Diamond-like carbons play an important role, being a key element in numerous everyday-life applications, in the information technology, telecommunications and automotive market. Their great versatility arises from the strong dependence of the physical properties on the ratio of  $sp^2$  (graphite-like) to  $sp^3$  (diamond-like) bonds. Here I will review the main deposition methods, characterisation techniques and applications of graphene, nanotubes and diamond-like carbons. I will focus in particular on the use of Raman spectroscopy to fingerprint each carbon species and to extract the most relevant structural information.

## Structure Dependent Conductive, Field Emission and Mechanical Properties of Carbon Nanotubes Grown by Different Methods

<sup>1</sup>J. Andzane, <sup>2</sup>J. Tobin, <sup>2</sup>Z. Li, <sup>1</sup>J. Prikulis, <sup>2</sup>J.D. Holmes, <sup>1</sup>D. Erts

<sup>1</sup>*Institute of Chemical Physics, University of Latvia, Riga, Latvia*  
<sup>2</sup>*National University of Ireland, Cork, Ireland*

Conductive, field emission and mechanical properties of carbon nanotubes (CNTs) grown using chemical vapor deposition and supercritical fluid methods [1], were analysed *in situ* by using a scanning tunneling microscope that is compatible with a transmission electron microscope. The investigated nanotubes have both tube and “bamboo” like structures.

Field emission characteristics for all CNTs were determined and put into the Fowler-Nordheim equation. CNT failure emission currents and voltages were determined for all types of CNT.

Conductivity of the nanotubes were measured in two contact configurations. “Bamboo” like structures exhibit substantially higher resistance in comparison to tube like CNTs. Observed particularities in I(V) characteristics of “bamboo” like structures are explained by the presence of different junctions inside the nanotubes.

Nanotube failure currents and voltages were determined and compared. Using thermoelectric heating, the conductivity of inhomogenities within the CNTs was studied. The highest heat dissipation which may lead to thermal damage is expected to occur in the spots of highest resistance. Nanotube failure locations were compared for different nanotubes.

The Young’s modulus of MWCNT was obtained from resonance frequency and geometry measurements. The Young’s modulus depends on the diameter, and in this case varied within the range of 3 – 2000 GPa.

### **References**

1. Z. Li, J. Andzane, D. Erts, J.M. Tobin, K. Wang, M.A. Morris, G. Attard, J. D. Holmes. *Adv. Mater.*, 19, 3043 (2007).
2. D. Erts, H. Olin, L. Ryen, E. Olsson, A. Thölen, *Phys. Rev. B* **61**, 12 725 (2000).

# ***In situ* Characterization of Bistable Nanoelectromechanical Devices Based on Semiconductor Nanowires**

<sup>1</sup>D. Erts, <sup>1</sup>J. Andzane, <sup>2</sup>J. D. Holmes

<sup>1</sup>*Institute of Chemical Physics, University of Latvia, Riga, Latvia*

<sup>2</sup>*Department of Chemistry, National University of Ireland, Cork, Ireland*

During the past few years nanowires and nanotubes have emerged as promising components of nanoscale electrical, mechanical and nanoelectromechanical systems (NEMS). The internal operating frequencies of NEMS may achieve giga and tera hertz, and NEMS power consumption and heat capacity is extremely low. One of the most important advantages of the devices based on NEMS is the high integration level that can be achieved. Logic elements containing NEMS are attractive for future applications as biological and chemical sensors based on force and mass detection, ultrahigh frequency resonators, nanotweezers, pulse generators etc.

Most of the NEMS operate as three terminal devices; however, an appealing advancement is the development of two terminal NEMS. An attractive way to demonstrate two terminal NEMS devices is by investigating them *in situ* inside electron microscopes [1,2]. The advantage of using *in situ* technique is that the process is visualized and all the alignments can be performed directly.

A scanning tunnelling microscope compatible with a transmission electron microscope (TEM-STM) [3] was used in the experiments. Semiconductor nanowires were used as the active elements of NEMS.

Here we present two terminal NEMS devices applicable as EPROM (erasable read only memory), RAM (random access memory). If compared to carbon nanotube based NEMS, devices based on nanowires can offer improved control of the size and electrical behavior. These nanowire devices were shown to be more mechanically stable than those based on carbon nanotubes because of their higher strength.

## **References**

1. K.J.Ziegler, D.M.Lyons, J.D. Holmes, D.Erts, B.Polyakov, H.Olin, E. Olsson, K.Svensson. *Appl. Phys. Lett.*, **84**, 4074 (2004)
2. C. Ke, H. D. Espinosa, *Small*, **2**, 1484 (2006)
3. D. Erts, H. Olin, L. Ryen, E. Olsson, A. Thölen, *Phys. Rev. B* **61**, 12 725 (2000).

## Conductive properties of semiconductor nanowire arrays

<sup>1</sup>P. Birjukovs, <sup>1</sup>K. Didriksone, <sup>2</sup>J. Svirkstis, <sup>3</sup>N. Petkov, <sup>3</sup>J.D.Holmes, <sup>1</sup>D. Erts

<sup>1</sup>*Institute of Chemical Physics, University of Latvia, Riga, Latvia,*

<sup>2</sup>*Department of Chemistry, University of Latvia, Riga, Latvia*

<sup>3</sup>*Department of Chemistry, National University of Ireland, Cork, Ireland*

Nanoporous templates as hosts for nanowires offer a viable method for forming high density arrays of ordered, crystalline nanowires. Complete filling of the pores is vital in order to create electronic and optoelectronic devices.

We are using conductive AFM and macrocontacts from both sides of membranes to determine the resistance of individual nanowires within a matrix. This approach was also used to conclude whether the nanowires went all the way through the filled porous membrane [1,2]. The drawback of this approach is that during two point measurements the contact resistance can not be extracted from the summary resistance.

Access to the full length of nanowires inside membranes permit conductivity measurements along the nanowire and exclude contact resistance from resistivity measurements.

Anodized aluminum oxide membranes containing semiconductor nanowire arrays were incorporated in an epoxy matrix and the individual nanowires were exposed by polishing and etching. Exposed surfaces were visualized by using the scanning electron microscope Hitachi S 4800. Conductive AFM (Asylum Research) in contact mode was applied for the surface conductivity mapping. The current through the individual nanowires of different length was measured and resistivity of the nanowires was determined. The resistance values are compared with the nanowire resistance obtained by the two and four point measurements.

### References

1. D. Erts, B. Polyakov, B. Daly, M. A. Morris, S. Ellingboe, J. Boland, J. D. Holmes. *J. Phys. Chem. B*, **110**, 820-826 (2006).
2. B. Polyakov, B. Daly, J. Prikulis, V. Lisauskas, B. Vengalis, J. D. Holmes, and D. Erts. *Adv. Mater.*, **18**, 1812-1816 (2006).

# MAGNETIC NANOCRYSTALLINE MATERIALS

\*R.Grössinger, R.Sato Turtelli, H.Sassik  
*Institute of Solid State Physics, Techn. Univ. Vienna, Austria*

The magnetic properties of magnetic materials (soft magnetic, hard magnetic, magnetostrictive) depends essentially on the grain size of the material. For grain sizes between 10 and 50 nm magnetic exchange coupling can be obtained. For uncoupled grains below 10 nm size superparamagnetism is observed. For all magnetic ordered materials the coercivity is a function of the grain size and exhibit a maximum. This effect is shown in Fig.1 for soft magnetic materials and in Fig.2 for hard magnetic materials.

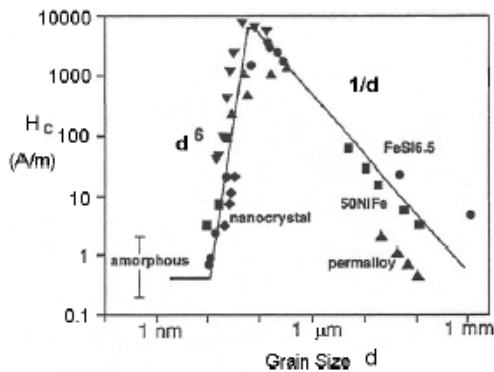


Fig. 1: Coercivity  $H_c$  versus grain size  $D$  for soft magnetic alloys [1]

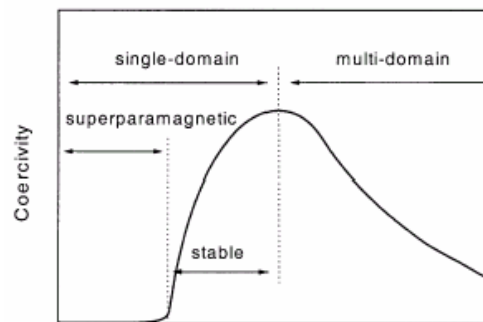


Fig.2 Dependence of the coercivity on the grain size of had magnetic materials according to [2]

In both cases the ratio between the so-called magnetic exchange lengths to the grain size plays the essential role. For hard magnetic material the exchange length resulting from a competition between quantum-mechanical exchange and magnetocrystalline anisotropy is most important, whereas for soft magnetic material the stray field between the grains polarise the neighbouring grains.

In this paper representative examples of the effect of exchange coupling for hard magnetic materials (remanence enhancement, reduction of coercivity, improved magnetizing), soft magnetic materials (low coercivity, high permeability) and magnetostrictive materials (reduction of the effective anisotropy; high  $d\lambda/dH$ ) will be given.

## References

- [1] Herzer G., *Physica Scripta* **1993**, T49, p. 307-314.
- [2] G.C.Hadjipanayis, *J. Magn. Magn. Mat.* 200 (1999) 373-391

## Magnetostriction in Fe-Ga Rapidly Solidified Alloys

<sup>1\*</sup>Nasir Mehmood, <sup>1</sup>R. Sato Turtelli, <sup>2</sup>F.Kubel, <sup>1</sup>R.Grössinger

<sup>1</sup>*Inst. f. Festkörperphysik, Techn. Univ. Vienna, Austria*

<sup>2</sup>*Inst. f. Chemische Technologien und Analytik; T.U.Vienna, Austria*

Galfenol (Fe-Ga) shows magnetostriction values up to to 400ppm. Therefore it is a promising and mechanically robust material for magnetostrictive sensor and actuator applications. Ribbons or foils of polycrystalline  $\text{Fe}_{100-x}\text{Ga}_x$  with  $15 < x < 20$  with different thicknesses were produced by melt spinning and splat cooling techniques in order to perform structural, magnetostriction and magnetic properties measurement. The magnetostriction was measured along the ribbon axis using a strain gauge method in combination with a 50 kHz ac-bridge in a pulsed field system. The magnetic field was applied perpendicular to the ribbon surface, along the ribbon axis and perpendicular to the ribbon axis. The ribbon was glued to a glass substrate to avoid any bending of the ribbons during measuring the magnetostriction. The maximum observed magnetostriction values are of the order of -40 ppm, which is much less as compared to earlier reported values of ribbons which gave values of thousands of ppm. Experiments were the ribbon shaped samples were partly or complete free showed that applying a magnetic fields causes the sample to move parallel to the direction of magnetic field in order to minimize the demagnetizing field thus causing strong bending leading to a large “magnetostriction” signal. An X-ray diffraction study showed pure Fe-BCC structure with a statistical Ga substitution, however also clear indications of a strong texture perpendicular to the ribbon surface were found.

# Highly ordered superparamagnetic FeAu nanoparticles.

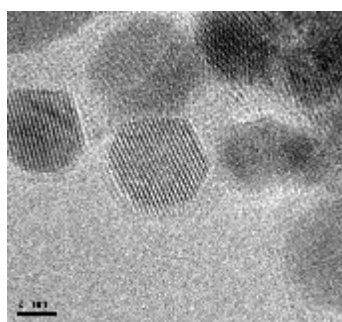
<sup>1\*</sup>A. Zelenáková, <sup>2</sup>J. Kováč, <sup>3</sup>V. Zelenák

<sup>1</sup>Department of Solid State Physics, University of P. J. Šafárik, Park Angelinum 9, Košice, Slovakia

<sup>2</sup>Institute of Experimental Physics, Slovak Academy of Sciences, Watsonova 44, Košice, Slovakia

<sup>3</sup>Department of Inorganic Chemistry, University of P. J. Šafárik, Moyzesova 11, Košice, Slovakia  
\*[adriana.zelenakova@upjs.sk](mailto:adriana.zelenakova@upjs.sk)

Magnetic nanoparticles have attracted considerable interest due to their significance in technological applications as well as for the fundamental physics. Below a critical size of particles, the magnetic moment in single domain fluctuates in direction due to thermal agitation, leading to superparamagnetic behavior above the blocking temperature  $T_B$ , and to spatial freezing of these moments below  $T_B$ .



Highly ordered superparamagnetic iron-gold nanoparticles were prepared by a reverse micelle method. The ferromagnetic iron formed a core of the nanoparticles while the diamagnetic gold a shell on the surface of the core. The presence of a gold coating inhibits oxidation and allows the particles to be stable. TEM observation showed that the Fe@Au nanoparticles are isolated without aggregation and of clearly spherical shape with average size 10 nm.

Fig. 1. HRTEM micrograph of the Fe@Au nanoparticles.

The zero-field-cooled (ZFC) and field-cooled (FC) magnetization curves measured in the DC field of 5000 Oe using SQUID, Fig. 2a, exhibit the irreversibility and narrow maximum of ZFC at the peak value of  $T_B \sim 20$ K. This indicates that below blocking temperature  $T_B$ , the magnetic moment of each particle is blocked along its easy magnetization axis, whereas above  $T_B$  the particles are characterized by superparamagnetic behavior. The shape of the ZFC curve also suggests a relatively narrow size distribution of the Fe@Au nanoparticles.

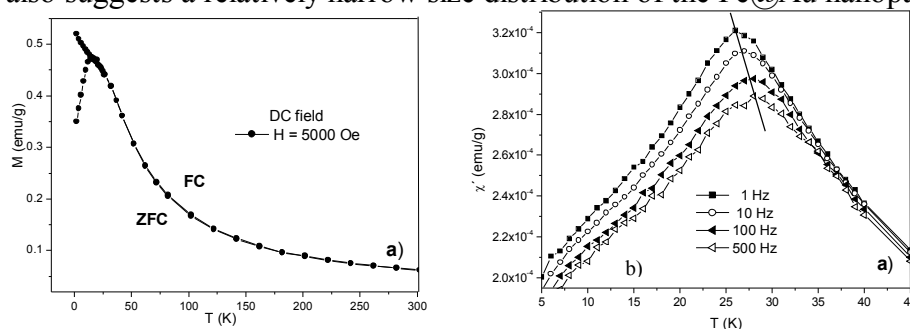


Fig. 2. Temperature dependence of magnetization (a) measured in DC magnetic field, (b) real component of the AC susceptibility measured at different frequencies (1-500 Hz).

To investigate the presence of inter-particle interaction, we performed AC susceptibility measurements at different frequencies (1-500 Hz) employed a SQUID-based magnetometer. It is evident from Fig. 2b, that the real part of the AC susceptibility  $\chi'$  is frequency dependent and the peak position increases with increasing of frequency. This is qualitative confirmation of blocking/freezing process in Fe@Au nanoparticles system. The qualitative analysis of measured data confirms the existence of inter-particle interaction in system.

# Properties of Fe Nanoparticles Produced by Isolation from Cu Matrix

<sup>1</sup>Ondrej Milkovič, <sup>1</sup>Štefan Nižník, <sup>2</sup>Ivan Škorvánek, <sup>2</sup>Jozef Kováč

<sup>1</sup>Department of Material Science, Faculty of Metallurgy, Technical University of Košice  
Park Komenského 11, 040 01, Košice, Slovakia

<sup>2</sup>Slovak Academy of Science, Watsonova 47, 040 01, Košice, Slovakia

The aim of this work is to characterize the nanoparticles produced by innovated method. The idea of method has published by prof. Longauer in paper [1]. In generally, it is possible to divide the method into two basic steps. At first, nanoparticles are prepared by precipitation in supersaturated solid solution. Precipitation reaction can be controlled by suitable heat treatment, which is main operation for controlled particles formation in nanometer scale and evolution of their size distribution [2, 3]. Second step of submitted method is isolation of prepared nanoparticles.

This paper refers about properties of iron nanoparticles generated by precipitation reaction in Cu-Fe alloy, whereby conditions for solution and ageing annealing were studied in previous work [4]. Accordingly, the conditions for nanoparticles isolation were published in paper [5].

Transmission electron microscopy observation of nanoparticles in bright field is documented in Figure 1. The two main structure phases were found by selection electron diffraction: magnetite ( $\text{Fe}_3\text{O}_4$ ) and *bcc* – iron ( $\alpha$  - Fe). These two phases can be observed in Figure 2 as a typical core-shell structure in larger particle with martensitic twin-like transformation in core *bcc* – iron.

Magnetic measurement of nanoparticles magnetic moment in dependence on temperature is showed in Figure 3. Documented magnetization curves taken in zero-field-cooling (ZFC) and field-cooling (FC) modes taken with  $H_{\text{app}} = 500$  Oe. ZFC curve mentioned the transition to blocked state at  $T_B = 65$  K, which is characteristic for superparamagnetic nanoparticles.

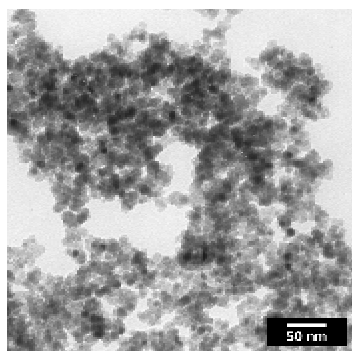


**Fig 1** Fe nanoparticles with diameter up to 10 nm.

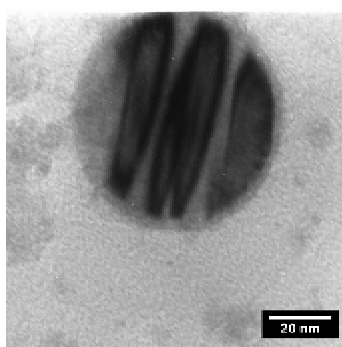


**Fig 2** Core-shell structure of nanoparticle

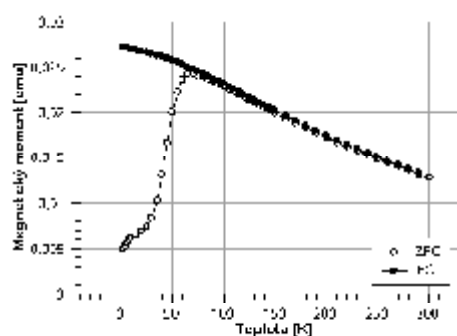


**Fig 3** Magnetization curve of Fe nanoparticles with diameter up to 10 nm.

- [1] LONGAUER, S.: *Nanoved.* 2003, Vol. 1, Iss. 1.
- [2] KITA, K. – MONZEN, R. *Scripta Materialia.* 2000, Vol. 43, Iss. 11, p. 1039-1043.
- [3] GRÄTZ, H. *Scripta Materialia.* 1996, Vol. 34, Iss. 8, p. 1209-1217.
- [4] MILKOVIČ, O. – HALAMA, M. – LONGAUER, S. – NIŽNÍK, Š. *Acta Metallurgica Slovaca.* 2007, Vol. 13, Iss. 1, p. 694-697.
- [5] NIŽNÍK, Š. – LONGAUER, S. – MILKOVIČ, O. *Acta Metallurgica Slovaca.* 2007, Vol. 13, Iss. 2, p. 210-213.

## Recent advances on soft magnetic nanocrystalline alloys

<sup>1</sup>I. Škorvánek, <sup>1</sup>J. Marcin, <sup>1</sup>J. Turčanová, <sup>1</sup>J. Kováč, <sup>2</sup>P. Švec and <sup>2</sup>D. Janičkovič

<sup>1</sup>*Institute of Experimental Physics, Slovak Academy of Sciences, SK- 040 01 Košice, Slovakia*

<sup>2</sup>*Institute of Physics, Slovak Academy of Sciences, SK-842 28 Bratislava, Slovakia*

The reduction of the grain sizes to the nanometer range may vary drastically the physical properties of materials, including the magnetic behavior. Typical examples of such systems are nanocrystalline Fe-based alloys prepared by devitrification of melt-spun amorphous precursors, which belong to an important group of soft magnetic materials. The properties of these materials can vary widely, depending on the size and volume fraction of the nanocrystalline grains as well as on the magnetic properties of the intergranular amorphous matrix phase. In order to further optimize the magnetic performance of the nanocrystalline alloys it is important to deepen knowledge about the influence of various processing techniques that can be used to tailor their properties for specific applications.

In this talk, our attention is devoted to the study of the effects of different heat treatments on soft magnetic characteristics in the series of FeCoNbB, FeCoZrB and FeCoMoBCu nanocrystalline alloys for high temperature applications. The magnetic properties of these alloys are discussed in terms of their microstructure. We report on a beneficial effect of both longitudinal and transverse magnetic field applied during the heat treatments. A heat treatment under the presence of longitudinal magnetic field results in squared hysteresis loops that are characterized by very low coercivities. Sheared loops with good field linearity and low coercivity were achieved for all alloys after annealing in transverse magnetic field [1]. Such characteristics are of particular interest for the high frequency transformers and the magnetic sensors. An important step toward the obtaining the soft magnetic Fe-based nanocrystalline materials with high saturation induction exceeding that of the conventional FeSi alloys was reported recently by Ohta and Yoshizawa [2]. Their FeCuBSi-based alloys with an improved performance at room temperature show good prospects for the industrial applications. We report also on a recent attempt to utilize the Fe-based nanocrystalline alloys as media for magnetic refrigeration near room temperature [3].

### References

- [1] I.Škorvánek, J. Marcin, J. Turčanová, M. Wojcik, K. Nesteruk, D. Janičkovič, P. Švec, *J. Magn. Mater.* 310 (2007) 2494
- [2] M. Ohta, Y. Yoshizawa, *Jpn. J. Appl. Phys.* 46 (2007) L477
- [3] I.Škorvánek, J. Kováč, J. Marcin, P. Švec, D. Janičkovič, *Mat. Sci. Eng. A* 449-451 (2007) 460

This work was supported by the grants VEGA 2/7193, APVV-0413-06, COST P17 and Cex-NANOSMART

## PHASE ANALYSIS OF HITPERMS

<sup>1</sup>Sitek, J., <sup>2</sup>Butvin, P., <sup>2</sup>Butvinová, B., <sup>1</sup>Kañuch, T.,

<sup>1</sup>Department of Nuclear Physics and Technology, SUT, Bratislava, Slovakia

<sup>2</sup>Institute of Physics, SASc, Bratislava, Slovakia

Two different kinds of substituted HITPERMs were analyzed by Mössbauer spectroscopy. The first alloy contained vanadium ( $\text{Fe}_{57}\text{Co}_{20}\text{Nb}_7\text{V}_4\text{B}_{12}$ ) and second one chromium ( $\text{Fe}_{57}\text{Co}_{20}\text{Nb}_7\text{Cr}_4\text{B}_{12}$ ). Samples were annealed at the temperature 540 °C and 580 °C in vacuum and in argon atmosphere. Mössbauer spectra represented nanocrystalline state. Crystalline component consisted of two subspectra, which indicate that iron atoms are situated in two different sites. Besides amorphous part the interface component was identified represented by quadrupole doublet in Mössbauer spectrum. Intensity of the second and fifth line of the spectrum reflects direction of net magnetic moment of amorphous component. Comparing annealed samples we found that net magnetic moment is more deflected from the ribbon plane for argon-annealed sample in accordance with magnetic anisotropy seen on corresponding hysteresis loops. The annealing at the 580° C caused decrease of amorphous component and increase of interface phase. This phenomena suggest that interface takes part in the structural transformation. Mössbauer and magnetic results also revealed that alloy containing chromium crystallizes faster than alloy with vanadium.

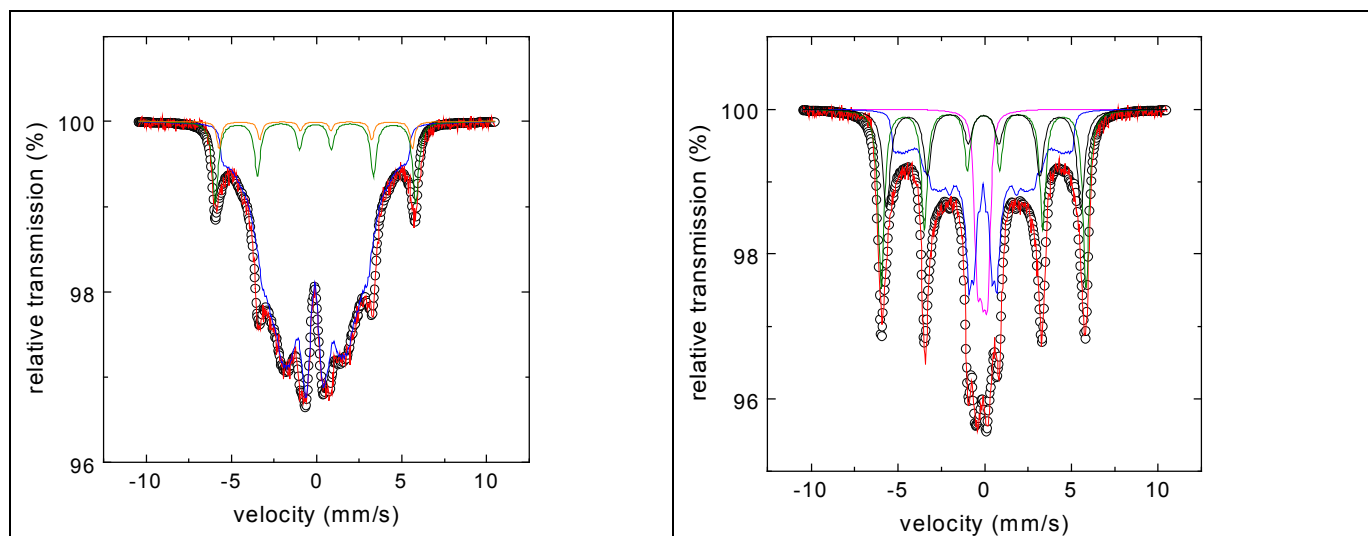


Fig.1 Mössbauer spectra of  $\text{Fe}_{57}\text{Co}_{20}\text{Nb}_7\text{V}_4\text{B}_{12}$  alloy at a) 540° C - left b) 580° C – right

The authors thank for partial support from grants VEGA 1/3189/06, 2/5099/27 and APVT 20-008404.

## Magnetism of Ni nanoarrays in porous silicon

<sup>1\*</sup>P. Granitzer, <sup>1</sup>K. Rumpf, <sup>1</sup>M. Hofmayer, <sup>1</sup>S. Ausserlechner, <sup>2</sup>P. Pölt, <sup>2</sup>S. Simic, <sup>1</sup>H. Krenn

<sup>1</sup>*Institut für Physik, Karl Franzens Universität Graz, Universitätsplatz 5, A-8010 Graz, Austria*

<sup>2</sup>*Institut für Elektronenmikroskopie und Feinstrukturforchung, Technische Universität Graz, Steyrergasse 17/III, A-8010 Graz, Austria*

The fabrication of nanoscopic silicon based membranes has been carried out by using a non-expensive electrochemical preparation technique. For these purposes an n<sup>+</sup>-silicon wafer is anodized to create oriented pores with diameters adjustable between 40 nm and 100 nm showing a length up to 50 μm. Dendritic growth could be sufficiently suppressed to achieve clearly separated channels with a quite regular self-assembled pore-arrangement. The pores are filled with a ferromagnetic metal (Ni) to obtain an array of nanowires. Metal-deposition within such high-aspect-ratio pores down to the pore-tips is a great challenge but have been successfully grown. The metal-loading consists of precipitations of different shape from elongated particles to wires reaching an extension of several micrometers (aspect ratio 1:100). The achieved nano-composite can be varied either by modification of the nano-architecture of the silicon template or by altering the metal deposition process. Structural characterization of the templates as well as of the deposited metal-particles is performed by scanning electron microscopy by recording the backscattered electrons and EDX-mapping, respectively, to get chemical element sensitive information. The magnetic properties of the nanocomposites depend on the pore-arrangement of different templates as well as on the various deposited metal structures with special geometry and spatial distribution. The magnetic behavior can be divided into two parts. At low magnetic field, ferromagnetic spin magnetism is observed, whereas at high magnetic field beyond the saturation magnetization of Ni a giant paramagnetic orbital magnetism prevails, which can not be saturated. This non-saturation behavior is due the orbital motion of carriers around the Ni-nanowires. Apart from conventional SQUID-magnetometry, the magnetic state of the samples is also investigated by magneto-optical Kerr effect (MOKE) and Faraday rotation. The relationship between the structural arrangement and the magnetic response is figured out, with the intention to fabricate tailored magnetic properties of ferromagnet/silicon nanostructures.

*Acknowledgement: Financial support by the Austrian FWF project P 18593 and NAWI Graz project is appreciated.*

# Kinetics of preparation of $\alpha$ -iron nanoparticles from the natural ferrihydrite precursor

<sup>1</sup>O. Schneeweiss, <sup>2</sup>J. Filip, <sup>1</sup>M. Hapla, <sup>2</sup>R. Zbořil, <sup>2</sup>M. Mašláň

<sup>1</sup>Institute of Physics of Materials, AS CR, Žitkova 22, 616 62 Brno, Czech Republic

<sup>2</sup>Centre for Nanomaterial Research, Palacky University in Olomouc, Svobody 26, 771 46 Olomouc, Czech Republic

Nanocrystalline/amorphous natural ferrihydrite was used as the precursor for preparation of nanocrystalline  $\alpha$ -Fe powder using heat treatment in a controlled atmosphere. Structure and phase composition of the precursor and the final powder were characterized by X-ray diffraction (XRD) and Mössbauer spectroscopy (MS) and TEM. Annealing in hydrogen atmosphere induces transformation to magnetite  $\text{Fe}_3\text{O}_4$  and/or  $\alpha$ -Fe. Transformation temperatures were estimated from the temperature dependences of magnetic moment (thermomagnetic curve – TMC). TMCs of the isothermal annealing in hydrogen atmosphere at 360°C and 600°C are shown in Fig. 1 together with the results of Mössbauer phase analysis. Magnetic properties were characterized according to MS and hysteresis loops parameters. The values of coercivity and behavior by approaching to saturation were typical for an assembly of isolated magnetic nanoparticles. The kinetics of the transformation was described using Avrami relation applied on the data of the isothermal time dependence of magnetic moment measurements and subsequently the activation enthalpy of transformation was estimated using Arrhenius plots of their parameters. Comparison of the changes of activation enthalpies derived from a various stages of the annealing indicates effect of several processes on formation of  $\alpha$ -Fe nanoparticles.

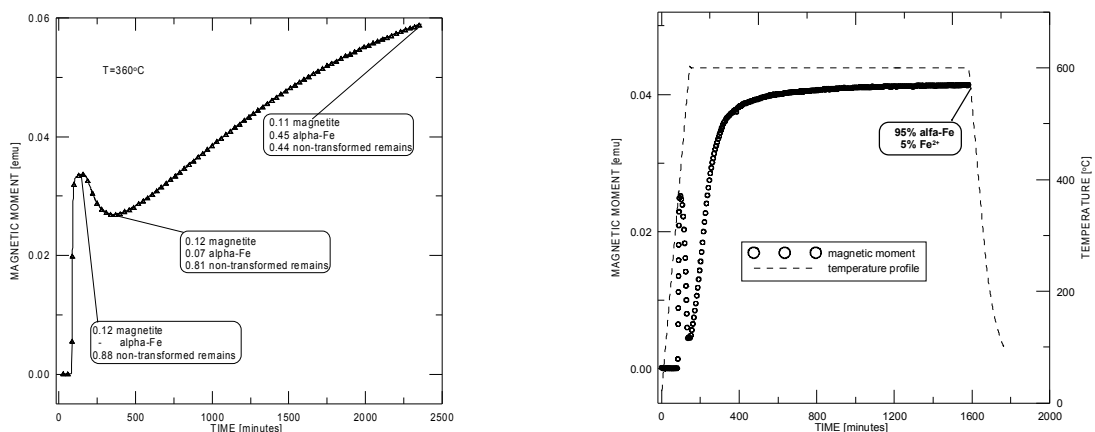


Fig. 1. Temperature dependence of magnetic moment during isothermal annealing of the ferrihydrite precursor in hydrogen atmosphere at 360°C (left) and 600°C (right). The given phase compositions were derived from Mössbauer spectra.

# **Nano-crystalline and nano-structured electrocatalysts – new challenges in clean electrochemical energy and chemical production**

**Petr Krtil**

*J. Heyrovsky Institute of Physical Chemistry v.v.i., Academy of Sciences of the Czech Republic,, Dolejskova 3, 18223 Prague, Czech Republic*

The vigorous electrocatalytic research witnessed by the scientific community over last three decades has been fueled by two principal applications of electrocatalytic systems – fuel cells and technical electrolysis. The primary interest in exploring the nano-sized materials in these applications can be linked to the fact that state of the art electrocatalysts are (as a rule) based on exploration noble metals or noble metal oxides supply of which is limited. The original extensive approach aimed at better utilization of the electrocatalyst and anticipated independence of the electrocatalytic reactivity on the electrocatalysts size. This approach tough successful in its original intention, however, revealed significant variability of the nano-crystalline/nano-particulate electrocatalysts activity, which in some cases surpasses that of the microcrystalline electrocatalysts.

Since all electrocatalytic processes are of redox nature (i.e. electrons are one of the reactants) one can track the unusual electrocatalytic behavior of nano-size electrocatalysts to changes in electronic structure or in dimensionality of the surface. The changes of the electronic structure may be related either directly to the size of electrocatalysts (due to the quantum confinement) or to the size-stabilization of meta-stable materials of unusual electronic structure. In addition to it the electrocatalytic behavior may be affected also by large number of low dimensionality sites (e.g. crystal edges and vertices) present on the surface of nano-sized electrocatalysts. These effects were subject of systematic research recently with an overall objective to rationalize the reactivity of these materials in terms of their corresponding surface structure and density of states distribution allowing thus in mid-term for a rational design and synthesis of advanced electrocatalysts.

The major aspects of the current state of the art electrocatalytic research will be shown on three examples: Pt-Ru surface nano-alloys for methanol oxidation, nano-crystalline gold electrocatalysts for oxygen reduction and nano-crystalline Ru based oxides for electrolytic gas evolution. Particular attention will be paid to describe the application of diffraction, microscopic and electrochemical techniques used to determine the solid state characteristics namely the crystallographic orientation of the surface and its consequence in electrocatalytic reactivity.

# Novel hybrid physical vapour deposition systems for preparation of nanostructured thin films

<sup>1</sup>J.Lančok, <sup>1</sup>J. Bulíř, <sup>1</sup>P. Pokorný, <sup>1</sup>M. Novotný, <sup>1</sup>F. Fendrych, <sup>2</sup> C. Garapon  
<sup>1</sup>*Institute of Physics AS CR, Prague, Czech Republic*  
<sup>2</sup>*LPCML-CNRS, Lyon France*

Since modern technology is shifting towards miniaturisation, it is highly desirable to explore techniques to fabricate the nanocomposites with outstanding physical properties also in the form of thin films (*applications as sensors, planar microwave elements etc.*). The Physical Vapour Deposition (PVD) methods of thin film growth have been known as a convenient way to control the crystallographic orientation using a proper substrate. PVD techniques used for preparation of nanogranular systems results in a distribution of particle sizes, however a random orientation of the particles and difficulty to control grain sizes and distances between them. Thus a new fabrication method, which allows production of monodisperse periodical nanogranular structures with controlled particle size, is primarily important. Due to this we suggest to develop the novel hybrid systems allowing the combination of different physical evaporation technique such as magnetron sputtering, pulsed laser ablation, plasma jet, electron beam evaporation and auxiliary ion beam sources and optimised the process in respect to the deposited materials and nanostructures.

The experiences with preparation of thin waveguiding nanostructures (Eu doped  $Y_2O_3$  and Yb in amorphous alumina) and magnetic nanocomposites films  $(Fe/Co)_p-(X-N)_{1-p}$ , ( $X = Ta, Al, Ti, etc.$ ) and oxides  $(Fe/Co)_p-(Y-O)_{1-p}$ , ( $Y = Al, Hf, Si$ ) with outstanding fluorescence and magnetic properties, respectively will be presented.

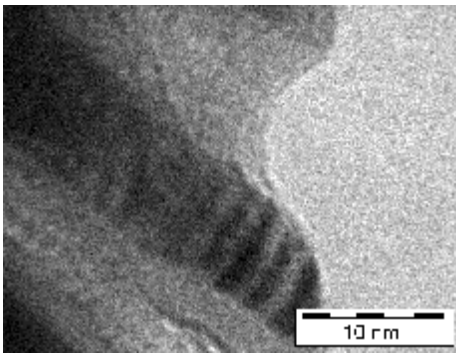


Fig.1 HRTEM of Eu doped  $Y_2O_3$ : alumina nanostructures prepared by target alternating laser ablation.

## **Microstructure and properties of PVD WC/C coatings**

<sup>1</sup>F. Lofaj, <sup>1</sup>M. Ferdinandy, <sup>2</sup>A. Juhász

<sup>1</sup>*Institute of Materials Research of SAS, Kosice, Slovakia*

<sup>2</sup>*Loránd Eötvös University, Budapest, Hungary*

Thin coatings of WC/C on tool steel substrate have been prepared using a combined Plasma Enhanced (PE) PVD method based on the sublimation and decomposition of tungsten hexacarbonyl in low pressure and temperature plasma. The thickness of the coatings was 300 nm and its microstructure was controlled by means of variations of vapor pressure, bias voltage and current density on the substrate. Phase composition of the coatings was investigated by X-ray diffraction, microstructure and local chemical composition by SEM/EDX. Nanohardness and the elastic properties of the coatings were investigated using instrumented indentation and these parameters were used to determine the optimum conditions for the coating preparation.

# Nanoscale surface modification of the III-V semiconductor materials through sulfur passivation

E.V. Kunitsyna, T.V. L'vova, M.S. Dunaevskii, Ya.V. Terent'ev, Yu.P. Yakovlev

*Ioffe Physico-Technical Institute RAS, St Petersburg, Russia*

Fast photodiodes based on GaSb and InAs for the 1.6-5.0  $\mu\text{m}$  spectral range are extremely important now for high-resolution laser diode spectroscopy of gases and molecules, ecological monitoring and medicine [1,2]. Progress in the photoelectrical and noise characteristics of the photodiodes can be provided by decreasing of surface component of dark current as well as by improving material morphology and interface abruptness. It is clear that structural and chemical characteristics of the InAs and GaSb substrates effect drastically on the heterostructure surface/interface quality and, as a result, on performance of the devices. Consequently, considerable advances in substrate processing technology, including sulphur surface passivation techniques are required.

In this paper, evolution and modification of GaSb(100) and InAs(100) surfaces due to  $\text{Na}_2\text{S}_x$  passivation has been studied with PL, STM, AFM, TEM, X-ray diffraction methods, taking the oxidized surfaces chemically prepared in a standard way as a reference. One of the main problems of epitaxial technology is damage of the III-V substrate morphology under annealing. For native oxidized GaSb (InAs) surface the annealing promotes chemical reactions between the  $\text{Ga}_2\text{O}_3 \times \text{Sb}_2\text{O}_3$  ( $\text{As}_2\text{O}_3 \times \text{In}_2\text{O}_3$ ) oxide layer and the semiconductor material. These reactions result in the deep chemical etching of the surface, which damages its morphology. The  $\text{Na}_2\text{S}_x$  treatment removes the undesirable oxides with minimal surface etching and forms a thin protecting overlayer which consists of the sulfur atoms covalently bonded to the surface In atoms in the case of (100) InAs and to Sb atoms in the case of (100) GaSb, respectively. The AFM images of the S-passivated materials reveal atomically flat surfaces with clearly distinguished atomic steps. We suggest that this nanoscale relief is formed by the (100)Sb-S( $\text{S}_2$ )-terraces fragments for GaSb and (100)In-S( $\text{S}_2$ )-terrace fragments for InAs, respectively. Then sulfide overlayer can be removed by annealing at low temperatures without surface roughening. Under epitaxy the plural atomic steps on the substrate act as growth crystallization centres providing better crystalline quality of the grown heterostructures as well as a decrease of dislocation density at the interface.

The method of  $\text{Na}_2\text{S}_x$  passivation has shown great effectiveness for LPE and MBE growth of III-V-based heterostructures.

The work supported in part by the Russian Foundation of Basic Research (RFBR) under Grant No.07-02-01359.

- [1] M.H.M. Reddy, J.T. Olesberg, C. Cao and J.P. Prenias, *Semicond. Sci. Technol.* 21, 267 (2006)  
[2] E.V. Kunitsyna, I.A. Andreev, M.P. Mikhailova, et al., *Proc. SPIE* 4340, 244(2000)

## Properties of nanocomposite films prepared by technology of discontinuous periodic multilayers

I. Vávra<sup>1</sup>, P. Lobotka<sup>1</sup>, J. Sobota<sup>2</sup>, Š. Gaži<sup>1</sup>, K. Sedláčková<sup>1</sup>, P. Majchrák<sup>1</sup>, J. Dérer<sup>1</sup>

<sup>1</sup>*Institute of Electrical Engineering SAS, Bratislava, Slovakia*

<sup>2</sup>*Institute of Scientific Instruments, AS CR, Brno, Czech Republic*

We report on the technology and properties of nanocomposite (of metal-insulator type) thin films prepared by magnetron sputtering in the form of periodic multilayer. For the deposition of metallic component of multilayer the dc magnetron sputtering was used. In accordance with Petrov et al. [1] the discontinuous growth of metallic component is supported by the deposition at relatively high ( $10^{-1}$  Pa) Ar pressure. Second, insulating component is prepared by rf sputtering at low pressure ( $10^{-2}$  Pa). At these conditions the insulating layer overlaps the metallic crystallites the surface planarization for subsequent deposition is guaranteed. The main advantage of the multilayer technology is the possibility to adjust the distance between neighboring nanocrystallites in normal to the film plane direction (by insulator thickness choice) and also in film plane by deposition parameters.

The detailed structural analysis was performed by in-plane and cross-sectional transmission electron microscopy. Good embedding in amorphous insulating matrix and structural perfection of nanocrystallites were confirmed (Fig.1).

Thanks to structural perfection the discontinuous periodic multilayers are suitable objects for the physical properties studies. We present the single electron transport effects in Ni/CN<sub>x</sub>, the superconductivity in NbN/AlN and interlayer and intergranular exchange and dipolar coupling in Fe/SiO<sub>2</sub> nanocomposites.

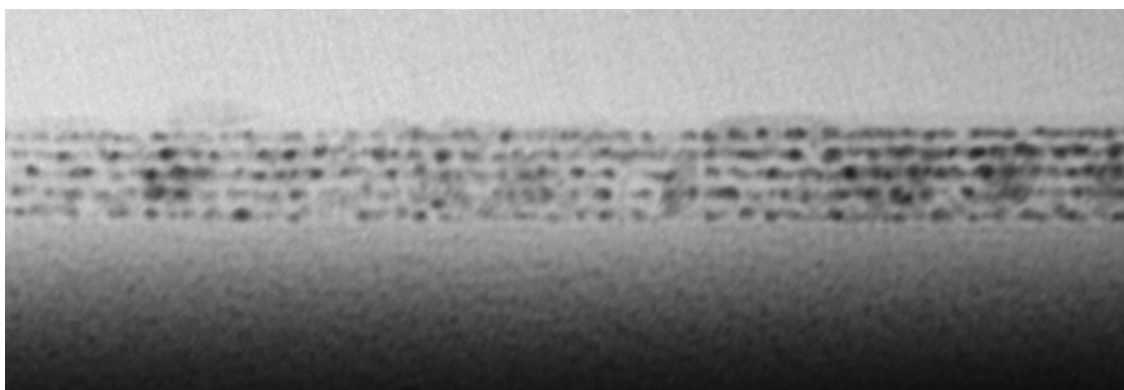


*Fig.1. Cross-sectional TEM micrograph of Ni/CN<sub>x</sub> periodic multilayer. The discontinuity of Ni layers (dark crystallites) and continuity of CN<sub>x</sub> matrix is evident.*

[1] Petrov et al. J. Vac. Sci. Technol. A21, S117(2003).

## Novel structural concepts of ceramic based nanocomposites: Towards enhanced functionality

Csaba Balázsi

*Ceramics and Composites Laboratory, Research Institute for Technical Physics and  
Materials Science, Hungary, H-1525 Budapest, P.O. Box 49,  
email: [balazsi@mfa.kfki.hu](mailto:balazsi@mfa.kfki.hu)*

Nanotechnology research aims to provide a fundamental understanding of phenomena and materials that enable the creation and use of devices and systems that have novel properties and function. The target of this research was to work out new methods for preparing synergistic ceramic matrix composites with new properties.

Primarily the interactions between *silicon nitride matrix* and graphite micrograins, carbon black nanograins, carbon fibres and *carbon nanotubes* were investigated. Carbon nanotubes present exceptional mechanical, superior thermal and electrical properties, therefore there are high expectations for improvement of quality of nanotube added nanocomposites. Our experimental work has been performed to control the preparation of colloidal ceramic slurry and the structural changes during shaping and sintering. Several sintering techniques PLS (Pressureless Sintering), HIP (Hot Isostatic Pressing), HP (Hot Pressing), FAST (Field Activated Sintering) were applied. Structural, morphological and mechanical properties were examined to follow the interactions between ceramic matrix and different carbon additions.

The development of gas sensing devices and their arrays based on *open structured and nanostructured tungsten oxides* will be also presented. In the beginning the work was concentrating on the preparation processes of new polymorphs of tungsten oxide, in bulk and thin film form. The target is to develop advanced gas sensors for high temperature applications. The cubic and hexagonal tungsten oxides have been found to be sensitive to NH<sub>3</sub> and NO<sub>2</sub> gases.

Our further aim was to develop composite materials for biomedical applications. In the first stage *hydroxyapatite* powders were prepared, the size of grains was in the nano and micro region. A new method has been worked out for covering hydroxyapatite substrate by calcium phosphate nano and micro layers or fibres. A layered structure of this type may increase the strength of composite. In the next step different porous ceramics and layers will be prepared and examined to improve both the bio-compatibility and strength.

- [1] Cs. Balázsi, B. Fényi, N. Hegman, Zs. Kövér, F. Wéber, Z. Vértesy, Z. Kónya, I. Kiricsi, L. P. Biró and P. Arató, Development of CNT/Si<sub>3</sub>N<sub>4</sub> composites with improved mechanical and electrical properties, Composites Part B: Engineering (2006), 418-424.
- [2] Cs. Balázsi, F. Wéber, Zs. Kövér, Z. Shen, Z. Kónya, Zs. Kasztovszky, Z. Vértesy, L.P. Biró, I. Kiricsi and P. Arató, Application of carbon nanotubes to silicon nitride matrix reinforcements, Current Applied Physics Vol. 6, Issue 2, (2006), 124-130.
- [3] Cs. Balázsi, K. Kalyanasundaram, E. O. Zayim, J. Pfeifer, A. L. Tóth, P.-I. Gouma, Tungsten oxide nanocrystals for electricchromic and sensing applications, 1st ICC, 25-29 June 2006, Toronto, Canada, Proceedings of the 1st International Congress on Ceramics, Ed. Stephen Freiman, Published by Wiley.
- [4] Cs. Balázsi, E. Ö. Zayim, Preparation and characterisation of WO<sub>3</sub>.1/3H<sub>2</sub>O thin films, Mat. Sci. Forum 537-538 (2007) 113-120.
- [5] Cs. Balázsi, F. Wéber, Zs. Kövér, E. Horváth, Cs. Németh, Preparation of calcium-phosphate bioceramics from natural resources, J. Eur. Ceram. Soc. Vol. 27, Iss. 2-3, (2007) 1601-1606.
- [6] Bishop A, Balázsi Cs, Jason H.C. Yang, Gouma P: Hydroxyapatite Biocomposite Coatings Prepared by Electrospinning for Advanced Prosthetics, Polymers for Advanced Technologies Iss 11-12 (2006) 902-906.

## CERAMIC NANOCOMPOSITES

Ján Dusza and Pavol Šajgalík

Institute of Materials Research, SAS, Watsonová 47, 043 53 Košice, Slovak republic

e-mail: [jdusza@imr.saske.sk](mailto:jdusza@imr.saske.sk)

The aim of this presentation is to summarize the results of the worldwide activities in the field of research, development and characterization of ceramic nanocomposites mainly silicon nitride and alumina based ceramic nano-composites during the last two decades. The main processing routes are summarized and the principal microstructure parameters are described. The relationships between rupture strength, Weibull modulus and defects-fracture origins are discussed and the possibilities of strength improvement through improved processing steps and microstructure design are discussed. The possible strengthening and toughening mechanisms are described and the relationships between the fracture toughness, microstructure and fracture micromechanisms are discussed. The effect of the temperature on deformation, crack growth and creep failure of the ceramic nanocomposites are characterized.

## Microstructure and Creep Deformation of Si<sub>3</sub>N<sub>4</sub>-SiC Micro/Nanocomposite

<sup>1</sup>M. Kašiarová, <sup>2</sup>B. Shollock, <sup>2</sup>A. Boccaccini, <sup>1</sup>J. Dusza

<sup>1</sup>*Institute of Materials Research, Slovak Academy of Sciences, Watsonova 47, 043 53 Košice, Slovak Republic*

<sup>2</sup>*Department of Materials, Imperial College London, South Kensington Campus, London SW7 2AZ, UK*

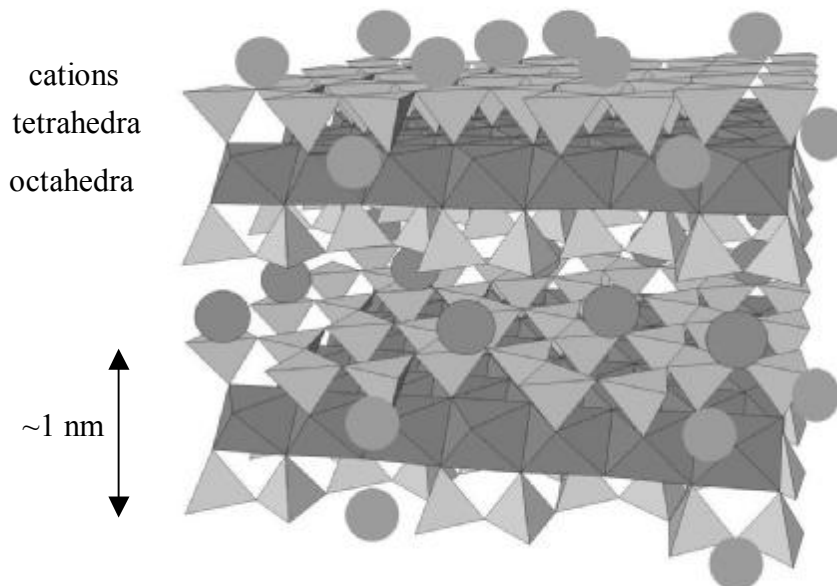
Silicon nitride–silicon carbide nanocomposite has been prepared by an *in situ* method that utilizes C+SiO<sub>2</sub> carbo-thermal reduction during the sintering process. The developed material consists of a silicon nitride matrix with an average grain size of approximately 140 nm with inter- and intra-granular SiC particles with sizes of approximately 150 and 40 nm, respectively. The creep behavior was investigated in bending at temperatures from 1200° to 1400°C, under stresses ranking from 50 to 150 MPa in air. The stress exponents are in the interval from 0.8 to 1.28. Value of stress exponent about 1 and TEM observation confirmed that the main creep mechanism is solution precipitation. After creep test no cavitation was observed in the microstructure of Si<sub>3</sub>N<sub>4</sub>-SiC micro-nanocomposite. A significantly enhanced creep resistance was achieved by the incorporation of SiC nanoparticles into the matrix. This is because of a change of the microstructure and grain boundary chemistry leading to a change of creep mechanism and creep rate.

## Clay minerals used in polymer-clay composites

Peter Komadel, Jana Hrachová

*Institute of Inorganic Chemistry, Slovak Academy of Sciences, 845 36 Bratislava, Slovakia*

Occurrence, mineralogical composition and properties of industrially important raw clay materials, bentonites, will be discussed. The properties of various clays depend strongly on the dominant mineral present, kaolinite in kaolins and smectite in bentonites. While chemical composition of kaolinite varies within a relatively narrow range; smectites differ substantially. Structure and its effect on the properties of clay minerals will be analysed in detail. Both dioctahedral (montmorillonite, nontronite, ...) and trioctahedral (saponite, hectorite...) smectites are composed of negatively charged layers and exchangeable cations. This is due to non-equivalent substitution in tetrahedral and/or octahedral sheets of their layers and it is compensated by the positive charge of exchangeable cations. present on the external surfaces and in the



Montmorillonite structure

Thickness of montmorillonite layers of 0.96 nm is in nanoscale range and single layers of minerals saturated with monovalent cations are found in water dispersions. Calcium and sodium cations dominate in most natural smectites, which are hydrophilic as well as minerals containing other inorganic cations. Ion exchange with organic cations, most commonly with tetraalkylammonium species, produces organosmectites (or organoclays), substances of substantially increased hydrophobic properties. Organic cations modify also the availability of the interlayers of the mineral. Organoclays are well known as adsorbents of hydrophobic pollutants from water and as inorganic components in polymer-clay (nano)composites.

## Properties of rubber/clay composites

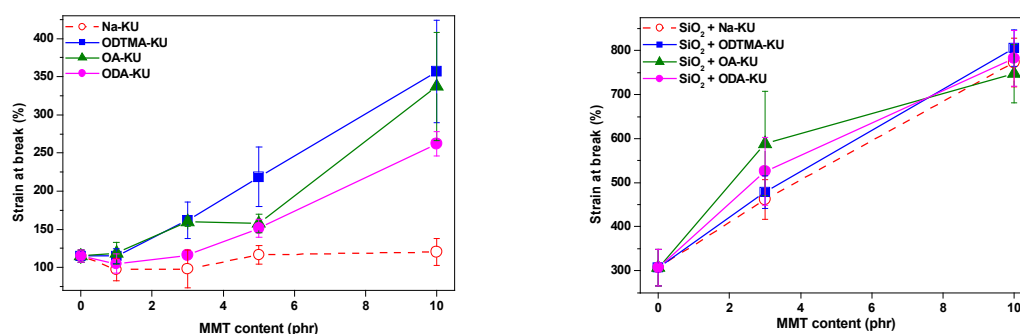
<sup>1\*</sup>Jana Hrachová, <sup>1</sup>Peter Komadel, <sup>2</sup>Ivan Chodák

<sup>1</sup>*Institute of Inorganic Chemistry, Slovak Academy of Sciences, Dúbravská cesta 9, SK-845 36 Bratislava, Slovakia, e-mail: [uachjana@savba.sk](mailto:uachjana@savba.sk)*

<sup>2</sup>*Polymer Institute, Slovak Academy of Sciences, Dúbravská cesta 9, SK-842 36 Bratislava, Slovakia*

When a polymer material is reinforced by a particle that is nanometric in at least one dimension, the resulting polymer composite usually exhibits remarkable improvements in material properties relative to the pristine polymers or conventional composites. Nanocomposites can be divided into three categories depending on whether the filler has one, two, or three dimensions in the nanometer range. Some clay minerals as montmorillonites in exfoliated form are representative of the first type of nanoparticles filler, since the silicate layers are 1 nm thickness, but up to several microns in diameter [1]. In order to improve the clay dispersion in polymers, montmorillonite needs to be organically modified. This modification is achieved by substituting long-chain alkylammonium cations for the inorganic cations. The aim of the modification is to increase the interlayer spacing and the hydrophobicity of the clay.

Kunipia-F, a commercial highly purified Na-montmorillonite (Kunimine Industries, Co., LTD., Japan) and its organic derivatives prepared by ion exchange with octadecyltrimethylammonium (ODTMA), oleylammonium (OA) and octadecylammonium (ODA) cations were used as aluminosilicate fillers for rubber matrix. Natural rubber-layer silicate composites were prepared by direct polymer melt intercalation, in some cases the mixtures of rubber and clay contained also silica as a conventional reinforcing filler. The effect of clay or organoclay loading from 1 up to 10 phr (parts by weight per hundred parts of rubber) on the tensile properties (stress at break, strain at break and modulus M100) was measured. As expected, much higher values of mechanical properties are observed in the presence of silica. The stress at break and strain at break of the materials systematically increase with increasing clay content.



In the presence of silica, the organic cation in montmorillonite has negligible effect; but 15 mass % of SiO<sub>2</sub> increases substantially the stress and strain at break values for all montmorillonite contents. The filler modification leads to higher values of strength and elongation compared to unmodified filler in the NR matrix. Modification of montmorillonite by different organic ammonium salts results in altered reinforcing and plasticizing effects of the filler in composites with rubber matrix.

- [1] S. Xue, T.J. Pinnavaia (2007) Overview of Clay-based Polymer Nanocomposites: In *Clay-based Polymer Nanocomposites* (CPN), CMS Workshop Lectures, Vol. 15, K. A. Carrado, F. Bergaya eds., The Clay Minerals Society, Chantilly, VA, USA, 2–32.

## **Kinetics of mechanochemical synthesis of Me/FeS nanoparticles (Me=Cu, Pb, Sb)**

<sup>1\*</sup> P. Baláž, <sup>1</sup> E. Dutková, <sup>2</sup> I. Škorvánek, <sup>3</sup> J. Kováč, <sup>3</sup> A. Šatka, <sup>3</sup> E. Gock

<sup>1</sup>*Institute of Geotechnics, Slovak Academy of Sciences, Watsonova 45, 043 53 Košice, Slovakia*

<sup>2</sup>*Institute of Experimental Physics, Slovak Academy of Sciences, Watsonova 47 045 01 Kosice, Slovakia*

<sup>3</sup>*Department of Microelectronics, Slovak University of Technology and International Laser Centre, Ilkovičova 3, 812 19 Bratislava, Slovakia*

The mechanochemical reduction of copper sulphide (Cu<sub>2</sub>S), zinc sulphide (ZnS), lead sulphide (PbS) and antimony sulphide (Sb<sub>2</sub>S<sub>3</sub>) with elemental magnesium Mg in a planetary mill has been studied. The Me/MgS nanocomposites have been characterized by XRD and SEM methods. The mechanochemical process is rather straightforward with elemental copper, zinc, lead and antimony, respectively and magnesium sulphide being the only solid state products. The process kinetics described by XRD shows that 100% of the reduction is complete after 60 min of milling in the case of Cu/MgS and Sb/MgS system 96% conversion to Zn and 88% conversion to Pb resulted in after 60 min in the case of Zn/MgS and Pb/MgS, respectively. In these systems Mg content is consumed faster than ZnS and PbS content, respectively. Particles in the nanometer size range have a strong tendency to agglomerate due to their relatively large specific surface area. Unlike the conventional high-temperature reduction of metal sulphides the mechanochemical reduction is fast and ambient temperature and atmospheric pressure are sufficient for its propagation. The mechanochemical reduction of MeS with Mg is a suitable system for a large-scale mechanochemical preparation.

# Highly ordered nanoporous materials and their perspective applications

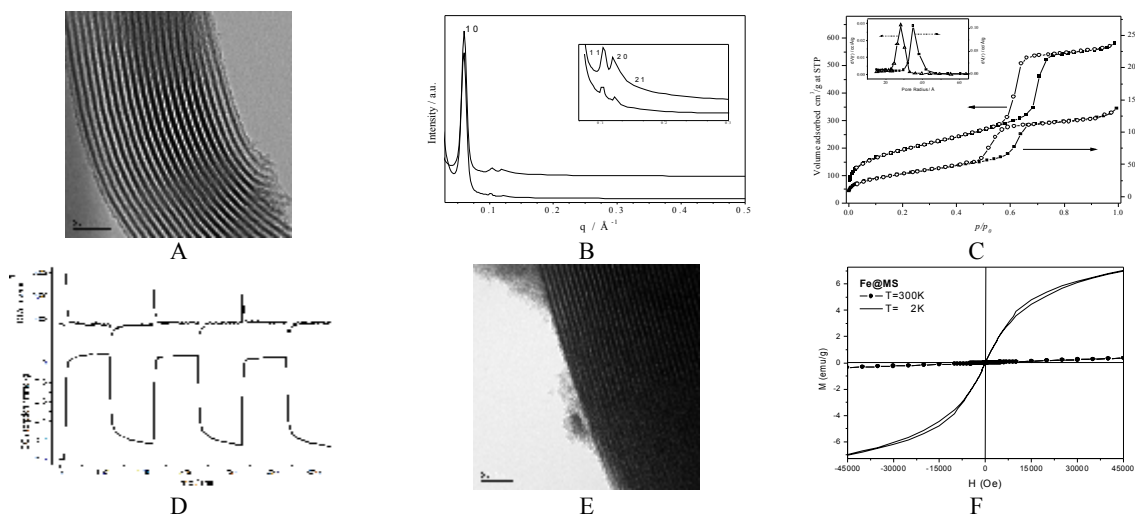
Vladimír Zelenák

Department of Inorganic Chemistry, P.J. Šafárik University, Moyzesova 11, 04154 Košice, Slovak republic, e-mail: [vladimir.zelenak@upjs.sk](mailto:vladimir.zelenak@upjs.sk)

Self-organized aggregates of surfactants and block copolymers (micelles, microemulsions, lyotropic liquid crystalline phases) are recently used as structure directing media in the synthesis of a huge variety of materials in nanoscale level. These aggregates may be used as structural templates, the size and structure of which determines the properties of the newly-formed material. After use of the concept of self-organised structures in synthesis of the mesoporous silica MCM-41 in 1992, the research in ordered mesoporous materials accelerated and new materials, their characterization but also of their potential applications were the subjects of many studies. The large surface areas, well-defined pore structure in the mesopore range and narrow pore size distribution make these materials attractive for application in the fields of adsorption, catalysis or magnetism. In our contribution we will present the use of mesoporous silica (MS) for (i) sorption of greenhouse gases, notably carbon dioxide and (ii) the use of MS as a reactor for nanocasting of magnetic particles.

First we have grafted surface of mesoporous silica by amines. Amines bind on the surface of mesoporous solid can capture carbon dioxide by way, which resembles process of CO<sub>2</sub> separation by liquid alkanolamines - the most widely developed commercial technology for carbon dioxide capture. Such solid sorbents take advantage of high surface area, selectivity to carbon dioxide and high mass transfer. In our contribution we discuss the influence of pore connectivity in MS, the type of amine ligand and the synthesis conditions, on the carbon dioxide sorption over the prepared materials. The discussion is based on the results of HRTEM (Fig. A), SAXS (Fig. B), nitrogen adsorption/desorption measurements (Fig. C) or cycling carbon dioxide sorption/desorption (Fig. D).

In the second topic we have used the mesoporous silica as a mold for nanocasting of iron particles. The prepared composite materials were characterized by wide-angle and low-angle XRD measurements, HRTEM (Fig. E) and magnetic measurements (Fig. F). The temperatures and the field dependence of magnetization measured on SQUID-based magnetometer confirm that the interactions among particles in composite sample Fe@MS are blocked at temperature 15K. The dc field dependence of magnetization at room temperature reveals the paramagnetic interaction between particles. In low temperatures region (2-50 K) the ferromagnetic dipole-dipole interactions among particles were present.



# DNA biochips for microbial pathogen detection

BARÁK Imrich<sup>1</sup>, BARBARO Massimo<sup>2</sup>, BLAŠKOVIČ Dušan<sup>1</sup>, MULLEROVÁ Denisa<sup>1</sup>,

CAMPO Alessandra, and RAFFO Luigi<sup>2</sup>

<sup>1</sup>Institute of Molecular Biology, SAS, 845 51 Bratislava 45, Slovak Republic

<sup>2</sup> DIEE, University of Cagliari, Italy

Number of pathogenic tick-borne bacteria cause diseases in humans and animals. Wide range of conventional methods as PCR, immuno based detection, cultivation, reverse line blot or microscopy is available for identification of bacterial pathogens. Although, these methods are used for many years, they do not allow simultaneous detection of wide spectrums of bacteria.

DNA hybridization together with polymerase chain reaction (PCR) amplification and DNA array technology is recently being used also for detection of wide range of pathogenic bacteria important from medical, veterinary and epidemiology point of view. The typical detection limit is in the picomolar range. We have developed the oligo-chip for detection of different tick borne pathogens. This method is based on detection of fluorescent signal after hybridization reaction by using laser scanner. We also prepared an electronic device for detection of specific contact of two single complementary strands of DNA. This method will allow simple detection without using the fluorescent probes and expensive laser scanner. For this purpose a novel solid-state sensor for detection of bio-molecular processes was developed. The device is compatible with a standard CMOS process, providing fully electronic readout and large-scale of integration of biosensors on a single chip. A model of the device was developed and simulated. CMOS-type sensor for detection of DNA hybridization is the semiconductor sensor measuring a change in the electric charge immobilized on the surface of the sensor. When hybridization occurs, a shift in effective threshold voltage can be measured and related to a change in the total amount of charge on the active surface. Recently we have prepared a second generation of electronic device with additional abilities to detect signal of DNA hybridization and microfluidic system to deliver DNA to the surface of the sensors.

DNA chips represent robust technology for fast, sensitive, relatively cheap and simultaneous detection of microorganisms in biological samples.

## Acknowledgements

The work in author's laboratory is supported by grant NMP4-CT-2004-013523 from EU and by grant APVT-51-009205 from Ministry of Education of Slovak Republic. Part of this work has been facilitated also through the International Consortium on Ticks and Tick-borne Diseases (ICTTD-3) supported by the INCO-DEV program of the European Union and by the EU-IST-FET program (BEST).

# Properties of nanofabricated biosensors based on DNA aptamers

Tibor Hianik

*FMFI UK, Bratislava, Slovakia*

Biosensors based on DNA or RNA aptamers (aptasensors) are of considerable interest as an alternative to the biosensors based on antibodies. Several problems related to the practical application of aptamers are still under solutions, for example how immobilization of aptamers to the supported films and their microenvironment will affect the aptamer structure and aptamer-ligand interactions. Problems are connected with application of aptamers in a complex biological systems, where interferences with other molecules could take place and especially So far mostly radio labeled aptamers were used, however, to be widely employed in clinical practice, aptamers must be detected via a nonradioisotope method with a comparable sensitivity, e.g. aptamers can be covalently linked to an enzyme, or fluorescently labeled aptamers can be exploited. Moreover, most reliable and cost effective would be exploitation of the direct physical methods that do not require labeling of aptamers by additional chemical ligands. This highly promising route is currently in considerable focus of many laboratories. Among perspective analytical methods for detection protein-aptamer interaction the electrochemical indicators can be used [1]. Another popular method is based on mass detection using quartz crystal microbalance technique. Despite high analytical value of this relatively simple method, this can not provide sufficient information about processes at complex surfaces [2]. The changes in the mass of the crystal can be masked by viscoelastic properties of the layers and the friction between the biolayer and surrounding liquid. Therefore complex impedance of crystal oscillation should be measured and analyzed. This transverse shear mode (TSM) method has been only recently applied for study the protein-aptamer interactions and already demonstrates high potentiality for detailed study of the mechanisms of molecular interactions at surfaces. In this contribution the focus is on application of electrochemical indicators and TSM method for study the protein-aptamer interactions. The aptamers sensitive to thrombin are used for fabrication of biosensors. The attention is given to the methods of immobilization of aptamers to a solid support and how this affect the interaction of thrombin with the aptamer. The effect of aptamer structure, presence of thrombin inhibitor heparin and the ions and pH on the binding properties of aptamer are presented. The advantage of electrochemical indicators and TSM method for detection of thrombin-aptamer interactions are demonstrated.

## Acknowledgements

This work was supported by Agency for Promotion Research and Development under the contract No. APVV-20-P01705 and by the Slovak Grant Agency (Project No. 1/4016/07).

## References

- [1] T. Hianik, V. Ostatná, M. Sonlajtnerova, I. Grman, *Bioelectrochemistry*, 70 (2007) 127.
- [2] T. Hianik, X. Wang, S. Andreev, N. Dolinnaya, T. Oretskaya, M. Thompson, *DNA Analyst* 131 (2006) 1161.

# Investigation of artificial receptor – target molecule interactions for the development of biosensors based on molecular recognition

<sup>1</sup>J. Cirák, <sup>1</sup>M. Weis, <sup>2</sup>R. Janíček, <sup>2</sup>T. Hianik

<sup>1</sup> Department of Physics, Faculty of Electrical Engineering and Information Technology, Slovak University of Technology, 812 19 Bratislava, Slovakia

<sup>2</sup> Department of Nuclear Physics and Biophysics, Faculty of Mathematics, Physics and Computer Sciences, Comenius University, 842 48 Bratislava, Slovakia

The development and study of novel nanostructured materials attracts much attention because of potential applications in molecular electronics, optics, medicine and immunology as well as for the development of chemical sensors and biosensors [1]. Moreover, such studies are essential for the physics of interfaces and for low-dimensional physics. So far significant scientific interest in nanomaterials has been focused on the study of thin organic layers. Detailed study of mechanisms of molecular interactions is crucial for the development of biosensors based on molecular recognition coatings.

The interactions between calix[4]resorcinarene and dopamine in monolayers formed at the air-water interface were studied by analyzing their mechanical, thermodynamic, and electrical properties evaluated from measurements of pressure-area isotherms and of Maxwell displacement currents (MDC). An increased concentration of dopamine in the water subphase resulted in an increase of the area per calix[4]resorcinarene molecule, an increase of the collapse pressure, and a shift in the monolayer phase transitions from the gaseous to the liquid state and the liquid to the solid state towards higher molecular areas. A contactless method of recording MDC enabled to monitor changes in the charge state of the monolayer-constituting molecules [2] and the determination of a relationship between the phase state of the monolayer and the structural transitions of calix[4]resorcinarene. The changes of the MDC recordings started already in the gaseous state of the monolayer. On the basis of MDC values, we determined the normal component of the dipole moment of the calix[4]resorcinarene as well as that of its complex with dopamine. The dipole moment reached a maximum value of 1040 mD in the region of the phase transition from the liquid to the solid state of the monolayer. The results obtained suggest that the binding of dopamine with calix[4]resorcinarene depends on the orientation of the calixarene molecules in the monolayer. The calix[4]resorcinarene-dopamine interactions were also quantified in terms of the excess of Gibbs free energy, thereby allowing the evaluation of the energy of the calix[4]resorcinarene-dopamine bond, which was in the range from 1.95 kJ/mol up to 8.54 kJ/mol depending on the surface pressure. This value implies weak interactions between these molecules [3].

## References

- 1 K. K. Jain, *Med. Device Technol.* **14** (2003) 10
- 2 D. Barančok, J. Cirák, P. Tomčík, J. Vajda, *phys. stat. sol.* **169** (1998) 267
- 3 M. Weis, R. Janíček, J. Cirák, T. Hianik, *J. Phys. Chem. B* **111** (2007) 10626

## Synthesis, microstructures and cytocompatibility of new nanostructured amorphous Ti-based alloys for biomedical applications.

<sup>1</sup>H. Lefaix, <sup>1</sup>P. Vermaut, <sup>2</sup>D. Janickovic, <sup>2</sup>P. Svec, <sup>1</sup>R. Portier,  
<sup>3</sup>A. Asselin, <sup>3</sup>J. M. Sautier, <sup>1</sup>F. Prima

<sup>1</sup> *Laboratoire de Physico-Chimie des Surfaces, CNRS – ENSCP (UMR 7045), Ecole Nationale Supérieure de Chimie de Paris, 11 rue Pierre et Marie Curie 75231 PARIS cedex 05, France.*

<sup>2</sup> *Institute of Physics, Slovak Academy of Sciences, Dubravská Cesta 9, Bratislava, Slovak Republic.*

<sup>3</sup> *Laboratoire de Biologie Orofaciale et Pathologie, INSERM U714, Université PARIS 7, UFR d'Odontologie, Institut Biomédical des Cordeliers, 15-20 rue de l'École de Médecine F-75270 PARIS cedex 06, France.*

Since the discovery of glassy materials, and more recently, of quasicrystals, the research has mostly focused on the exceptional structure, the stability and the physical properties of these peculiar systems. Intense theoretical studies have highlighted an unexpected combination of properties, attractive to advanced technologies. Apparently unsuitable for structural devices due to brittleness, their excellent surface properties offer a new challenge for coating applications, considering the low coefficient of friction, the good corrosion and wear resistances, and the high surface hardness of these phases. Ti-based implants, frequently used for replacing failed hard tissue, have a poor wear resistance so that tribo-chemical reactions produce debris accumulation, resulting in adverse cellular responses. In that sense, amorphous materials and quasicrystals could be used in the field of biomaterials to improve their surface qualities. Among the over hundred quasicrystal forming systems, the ternary Ti-Zr-Ni alloy presents fundamental interest due to the most highly ordered and most stable icosahedral phase, as well as due to the presence of biocompatible Zr and Ti alloying elements. Our previous research outlined that a protective TiO<sub>2</sub>/ZrO<sub>2</sub> barrier, depleted in Ni, composed the surface oxide layer which ensured thus the biocompatibility of these alloys. However, the ternary diagram of Ti-Zr-Ni systems shows their ability to promote also large number of structures, from alpha phase to approximants or Laves phases. The production conditions have a strong effect on the final structural state. As a wide range of cooling rate might be used during the metallurgical process including solidification technology and coating applications, better understanding of the phase selection criterion as function of solidification route is essential to embody the utilization of these materials.

In the present work, nanostructured amorphous ribbons with composition Ti<sub>45</sub>Zr<sub>38</sub>Ni<sub>17</sub> have been produced by planar flow casting using different quenching rates. Among the all parameters involved in this technique such as temperature or atmosphere, the wheel velocity was chosen since it can be well-controlled. Experimented values were within range 10-40 m/s. A detailed characterisation of as-cast ribbons has been performed in order to understand effects of the quenching rate on the so-obtained structures, and precisely on the QC forming and glass forming abilities. Microstructures were compared using X-ray diffraction, and transmission electron spectroscopy. The *in-vitro* evaluation of cytocompatibility of such composite was carried out in organotypic culture of bone tissue. The cell behaviour was analysed around and upon the metallic surface by qualitative and quantitative measurements, characteristic of material/tissue interface: the cell adhesion, proliferation and differentiation.

**Keywords:** titanium, amorphous, quasicrystals, nanomaterials, biocompatibility.

## **Stress and Strain in Small Scale Materials**

R. Pippan, J. Keckes, G. Dehm

*Erich Schmid Institute for Materials Research, Austrian Academy of Sciences  
and  
Department Materials Physics, Montanuniversität Leoben, 8700 Leoben, Austria*

Materials with internal or external length scales in the micro- and nanometer regime, such as hard coatings, thin metallic films, and micro/nanocrystalline bulk materials, reveal mechanical properties which can significantly deviate from their conventional bulk counterparts. To explore the underlying deformation mechanisms microstructural characterization and miniaturized mechanical tests are usually required. A combination of both is offered by (novel) in situ tests performed in the focussed ion beam microscope (FIB), scanning electron microscope (SEM), transmission electron microscope (TEM) and X-ray diffraction facilities including the possibilities of synchrotron radiation. In this overview several examples are provided and discussed.

## A cantilever technique to determine stress distributions in residually stressed surface-near regions

<sup>1</sup>S. Massl, <sup>2</sup>J. Keckes, <sup>1</sup>R. Pippan

<sup>1</sup>*Erich Schmid Institute of Materials Science, Austrian Academy of Sciences, Austria*

<sup>2</sup>*Department Materials Physics, University of Leoben, Austria*

A method to determine stress distributions in residually stressed surface-near regions is presented. The developed technique is based on the fabrication of a cantilever (Fig.) by means of a focused ion beam workstation and allows the determination of residual stresses with a depth resolution on the nanometer scale and a lateral resolution on the micrometer scale. The calculation procedure only requires the dimensions of the cantilever, the distribution of the elastic constants and basic bending beam theory. The method can be applied to crystalline as well as amorphous materials.

It will be presented by determining depth profiles of residual stresses of a crystalline TiN coating and an amorphous SiO<sub>x</sub> thin film. Furthermore the three dimensional elastic stress field produced by a spherical indent on a thin Ni film is analyzed by means of the developed technique.

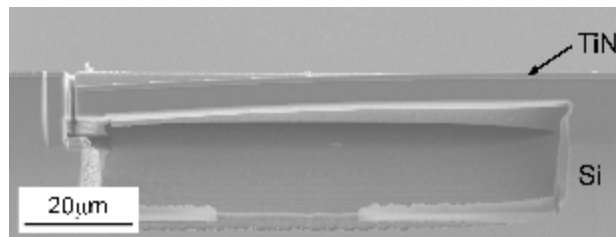


Fig. FIB-fabricated micro cantilever that deflects owing to the residual stresses in the TiN coating and the Si substrate.

## Stress measurement in small dimensions using micro-cantilever deflection technique

Kurt Matoy<sup>1,2</sup>, Helmut Schönherr<sup>3</sup>, Thomas Detzel<sup>3</sup>, Thomas Schöberl<sup>2</sup>, Reinhard Pippan<sup>2</sup>, Christian Motz<sup>2</sup>, Gerhard Dehm<sup>2</sup>

<sup>1</sup> *Kompetenzzentrum Automobil- und Industrie-Elektronik GmbH, A-9524 Villach, Austria*

<sup>2</sup> *Erich Schmid Institute of Material Science, Austrian Academy of Sciences, and Department Materials Physics, Montanuniversität Leoben, A-8700 Leoben, Austria*

<sup>3</sup> *Infineon Technologies AG, A-9500 Villach, Austria*

Thin films on substrates can reveal high internal stresses. As a consequence thin film systems are prone to deformation and may limit the lifetime of components. Thus, there is a strong need to determine the mechanical properties of thin film materials using well-defined mechanical tests. In this talk we present and critically compare experimental results obtained by micro-cantilever deflection experiments of free-standing films and nanoindentation measurement of identical films on a substrate. The investigated films are amorphous silicon oxide, silicon oxynitride and silicon nitride which are produced by plasma enhanced chemical vapour deposition. It is shown that the film materials behave linear elastically until fracture occurs. Hardness, Young's modulus and fracture stress show a clear correlation with the nominal nitrogen content determined from Fourier Transform Infrared Spectroscopy (FTIR). Furthermore, all the investigated mechanical parameters scale with the refractive index.

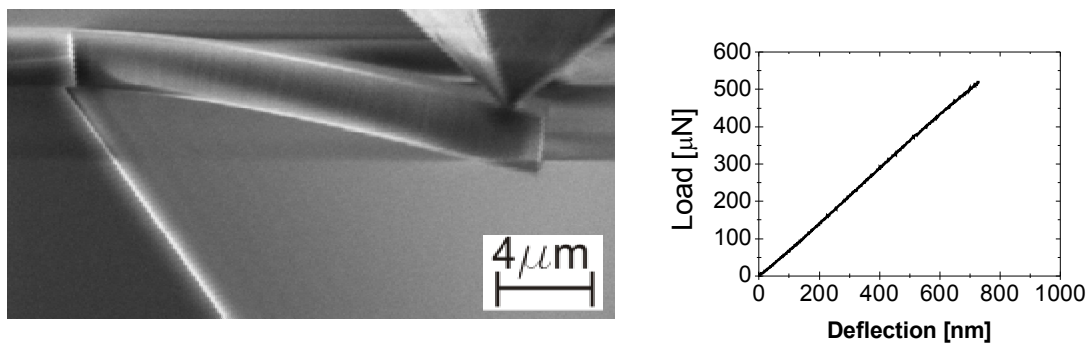


Figure.1. *In-situ* micro-cantilever deflection experiment of a 2.3 μm thick silicon oxide film in scanning electron microscope and load-deflection curve.

# Grain refinement of single crystals and alloys processed by high pressure torsion

<sup>1\*</sup>Hafok Martin, <sup>1,2</sup>Reinhard Pippan,

<sup>1</sup>*Erich Schmid Institute of Material Science, Austrian Academy of Sciences, Leoben, Austria*

<sup>2</sup>*CD Laboratory for local Analysis of Deformation and Fracture, Christian Doppler  
Forschungsgesellschaft, Leoben, Austria*

Severe plastic deformation comprises techniques for the grain refinement of bulk materials. One of these methods is high pressure torsion which was used to produce submicron and even nanostructured materials. The refinement of grains is achieved by high pressure torsion by imposing a combination of extreme high strains and a high hydrostatic pressure to the samples.

The presented study deals with single phase alloys and a single crystalline material, which were examined by scanning electron microscopy, electron back scatter diffraction and transmission electron microscopy. The structure refinement of the single crystal revealed the fragmentation process under the absence of initial boundaries and overall initial texture. In case of the single phase alloys the structure refinement as a function of the alloying content was examined and compared with the mechanical tests of high pressure torsion deformed samples to study the influence of structure size and alloy concentration on the mechanical properties.

# Thermophysical Properties by Different Measurement Techniques - The Project *High Temperature Metallic Melts*

<sup>1</sup>Thomas Hüpf, <sup>1</sup>Claus Cagran, <sup>1</sup>Boris Wilthan <sup>2</sup>Georg Lohöfer, <sup>1</sup>Gernot Pottlacher

<sup>1</sup>*Institute of Experimental Physics, Graz University of Technology, Austria*

<sup>2</sup>*Institut für Materialphysik im Weltraum, DLR, Linder Höhe, Köln, Germany*

Metallic Melts, such as liquid iron, are difficult to handle and to investigate. When molten metals become highly reactive (with the surrounding atmosphere as well as with the crucible) which causes contamination or changes of composition.

The handling of liquid metals is well developed in the metalworking industry (casting, injection molding, etc.), but basic research on fundamental properties, like electrical resistivity or density, often suffers from the uncomfortable characteristics of metallic melts.

The ‘Subsecond Thermophysics Workgroup’ at Graz University of Technology (TUG) operates a facility, which allows measurements of the liquid state thermophysical properties of most conducting elements (i.e., metals). The key to this facility is *speed*: The specimens (which are wire-shaped) are heated from room temperature up to the end of the liquid phase within about 50  $\mu$ s. This short time interval inhibits chemical reactions and keeps the wire from changing its position (as it cannot bend or collapse so quickly). As a result, all measurements have to be done very fast too and temperature can only be measured via thermal radiation. The technique is called ‘fast pulse-heating method’ because the specimens are heated by the passage of a large current pulse (about 10 000 A). Although very elegant and simple, this technique is not new and the first setup at TUG was already developed around 1979. Several pulse-heating laboratories existed around the globe, but the interest is currently decreasing (i.e., NIST, USA or CEA, France).

The current research at the Subsecond Thermophysics Workgroup is divided into a collaboration with the metalworking industry (Böhler Edelstahl GmbH), who is - among other things - interested in input data for casting simulations, and a joint research project together with the German Aerospace Center (DLR) in Cologne, where another approved technique to investigate metallic melts, namely electromagnetic levitation, is elaborated.

By using electromagnetic levitation, the gravitational forces on the liquid metal drop are compensated with electromagnetic fields which *levitate* the sample. As these fields may cause disturbances of the sample (e. g. melt flow) the measurements are planned to be carried out under  $\mu$ g-conditions (at the ISS or during parabolic flight experiments). Within this context, the measurement capabilities at TUG are an inexpensive and ‘ground based’ possibility for comparison of results obtained with different techniques.

The aim of the current work is to present the pulse heating setup at TUG and to discuss the latest results thereof. The joint-project with DLR Cologne is sponsored by the Austrian Space Applications Programme ASAP by FFG, Vienna.

# Structural Transformations in Fe-Based Nanocrystalline Alloys

<sup>1,3</sup>M. Miglierini, <sup>1</sup>T. Kaňuch, <sup>1</sup>M. Pavúk, <sup>1</sup>M. Pavlovič, <sup>2</sup>P. Švec, <sup>2</sup>D. Janičkovič, <sup>3</sup>M. Mašláň,  
<sup>3</sup>R. Zbořil, <sup>4</sup>Y. Jirásková, <sup>5</sup>G. Schumacher and <sup>6</sup>I. Zizak

<sup>1</sup>Slovak University of Technology, Bratislava, Slovakia

<sup>2</sup>Institute of Physics, SAS, Bratislava, Slovakia

<sup>3</sup>Nanomaterials Research Centre, Olomouc, Czech Republic

<sup>4</sup>Institute of Physics of Materials, AS CR, Brno, Czech Republic

<sup>5</sup>Hahn-Meitner-Institute, Berlin, Germany, <sup>6</sup>BESSY, Berlin, Germany

Disordered nature of structural arrangement in Fe-based metallic alloys gives rise to advantageous (from a practical application point of view) magnetic properties. Suitable heat treatment of metallic glasses produces the so-called nanocrystalline alloys. The latter attract a lot of scientific interest because, contrary to their amorphous counterparts, their magnetic parameters do not substantially deteriorate at elevated temperatures during the process of their practical exploitation. To benefit from their unique magnetic properties, the mechanism of stability comprising crystallization should be known. Here, we present a study of structural transformation of Fe-Mo-Cu-B NANOPERM-type alloys with the aid of Mössbauer spectrometry, conventional X-ray diffraction (XRD) as well as by *in situ* (during continuous heat treatment) diffraction of synchrotron radiation. Additional information is provided by atomic force microscopy (AFM), transmission electron microscopy, high resolution electron microscopy, differential scanning calorimetry, and positron annihilation spectroscopy. Some results are illustrated in the figures below using the Fe<sub>79</sub>Mo<sub>8</sub>Cu<sub>1</sub>B<sub>12</sub> alloy as an example.

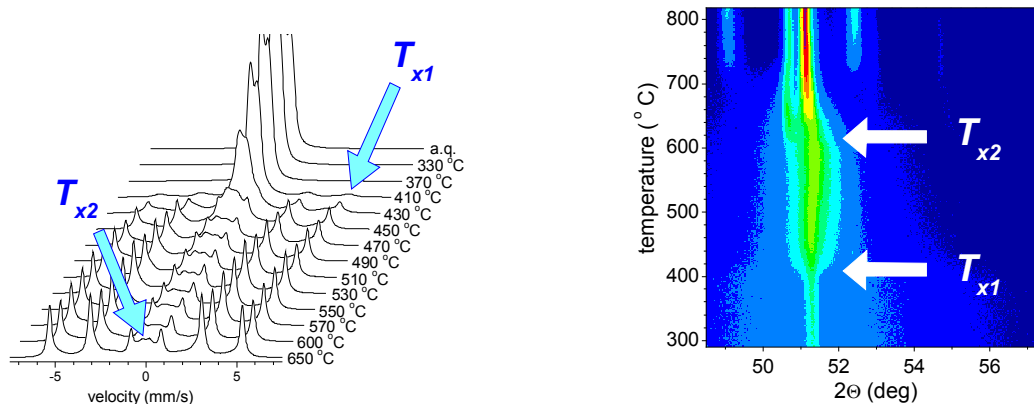


Fig. 1. Fe<sub>79</sub>Mo<sub>8</sub>Cu<sub>1</sub>B<sub>12</sub> alloy: conversion electron Mössbauer spectra (left) taken after 1 hour annealing at the indicated temperatures (a.q. – as-quenched). XRD intensities at 2 $\Theta$  angles (right) acquired with synchrotron radiation during *in situ* heating with the temperature ramp of 10 K/min. The onset of the first ( $T_{x1}$ ) and the second ( $T_{x2}$ ) crystallization steps is marked with the arrows.

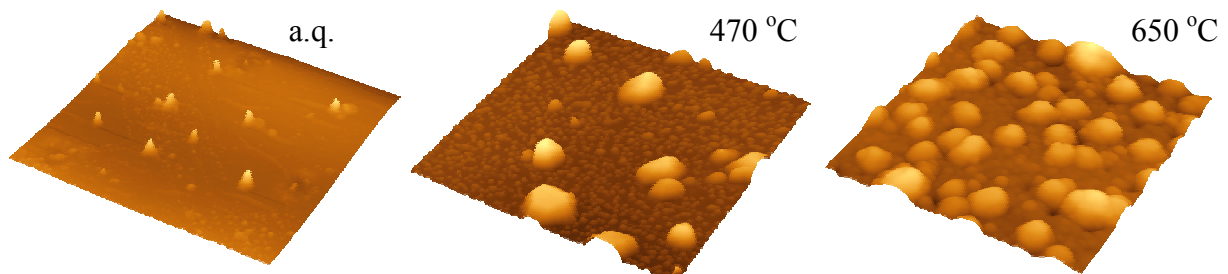


Fig. 2. Fe<sub>76</sub>Mo<sub>8</sub>Cu<sub>1</sub>B<sub>12</sub> alloy: AFM images taken after 1 hour annealing at the indicated temperatures.

This work was supported by the grants VEGA 1/4017/07, 2/5096/27, MSM6198959218, APVT 20-008404, and EC grants under IA-SFS contract RII 3-CT-2004-506008, EU/INTAS/07, and INTAS 06-100012-8683.

# Application of evanescent waves to nanostructures characterization

<sup>1</sup>J. Pištora, <sup>2</sup>J. Vlček, <sup>1</sup>M. Lesňák

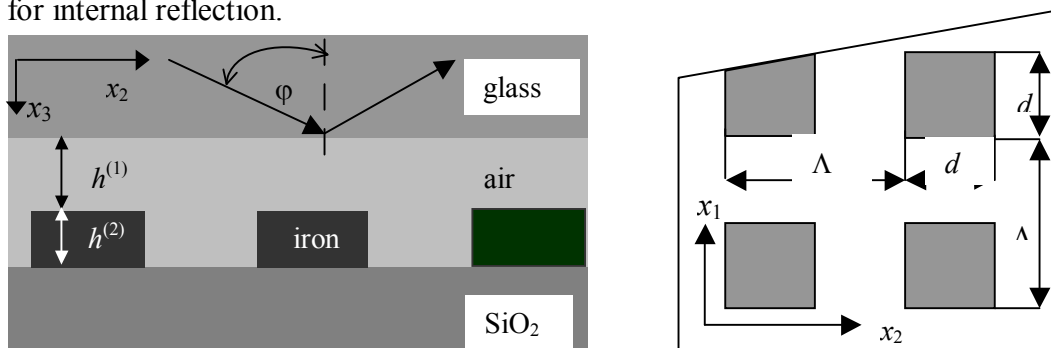
<sup>1</sup>Department of Physics

VSB – TU of Ostrava, 17. listopadu 15, 708 33 Ostrava – Poruba, Czech Republic.  
Tel: +420 597 323 129; Fax: +420 597 323 139; E-mail: [jaromir.pistora@vsb.cz](mailto:jaromir.pistora@vsb.cz)

<sup>2</sup> Department of Mathematics and Descriptive Geometry

VSB – TU of Ostrava, 17. listopadu 15, 708 33 Ostrava – Poruba, Czech Republic.  
Tel: +420 597 324 176; E-mail: [jaroslav.vlcek@vsb.cz](mailto:jaroslav.vlcek@vsb.cz)

In our contribution we analyze the concept of total internal reflection ellipsometry (TIRE) containing two-dimensional periodic system of metallic square dots. Obtained results demonstrate the dependence of ellipsometric response on air gap thickness, and, also the comparison for planar, lamellar and 2D binary periodic system is reached. The basic parameters of considered TIRE system setup are analogous as in [1]. The high refractive index medium (coupling prism) is represented by the BK-7 glass. The binary grating created as Fe square dots on the SiO<sub>2</sub> substrate is separated from the prism by thin air gap. The geometrical characteristics of the periodical structure are showed in the Fig. 1: grating period  $\Lambda = 260$  nm (the same in the directions  $x_1, x_2$ ) and square dots size  $d = 130$  nm do not change in the all samples. The thickness  $h^{(1)}$  of air gap is the variable parameter whereas the dot height  $h^{(2)} = 10$  nm is fixed. All the materials are supposed to be isotropic. As the refractive index of glass,  $n^{(0)}$ , is larger than this one of air gap,  $n^{(1)}$ , the dependence of ellipsometric angles  $\psi, \Delta$  on incidence angle  $\varphi$  upon the critical angle  $\varphi_c$  exhibits the specific feature that is typical for internal reflection.



The interaction of electromagnetic field with nanostructured metallic elements and their diffraction properties are determined by coupled wave method implemented as the Fourier modal method (FMM).

The modeling of total internal reflection ellipsometry demonstrates the extreme sensitivity of ellipsometric angles to the fill factor of the metallic grating elements, and, to the thickness of coupling gap. An interesting application is using this method for surface effects study especially for metallic and anisotropic media. We can observe relatively high sensitivity of dot shapes on ellipsometric angle dependence. The length change of 5 % of one side of square dots generates the ellipsometric angle shift (in  $\Delta$  scale) about 3 degrees. It means the TIRE method can be applied to the shape inspection of nanostructured dots.

- [1] J. Pištora, J. Vlček, P. Hlubina, M. Foldyna, O. Životský, “Total internal reflection ellipsometry of periodic structures”, Proc. of SPIE, Vol. 6180, pp. 61801E-1 – 61801E-5, 2006.

## On the mechanism of thermally activated solid-state reaction and formation of intermetallic nanograins in Al/Ti nanoscaled multilayer foils

<sup>1\*</sup>E. Illeková, <sup>2</sup>J.C. Gachon, <sup>3</sup>A. Rogachev, <sup>4</sup>J.C. Schuster

<sup>1</sup>*Institute of Physics, SAS, Dúbravská cesta 9, Bratislava, Slovakia*

<sup>2</sup>*LCSM UMR7555, Université Henri Poincaré, 54506 Vandoeuvre les nancy Cedex, France*

<sup>3</sup>*Institute of Structural Macromechanics and Materials Science, RAS, 142432 Chernogolovka – Moscow, Russia*

<sup>4</sup>*Innovative Materials Group, Universität Wien, A-1090 Wien Austria*

*\*Center of Excellence “NANOSMART”, Slovak Academy of Sciences, Bratislava, Slovakia*

Foils with a wide variety of layer numbers and thicknesses can be obtained with help of magnetron layer-by-layer deposition. Reactions in such multilayer nano-systems can be utilized for producing novel materials and coatings such as intermetallic layers for reactive micro-soldering in tiny devices, etc...

Fast growth of nanotechnology requires fundamental knowledge of heterogeneous reaction kinetics and mechanisms in nano-systems. Multilayer nanofilms represent promising subjects for experimental study of nano-heterogeneous reactions. The thermal effects or X-ray diffraction patterns produced by reactions between hundreds or thousands layers in extremely thin reacting medium allow the kinetic analyses by Differential Scanning calorimetry (DSC) or by time-resolved synchrotron radiation diffraction (TRSRD).

TiAl-based intermetallics due to their low specific weight, high specific strength and hardness, excellent creep strength and good oxidation resistance are promising materials for high temperature applications particularly in automotive and aerospace industries.

This contribution describes results obtained during the study of the slow synthesis of intermetallic Al/Ti foils, starting from elemental nanoscaled multilayers of Al and Ti prepared by plasma sputtering. Various foils with layer thicknesses from 4.5 nm up to 1000 nm, and layer numbers from 20 up to 4440 were produced. The process of structural transformation due to temperature controlled heterogeneous reaction is studied by DSC and TRSRD during continuous heating. In the heating rate controlled reaction, which starts below 570 K, more than one exothermal elementary transformation step is distinguished. The produced crystalline phases and their morphology are investigated by X-ray diffraction (XRD) and transmission electron microscopy (TEM). Aluminides  $\text{Al}_3\text{Ti}$ ,  $\text{AlTi}$  and  $\text{Ti}_3\text{Al}$  have been identified. The thermodynamic stability of the formed phases and kinetic parameters of the proceeding reaction are quantified. Kissinger and Suriñach methods have been used. The mechanism of the complex formation of the aluminides in the individual multilayers is proposed. Results demonstrate that total heat of reaction, activation energies and reaction mechanisms vary with the thickness of the individual layers of Al and Ti.

## Characterization of sulfonated poly(ether ether ketone) polymer electrolyte for fuel cells by FTIR spectroscopy

<sup>1\*</sup> G. Chikvaidze, <sup>2</sup>H. Luo, <sup>1</sup>G. Vaivars, <sup>1</sup>J. Kleperis

<sup>1</sup>*Institute of Solid State Physics of University of Latvia, Riga, Latvia;*

<sup>2</sup>*SA Institute of Advanced Material Chemistry, Univ. Western Cape, Cape Town, South Africa*

In our work the sulphonated poly(ether ether ketone) (SPEEK) ionomers were synthesized using original and simple method (patent application is in preparation). Homogeneous proton-conducting membranes were developed from the obtained SPEEK by solvent casting method. Membranes were assessed for their suitability in fuel cell applications. The membranes were characterized by FTIR to confirm sulphonation, and DSC and TGA to investigate the thermal stability. The proton conductivities of such membranes were found to be excellent in the order of  $10^{-2}$  S/cm in the fully hydrated condition at room temperature. The durability of the membranes was also tested.

SPEEK membrane is a hydrophobic polymer with an aromatic, non-fluorinated backbone, in which 1,4-disubstituted phenyl groups are separated by ether (–O–) and carbonyl (–CO–) linkages. Sulfonation is an electrophilic substitution reaction, in which the hydrogen ion on aromatic ring is substituted by sulfonic acid group (–SO<sub>3</sub>H). The presence of sulfonic acid group is increasing the acidity of polymer and makes the SPEEK highly hydrophilic. FTIR spectra were obtained using a Bruker EQUINOX 55 spectrometer equipped with Praying Mantis TM (DDR) accessory designed for examining samples by diffuse reflection spectroscopy. The spectra were measured in transmittance mode and in DDR mode over a wave number range of 7000-400 cm<sup>-1</sup>. Spectra are measured with resolution of 1 cm<sup>-1</sup>.

The presence of sulfonic acid group in SPEEK was confirmed by the strong characteristic peaks at 1239, 1088 and 1032 cm<sup>-1</sup>, were assigned to the symmetric and asymmetric O=S=O stretching vibrations, as their intensities with respect to the backbone carbonyl (C=O) band at 1651 cm<sup>-1</sup> increased with DS. These O=S=O stretching vibrations spectrum for unsubstituted PEEK were weak, meanwhile there is no significant difference in the carbonyl band for PEEK compared with SPEEK. Another evidence of the presence of sulfonic acid group is the appearance of the peak at 3460 cm<sup>-1</sup> in SPEEK samples, which is assigned to O-H vibration from sulfonic acid group. The spectrum shows that the O-H peak increased with SPEEK DS, thus indicating the polymers with higher DS are more acidic. The same findings were also reported by [1,2].

Thermogravimetric analysis (TGA) and proton conductivity measurements of membranes also will be presented.

### References:

1. M. H. D. Othman, A. F. Ismail\*, A. Mustafa, Physico-Chemical Study of Sulfonated Poly(Ether Ether Ketone) Membranes for Direct Methanol Fuel Cell Application. Malaysian Polymer Journal (MPJ), Vol 2, No. 1, p 10 -28, 2007
2. J. Ho-Young, C. Ki-Yun, S. Kyung-A, K. Wan-Keun, P.Jung-Ki. The effect of sulfonated poly(ether ether ketone) as an electrode binder for direct methanol fuel cell (DMFC). J Power Sources, Vol. 163, p 56-59, 2006.

## Organometallic Nanojunctions Probed by Different Chemistries: Thermal-, Photo, and Mechanochemistry.

<sup>1,2</sup>I. Štich, <sup>2</sup>M. Konôpka, <sup>2</sup>R. Turanský, <sup>3</sup>D. Marx

<sup>1</sup>*Institute of Physics, Slovak Academy of Sciences, Bratislava, Slovakia*

<sup>2</sup>*Center for Computational Materials Science, Slovak University of Technology (FEI STU),  
Bratislava, Slovakia*

<sup>3\*</sup>*Ruhr-Universität Bochum, Bochum, Germany*

Different methods of activation of chemical reactions are compared for organometallic nanojunctions. The study is based on density functional theory simulations. First we provide a comparison of thermal activation with mechanical activation, or mechanochemistry. Study of thiolate/copper junctions and interfaces provides evidence for vastly different reaction pathways and products. The differences are understood in terms of mechanical manipulation of coordination numbers and system fluctuations in the process of mechanical activation. Next we compare photo- and mechanochemistry. Azobenzene (AB) is an optically switchable molecule. Laser light is normally used to achieve molecular switching between gas phase *cis* and *trans* isomers of AB. Does the switching property hold also for anchored AB? What is the interplay between optical and mechanical switching? In order to answer these questions we study AB optomechanical switch which combines photo excitation with external pulling force to manipulate optical switching properties of AB anchored to gold tips by thiolate bonds. We focus on the separation between ground (S0) and first excited (S1) singlet states. We observe a pronounced dependence of the S0-S1 separation on the applied strain and a close interplay between optical and mechanical switching. Furthermore we find that ground-state mechanochemistry alone can be used to achieve switching. Pulling the *trans* isomer leads just to formation of gold nanowires and mechanical breakage of the electrodes. However, mechanochemistry with modest applied forces leads to *cis* → *trans* reversion. The reversion mechanism (rotation, inversion) strongly depends on the model tips used.

## How good conductors are pi-conjugated molecules ?

Z. Crljen

*Theoretical Physics Division, Rudjer Boskovic Institute,  
Zagreb, Croatia*

In the field of molecular nanoelectronics the transport properties of single molecule are of crucial importance. Molecular junction with  $\pi$ -conjugated molecules have often been studied primarily for their promising molecular wire behaviour. However, the discrepancies between theoretical predictions and experimental data have blurred out the ability of  $\pi$ -conjugated systems. The precise knowledge of the contact geometry of the molecular junction, as the adsorption site and bonding between the molecule and the electrode has been difficult to achieve experimentally and the dependence of the conductivity on the length of the molecule has not been precisely known.

In order to get a reliable description of the molecular conducting properties, details, such as the electronic structure of the electrodes, the electrode surfaces, the molecule, and the molecule-induced gap states, should be fully considered. Moreover, as the junction is subject to the nonequilibrium conditions the transmission should be obtained self-consistently for each bias voltage applied across the junction. To account for this we used a full self-consistent ab initio method based on the density functional theory and nonequilibrium Green's function technique [1].

We performed series of calculations of the conductance of certain classes of  $\pi$ -conjugated molecules: phenyl ethylene oligomers (Tou wires), phenylene vinylene oligomers (OPV) and polyynes. The considered geometry consisted of the molecule between the gold electrodes. We used a Au(111) surface in a 3x3 unit cell for electrodes and molecule chemisorbed to the surfaces through strong thiol bonds. Keeping the contact geometry for all of molecules the same, optimizing it with respect to the adsorption site we obtained the functional dependence of the conductance on the intrinsic molecular properties. In the low bias regime we found that polyynes, the one-dimensional chains of carbon atom with alternating single and triple bonds between carbon atoms, show the highest conductance with the value of 100  $\mu$ S at zero bias[2]. In Tou wires and OPV molecules, the conductivity shows the decrease proportional to the number of benzene rings in the molecule. We will show that the conductance of polyynes is stable with respect to the applied bias and the length of the molecule while in Tou wires and OPVn it exhibits the nonlinear behaviour as a consequence of different electronic structure around the Fermi level of the system. We will also observe that the dependence of the conductance on the molecular length clearly shows nonexponential decay, contrary to the known results of various semi-empirical theoretical approaches.  $\pi$ -conjugated molecules show a good molecular wire properties, with the metalliclike conductance in polyynes, which controllably reduces down with the number of phenyl rings in phenyl type oligomers. That may appear as a desired property in the designing of nanostructures with required characteristics.

References:

- [1] M. Brandbyge, J. L. Mozos, P. Ordejon, J. Taylor, and K. Stokbro, Phys. Rev. B 65, 165401 2002 .
- [2] Z. Crljen, and G. Baranovic, Phys. Rev. Lett. 98, 116801, 2007.

# Various aspects of immobilization of glucose sensitive proteins within hybrid silica gel matrices

**Igor Krupa,<sup>1</sup> Tomáš Nedelčev,<sup>1</sup> Dušan Chorvát, Jr.,<sup>2</sup> Igor Lacík,<sup>1</sup>**

<sup>1</sup> *Polymer Institute SAV, Dúbravská cesta 9, 84236 Bratislava, SLOVAKIA  
([upolkrup@savba.sk](mailto:upolkrup@savba.sk))*

<sup>2</sup> *International Laser Center, Ilkovičova 3, 812 19 Bratislava, SLOVAKIA*

Immobilization of proteins, enzymes and cells in the xerogel and/or hybrid xerogel matrices, most often in the form of monoliths and thin films, has been the area of interest with the outcome in many applications spanning from biosensors, bioselective chromatography, controlled release of drugs etc [1,2]. The preparation, structure and some physical characteristics of various types of hybrid xerogel matrices based on the organofunctional silanes is reported in this work. Tetraethoxysilane, 3-aminopropyl triethoxysilane and 3-epoxypropyl trimethoxysilane were used as building blocks, whereas glycerol and various polymeric additives were used as processing agents. The preparation of transparent material with controlled porosity over long period of use was one of the main aims of this work.

Fluorescence microscopy was used i.) to monitor the penetration of fluorescently labelled dextrans of different molecular weight into the formed hydrogels to determine their exclusion limit and ii.) to estimate diffusion coefficient of glucose (using fluorescently labelled glucose) within a silica gel.

Bovine serum albumin (BSA) and glucose binding protein (GBP) were immobilized into formed silica hydrogels as the model enzymes. Their leaching (BSA, GBP) and glucose-sensing properties (GBP) were monitored by UV-VIS and fluorescence spectroscopy. Sensitivity of GBB on the glucose was also investigated.

## Acknowledgement

The research was supported by the Scientific Grant Agency of the Ministry of Education of Slovak Republic and the Slovak Academy of Sciences (project No. 2/6114/26) and, in part, by Sixth Framework Program of the EU, IP-031867, P. Cezanne.

## Literature

1. W. Jin, J.D. Brennan, *Analytica Chimica Acta*, **2002**, 461, 1.
2. I. Gill, A. Ballesteros, *TIBTECH*, **2000**, 18, 282.

## Laser induced self-assembling formation of semiconductors nanohills for nanoelectronic and optoelectronic applications

<sup>1\*</sup>A.Medvid', <sup>2</sup>I.Dmitruk,P. <sup>1</sup>Onufrijevs, <sup>2</sup>I I.Pundyk ...

<sup>1</sup>Riga Technical University,Riga, Latvia

<sup>2</sup>Kyiv National University,Kjiv, Ukraine

Nanohills on a surface Ge single crystal were formed using basic frequency of Nd:YAG laser radiation at intensity of 30 MW/cm<sup>2</sup>. This structure is characterized by patterns related to C<sub>6i</sub> point group symmetry covering all the surface of the sample by translations symmetry [1]. In the case of SiO<sub>2</sub> on Si, the nanohills are formed by the second harmonics of Nd:YAG laser radiation at intensity of 20 MW/cm<sup>2</sup>. The nanohills form rows on micro-periodical structure. Photoluminescence from irradiated surfaces is found in visible range of spectrum. Peculiarities of photoluminescence from Ge and Si nanohills could be explained by Quantum Confinement effect in nanowires with gradual decrease of nanowire diameter from maximum on the plane of a semiconductor surface to minimum on the top of nanohill. It is semiconductor with graded band gap [2]. Photoluminescence from the surface of GaAs single crystal irradiated by the second harmonic of Nd:YAG laser at intensity 7.5MW/cm<sup>2</sup> is characterized by blue shift on 100 nm and increase of its intensity by 10 times in comparison with a nonirradiated sample. A shift of micro-Raman back scattering spectra is a good evidence of this suggestion. The calculated minimal diameters of nanowires on the top of nanohills [3] for Ge, Si and GaAs single crystals are 4 nm, 4.5 nm and 11.5 nm, correspondently.

### References

1. A. Medvid', Y. Fukuda, A. Michko, P. Onufrievs , and Y. Anma."2D lattice formation on a surface of Ge single crystal by YAG:Nd laser", *Appl. Sur. Sci*, Vol. 244/1-4, pp.120-123, 2005.
2. A.Medvid', L.Fedorenko, B.Korbutjak, S.Kryluk, M.Yusupov, A. Mychko. " Formation of grated band-gap in CdZnTe by Nd:YAG laser radiation "*Radiation Measurements*" , 2006, accepted.
3. L.E.Brus." Electron-electron and electron-hole interactions in smal semiconductor crystallites: The size dependece of the lowest exited electronic state", *J.Chem.Phys.*, Vol.80, pp.4403-4409, 1984.

**Abstracts**

**Poster contributions**

# The Dynamical Response to the Node Defect in Thermally Activated Magnetic Dot Arrays

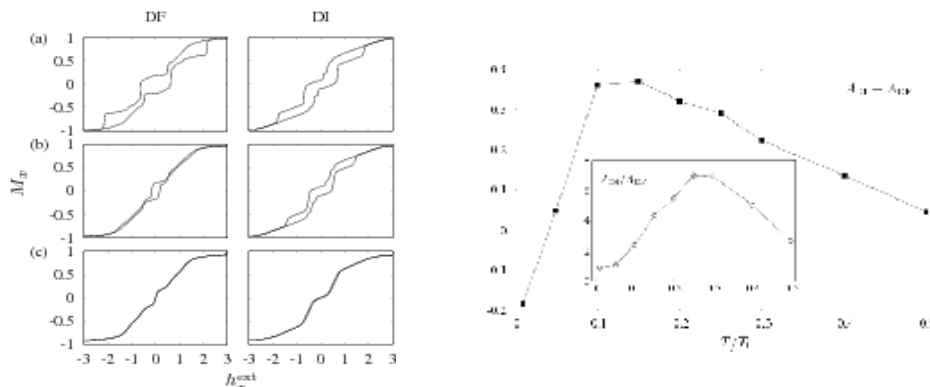
Pavel Baláž, Denis Horváth, Martin Gmitra

*Institute of Physics, P. J. Šafárik University, Košice, Slovakia*

The concept of nano-scaled monolayer two-dimensional structures consisting of identical and periodically ordered magnetic nanoparticles so-called magnetic dot arrays (MDAs) is compelling because of qualitatively new properties that could evoke potential applications concerning the magnetic memory devices. Despite of recent progress in fabrication, an occurrences of defects and damage have still a great influence on magnetic properties of MDAs. By this reason the aim of our study is to look for the dot vacancy effects. We focus on the vacancy located at the centre of 2d square lattice [1]. We have studied magnetic hysteresis and relaxation processes under the thermal fluctuations. For this purpose elementary model is considered where each dot is described by the point magnetic dipole. Thus the system of dots - dipoles interact via dipol-dipol interaction. The dynamics of dot moments has been simulated by integrating stochastic Landau-Lifshitz-Gilbert equation.

The left hand side figure bellow shows comparison of the system of conditionally averaged hysteresis loops simulated for MDAs without (DF) and with defect (DI) at different temperatures (measured in characteristic units  $T_0$ ) (a) 0.01 (b) 0.1 (c) 0.5. On the right hand side figure we depicted the temperature dependencies of differences resp. ratios (see the inset) of areas of loops for DI and DF MDAs cases. They demonstrate that the presence of defect influences dynamical properties of MDAs and the temperature changes sensitivity to magnetic defect. It means that properly chosen thermal activation can enhance the observability of magnetic defects in experimental conditions. Because of the temperature dependencies are non-monotonous, the optimal temperature, given by extremal defect sensitivity, can be chosen. The simulations have provided rough value 0.2  $T_0$ .

This work was partly supported by the Slovak Research and Development Agency under the contract No. RPEU-0006-06, VEGA 1/2009/05, APVT-51-052702 and APVV-LPP-0030-06.



[1] P. Baláž, D. Horváth, M. Gmitra, arXiv:0705.1889 (2007).

# Spin-polarized Current-pulse-induced Spin-switching in Spin-valves

Pavel Baláž<sup>1</sup>, Martin Gmitra<sup>2</sup>, Józef Barnas<sup>1</sup>

<sup>1</sup>*Department of Physics, A. Mickiewicz University, Poznań, Poland*

<sup>2</sup>*Institute of Physics, P. J. Šafárik University, Košice, Slovakia*

Spin-polarized current can transfer spin angular momentum from conduction electrons to localized moments and generate magnetization excitations [1]. This phenomenon is important for its wide range of technological applications, including magnetic memory and magnetic sensors. Despite advantages in current-induced magnetization switching in metallic spin valves, the straightforward application is still restricted due to high critical current densities. Such a high current density can produce significant Joule's heating that can thermally destabilize the spin valve. Therefore, it seems to be desired to design a current pulse which minimizes the switching time and also produces minimal Joule heating. We have performed relevant dynamical study in the standard spin valve Cu/Co(30)/Cu(10)/Co(4)/Cu and in the asymmetric valve Ir/Co(6)/Ru(2)/Co(4)/Cu(8)/Py(4)/Cu [2] at zero temperature. The dynamics has been described within the macrospin model using the generalized Landau-Lifshitz-Gilbert equation. The spin transfer torque has been calculated in the diffusion transport limit [3]. The influence of current pulse shape and Joule's heating on the switching time has been investigated. We have compared the spin-valve dynamics under a rectangular pulse and the pulse having finite rise and fall behavior. The detailed dependence of the diagrams of switching time and Joule's heating on the relevant pulse parameters has been obtained. We have found the areas comprising the short switching times and low level of Joule heating.

This work was supported by the EU through the Marie Curie Training network SPINSWITCH (MRTN-CT-2006-035327).

[1] J. C. Slonczewski, *J. Magn. Magn. Mater.* 195, L261 (1999)

[2] M. Gmitra, J. Barnas, *Phys. Rev. Lett.* 99, 097205 (2007)

[3] J. Barnas, A. Fert. M. Gmitra, et al., *Phys. Rev. B* 72, 024426 (2005)

# ECAP as the technique for consolidation of rapidly solidified Al based particles.

Martin Balog, Frantisek Simancik

*Institute of materials and machine mechanics, SAS, Racianska 75, 83102 Bratislava, Slovakia, tel.: +421/249268303, fax: +421/244253301*

The extremely high tensile strengths exceeding 1 GPa accompanied with good ductility and thermal stability are expected from specific Al-based alloys rapidly solidified (RS) at extreme cooling rates up to  $10^6$  °C.s<sup>-1</sup> – featuring significantly extended solid solubility of alloying elements, nanocrystalline or amorphous microstructures, presence of aperiodic phases [1]. However, associated heat flow limits thickness of material chilled down during quenching at such high cooling rates, so such materials can be obtained only in form of thin ribbons or fine powder particles. Since discrete particles lack broader technological feasibility, their synthesis into bulk materials is required. To establish good metallurgical bonding between particles, to break up surface oxide's envelopes and meanwhile to maintain metastable RS structures consolidation is basically circumscribed to compaction routes based on introduction of shear deformation - predominantly to well establish direct extrusion (DE). However, the resistance against plastic deformation of high strength RS particles leads to extreme extrusion pressures at moderate temperatures often exceeding the limits of conventional tooling [2]. Decreasing of this resistance by consolidation temperature increase is not possible, since it would result in devitrification / coarsening of their unique structures followed with irreversible loss of desired mechanical properties. Therefore an alternative consolidation technique assuring sufficient amount of shear deformation performed at lower temperatures while reducing extreme pressing loads should be explored.

In this study an approach utilizing the well known method of severe plastic deformation - Equal Channel Angular Pressing (ECAP) was proposed for consolidation purposes. Consolidation was illustrated on two different kinds of hard-to-compact materials - ultra-fine 1,3 μm Al 99,7 % gas atomized powder and AlFe2V4 melt-spun ribbons (MSR). ECAP provides high level of shear stresses without change of cross-section of compacts. Minimized redundant normal stresses leads to significant reduction of total pressing loads. The experiments have shown that the pressure during ECAP consolidation of studied materials was at least 3 times lower if compared with pressures attained in DE (at ratio of 11:1) at the same temperatures. From the other perspective, lower pressing loads allowed significant decrease of pressing temperature from 500°C (DE) to "safe" 200°C (ECAP). To apply shear strain under homogenous hydrostatic compressive pressure conditions, backpressure was needed to be accommodated in output ECAP channel.

ECAP of 1,3 μm Al 99,7 % powder yielded sound compacts consisting of ultra-fine elongated grains (transversal grain size ~200 nm) stabilized and strengthened with torn and homogeneously redistributed surface oxide fragments. Relatively high ultimate tensile strength (UTS) up to 310 MPa accompanied with ductility of  $A = \sim 10$  % was attained. High strength values reflect predominant effect of grain boundaries strengthening mechanism. Nanometric oxide dispersions effectively grain pinned compact's microstructures yielding high temperature UTS = 220 MPa at 300°C with excellent structural stability with no detected structural changes observed after 20 hours annealings at 350 °C. Relatively simple processing with excellent high temperature properties make presented material very promising in prospective structural applications in automotive and aircraft industries. Also in a case of hard-to-compact RS Al-Fe-V melt-spun ribbons [3] ECAP enabled their compaction into sound profiles at moderate temperatures of 350 C. No distinctive phase transformations of as-received MSR took place during ECAP. Microstructure of sound compacts was formed by  $\alpha$ -Al grains, randomly oriented spherical icosahedral particles with diameters mostly not exceeding 100 nm and small amount of Al<sub>10</sub>V intermetallic phase (also present in as-received MSR). ECAP led to full devitrification of amorphous phase traced in small amount within as-received MSR.

In this study ECAP as a consolidation technique has shown its great feasibility in consolidation of rapidly solidified high strength Al particles without danger of undesired structural changes during consolidation.

## References:

- [1] A. Inoue, H. Kimura, Mater. Sci. Eng. A 286 (2000) 1–10
- [2] M. Balog, J. Nagy, K. Iždinský, F. Simančík, Int. J. Mat. & Product Tech., Vol.23, Nos.1/2, (2005) 70-78
- [3] J. Nagy, M. Balog, K. Iždinský, F. Simančík, P. Švec, D. Janičkovič, J. Mat. & Product Tech., Vol.23, Nos.1/2, (2005) 79-90

## **Influence of Surface Properties on Determination of RQ Ribbon's Magnetic properties**

P.Butvin, B.Butvinová, Y.Halahovets, P.Šiffalovič

*Institute of Physics, SASc, Bratislava, Slovakia*

The surfaces of ribbons rapidly quenched on air more or less differ from the ribbon interior as a rule. Oxidic, hydroxidic and more complex contaminations are often observed on the surfaces by sensitive methods as XPS [1, 2]. This chemical surface-interior difference does not simply disappear during thermal treatment of an as-cast ribbon; it merely transforms and variably affects the interior too. The chemical difference manifests most after a non-vacuum anneal. It mainly results in affecting the structural transformation (partial crystallization) and implicitly also leads to specific contribution to the magnetic anisotropy.

The surfaces are rather rough [3] and this feature hardly changes during a standard annealing, be it performed in vacuum or in inert gas. Apart from influencing the effective magnetic anisotropy by stray fields, the roughness sometimes challenges optical methods used just to see the surface properties – e.g. Magneto-Optical Kerr Effect. It works fine with specular reflection but the diffuse reflection from a rough surface cuts down the intensity which reaches the detector and provides further obstacles which are treated in this work.

Being different, the surfaces can exert force on the interior (and vice versa). This is specifically significant for magnetostrictive materials, thus it concerns the majority of compositions used to prepare magnetic ribbons. As the tensile strength of the former majority amounts at least 200 MPa even after nanocrystallization, so some 2 $\mu$ m thick surface layers can exert 50 MPa on the interior of 20  $\mu$ m thick ribbon without breaking the surfaces. This is by far enough to induce a hard-ribbon-axis anisotropy by magnetoelastic interaction in a positively magnetostrictive ribbon whose surfaces squeeze (although not necessarily isotropic, the compressive stress is bi-axial in-plane one) the interior.

To illustrate the above measurement and interpretation problems, surface and volume hysteresis loops, loops observed at emulated biaxial squeeze and domain structures of Finemts and/or Hitperms are presented and discussed.

[1] S.P. Chenakin, M.A. Vasylyev, N. Kruse, A.B. Tolstogouzov, Surf. Interface Anal. 38 (2006) 1164.

[2] R.Jain, N.S.Saxena, K.V.R.Rao, D.K.Avasthi, K.Asokan, S.K.Sharma, Mat.Sci.Eng. A297 (2001) 105.

[3] M.Paluga, P.Švec, D.Janičkovič, P.Mrafko, C.F.Conde, J. Non-Cryst. Solids 353 (2007) 2039.



## Characterization of Hollow and Bamboo-Like Carbon Nanofibers

J. Dusza, L. Hegedúšová, Z. Bastl, J. Morgiel, P. Švec

Hollow carbon micro/nanofibers prepared by Catalytic Chemical Vapor Deposition have been characterized using scanning electron microscopy (SEM), transmission electron microscopy (TEM), high resolution electron microscopy (HREM) and electron spectroscopy for chemical analysis (ESCA). The dimensions, morphology of the fibers, the crystal structure and graphic layers arrangement and the chemical composition of their surface have been investigated. Two type of fibers have been identified; pipe – shaped and bamboo – shaped fibers. The pipe – shaped fibers are usually defects free and consist from distinct sandwich of graphite layers parallel to the fiber axes. The bamboo – shaped fibers often contains defects at the nano-level, their walls are built from domains with different crystalline structures. The fibers contains 99.05 at.% graphic and 0.95 at.% oxygen with the binding energy of O (1s) electrons of 532.7 eV which corresponds to carbon in C-O bonds.

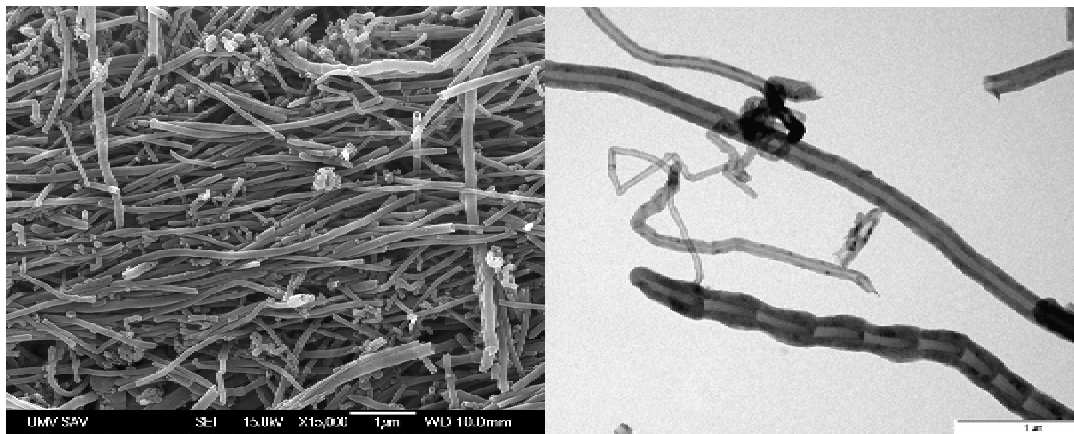


Fig. 1 SEM (a) and TEM (b) of carbon nanofibers

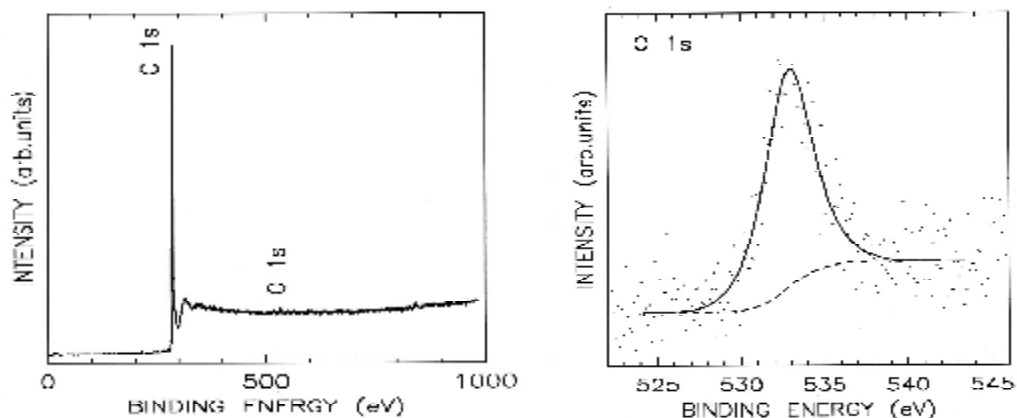


Fig. 2 Survey spectra of the carbon and oxygen

# Detection of the DNA hybridization using a thickness shear mode method. Effect of the oligonucleotide chain length and position of complementary DNA sequence

<sup>1</sup>Viktor Gajdoš, <sup>1</sup>Tibor Hianik, <sup>2</sup>Hana Drahovská, <sup>2</sup>Ján Turňa, <sup>3</sup>Agnieszka Kochman, <sup>3</sup>Włodzimierz Kutner, <sup>4</sup>Pankaj Vadgama

<sup>1</sup>FMFI UK, Bratislava, Slovakia, <sup>2</sup>PriFUK, Bratislava, Slovakia, <sup>3</sup>Institute of Physical Chemistry, Polish Academy of Sciences, Warsaw, Poland, <sup>4</sup>IRC in Biomedical Materials, Queen Mary & Westfield College, London, UK

We studied properties of the genosensor composed of 19-mer biotinylated single stranded oligonucleotide (ODN) with the nucleotide sequence corresponding to that of the *fimC* gene fragment of *Salmonella typhimurium*. This probe was immobilized onto the gold surface of the quartz crystal through avidin. The hybridization process was studied by means of the thickness shear mode method (TSM), that allowed us to determine changes of the resonant frequency of the crystal oscillation,  $\Delta f$ , and the motional resistance,  $R_m$ . The changes of  $\Delta f$  are connected with the changes of mass and also with contribution of the friction between biolayer and the surrounding buffer. The  $R_m$  value allowed us to determine contribution of the friction. The sensor selectively detects the target short chain 19-mer complementary oligonucleotides corresponding to the Salmonella gene as revealed by decrease of the oscillation frequency. No changes of frequency were observed following addition of target 19-mer with sequences characteristic to either *Campylobacter jejuni* or *Listeria monocytogenes*. However, addition of the relatively long 454-mer ODN inside which

the characteristic 19-mer gene were incorporated resulted in frequency changes much lower than one would expect for tight adsorption of the target to the sensor surface. The decrease of resonant frequency was accompanied by increase of the  $R_m$  value. The increase of the motional resistance suggests increased contribution of viscous forces. After approx 200 min a buffer flow was used to remove not hybridized molecules from the surface. As it is seen from the Fig. 1, this resulted decrease of  $R_m$  and increase of  $\Delta f$ . The model 30-mer ODN was used to investigate in

more detail the role of the position of complementary (10-mer) sequence for hybridization at surfaces. It has been shown, that for optimal hybridization the complementary sequence should be at the marginal part of long ODN.

## Acknowledgement

This work was supported by Slovak Grant Agency (Project No. 1/4016/07) and by Agency for Promotion of Research and Development, project No. APVT-51-013904.

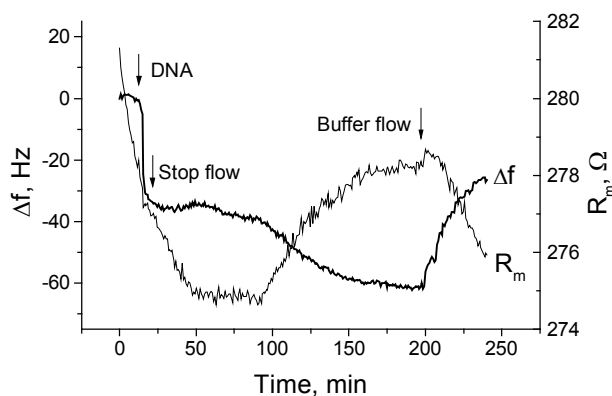


**Fig. 1** The changes of resonant frequency,  $\Delta f$ , and motional resistance,  $R_m$ , following addition of long 454-mer DNA and under buffer flow.

## Contact strength of Si<sub>3</sub>N<sub>4</sub>+SiC nanoceramics

<sup>1</sup>L. Hegedüsová, <sup>1</sup>J. Dusza, <sup>2</sup>M. Hnatko, <sup>2</sup>P. Šajgalík

<sup>1</sup>*Institute of Materials Research, Slovak Academy of Sciences, Košice, Slovak Republic*

<sup>2</sup>*Institute of Inorganic Chemistry, Slovak Academy of Sciences, Bratislava, Slovak Republic*

The paper deals with an investigation of strength of Si<sub>3</sub>N<sub>4</sub>+SiC based nanoceramics using two measuring techniques to include the opposite-sphere contact and four-point bending strength tests. Four-point bending strength was measured on specimens with different effective volumes and Weibull statistical analysis has been used for characterization of the strength values in the form of characteristic strength and Weibull modulus. The characteristic strength of the investigated nanocomposite was  $\sigma_0 = 675$  MPa and  $\sigma_0 = 832$  MPa with the Weibull modulus of 6,4 and 8,6. Contact strength of the investigated material was carried out using sphere on sphere and the obtained results are  $\sigma_{0S} = 1997$  MPa and  $m_S = 17,1$ . Additionally, cone cracks with similar size studied by the optical microscopy are formed during the contact strength test to control the Weibull's parameter and fracture. Lower radius of the spheres results in longer cone cracks and lower angle between the cracks and a sample surface, and vice versa. Finally, the Weibull parameter within the bending test is controlled by volume defects to result in significant strength degradation.

**Keywords:** Si<sub>3</sub>N<sub>4</sub>+SiC nanoceramics, bending strength, contact strength, Weibull's modulus, cone cracks.

## **Si<sub>3</sub>N<sub>4</sub>/SiC nanocomposite prepared by the addition of SiO<sub>2</sub> + C by hot pressing and gas pressure sintering methods**

M. Hnatko, Š. Lojanová, P. Šajgalík,

*Institute of Inorganic Chemistry, SAS, Bratislava, Slovakia*

The Si<sub>3</sub>N<sub>4</sub>/SiC nanocomposite with yttria and alumina as sintering additive was prepared by hot pressing and gas pressure sintering methods. The influence of carbon adds to the starting mixture on final densities and creation SiC nano-inclusions by carbothermal reduction of silica during sintering process were investigated. The final density of this way prepared sample was 99 % of the theoretical value calculated by the rule of mixtures. The microstructure and mechanical properties at room temperature of both samples were investigated.

## Phase transformations of Co-enhanced Finemet amorphous ribbons based on resistance-temperature correlation

T. Papaioannou<sup>1</sup>, P. Svec<sup>2</sup>, D. Janickovic<sup>2</sup>, E. Hristoforou<sup>1</sup>

<sup>1</sup>National Technical University of Athens, Iroon Polytechniou 9, Athens 15780, Greece

<sup>2</sup>Slovak Academy of Sciences, Bratislava, Slovakia

Phase transformations of  $(\text{Fe}_{1-x}\text{Co}_x)_{73.5}\text{Cu}_1\text{Nb}_3\text{Si}_{13.5}\text{B}_9$   $\{x=0, 0.5, 1\}$  amorphous ribbons, produced by the melt-spinning technique, were studied using resistivity to temperature  $R(T)$  at several heating rates. Differential scanning calorimetry (DSC) measurements were also performed at 10K/min and 40K/min heating rates. Isothermally annealed ribbons at various temperature-time sets were investigated with XRD, showing the previous amorphous condition and the resulted crystallized material. The nanostructured grains have been observed by transition electron microscopy (TEM).

The master alloys were produced by induction melting in vacuum furnace. Ribbons were cast with the planar flow technique under Ar atmosphere inside a quartz tube, through a ceramic nozzle and cooled over a spinning copper wheel. Ribbon dimensions were 6mm in width and  $\sim 25\mu\text{m}$  in thickness.  $R(T)$  at 2.5, 5, 10, 20, and 40 K/min heating rates took place (see Figure 1). The results demonstrated phase transformations, by means of the relative resistivity value drop over temperature (K). During cooling, the resistivity values are linearly proportional to temperature from 1000K to 300K, clearly indicating that the crystallization process had been completed during the heating step. DSC diagram (Figure 2), regarding the same ribbon verified the phase transformations observed by  $R(T)$ .

XRD response of the as-quenched ribbons illustrated the presence of the amorphous phase for all three compositions. The ribbons were exposed to 773, 823, 873 and 923 K for 30min, inside a vacuum chamber (approximately  $10^{-4}$  torr) and the obtained XRD response indicated the crystalline phase transformation. Figure 3 demonstrates the crystalline phase transformation concerning the  $(\text{Fe}_1\text{Co}_1)_{73.5}\text{Cu}_1\text{Nb}_3\text{Si}_{13.5}\text{B}_9$  composition. TEM micrographs (Figure 4) illustrated the nano-crystalline nature of the crystalline transformation (the given sample was treated at 823 K for 30min).

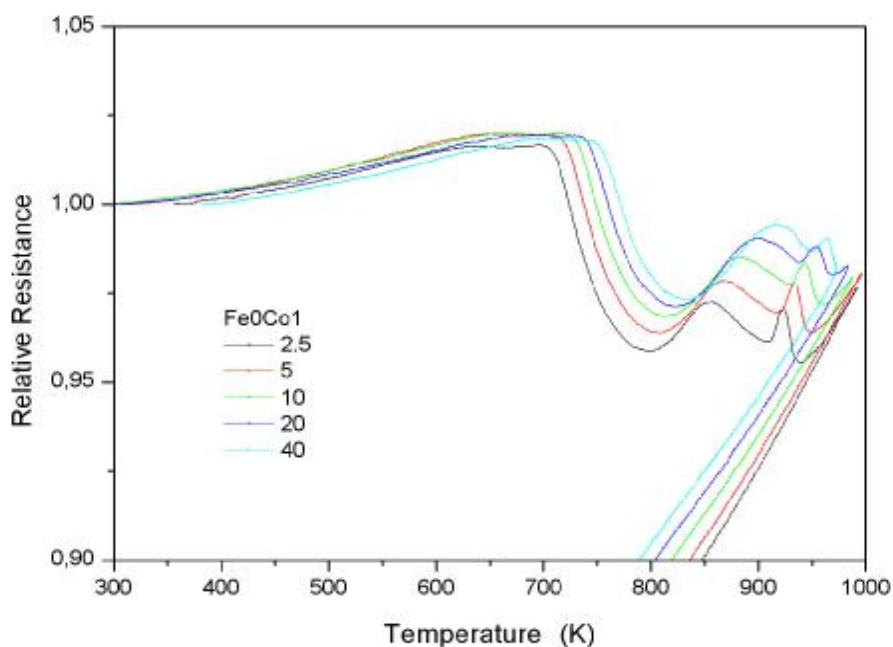


Fig. 1.  $R(T)$  for several heating rates (K/min) concerning a  $\text{Co}_{73.5}\text{Cu}_1\text{Nb}_3\text{Si}_{13.5}\text{B}_9$  ribbon.

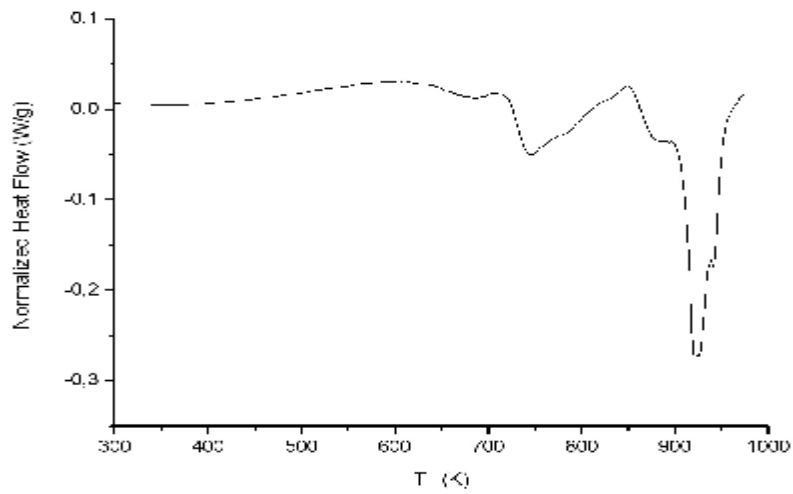


Fig.2. DSC response of  $\text{Co}_{73.5}\text{Cu}_1\text{Nb}_3\text{Si}_{13.5}\text{B}_9$  ribbon at 10 K/min in Ar atmosphere.

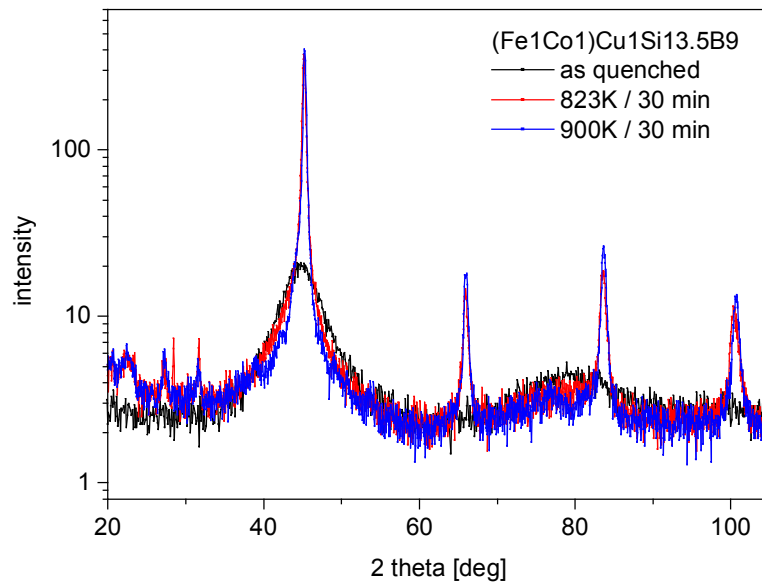


Fig.3. XRD measurements with ribbons parallel to x-rays.

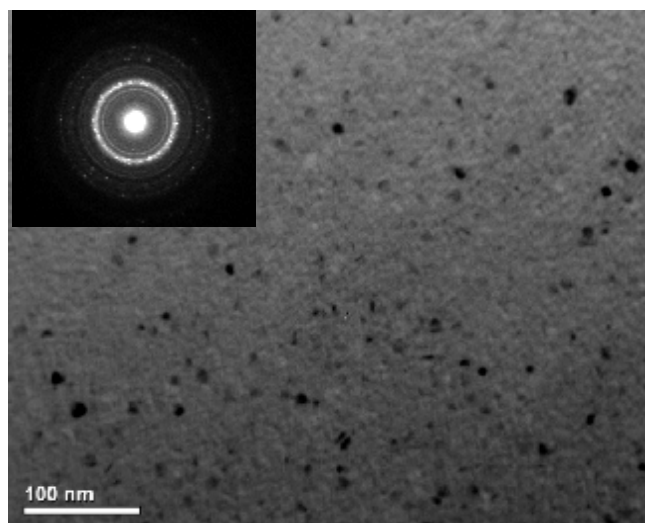


Fig.4. TEM micrograph after thermal treatment, illustrating nano-crystallization.

## **Microstructure and mechanical properties of silicon carbide based ceramics**

<sup>1</sup>A. Kovalčíková, <sup>1</sup>J. Dusza, <sup>2</sup>M. Balog, <sup>2</sup>P. Šajgalík

<sup>1</sup>*Institute of Materials Research, SAS, Watsonova 47, 043 53 Košice, Slovak Republic*

<sup>2</sup>*Institute of Inorganic Chemistry, SAS, Dúbravská cesta 9, 845 36 Bratislava 45,  
Slovak Republic*

The influence of the microstructure of liquid phase sintered and heat treated SiC+Si<sub>3</sub>N<sub>4</sub> composites and monolithic SiC ceramics on their mechanical properties, namely Young's modulus, Vickers hardness, indentation fracture toughness, flexural strength and thermal shock resistance was investigated. The hardness and the fracture toughness were determined by Vickers indentation method and Young's modulus was measured by resonance frequency method. Flexural strength measurement was performed by means of four-point bend testing. The characteristic flexural strength was increasing with silicon nitride content. Fractographic analysis of broken flexural specimens was used to characterize the fracture initiation origins. The strength of the investigated materials was degraded by the present processing flaws in the form of pores and clusters of pores. The fracture toughness was enhanced by changing the SiC grains size and aspect ratio after the heat-treatment at 1850°C/5 h. The main toughening mechanisms of crack deflection, crack bridging and crack branching are responsible for the toughness improvement.

Keywords: SiC ceramics, SiC+Si<sub>3</sub>N<sub>4</sub> composites, microstructure, flexural strength, Vickers hardness, indentation fracture toughness

# Effect of various types of polypropylene matrices on properties of carbon nanotubes-containing nanocomposites

Matej Mičušík,<sup>1</sup> Mária Omastová,<sup>1</sup> Igor Krupa,<sup>2</sup> Petra Pötschke,<sup>2</sup> Jürgen Pionteck,<sup>2</sup>  
Polycarpos Pissis,<sup>3</sup> Fahad S al Mubaddel<sup>4</sup>

<sup>1</sup> Polymer Institute, Slovak Academy of Sciences, Dúbravská cesta 9, 842 36 Bratislava, Slovakia

<sup>2</sup> Leibniz Institute of Polymer Research Dresden, Hohe Str. 6, 01069 Dresden, Germany

<sup>3</sup> Department of Physics, National Technical University, Zografou Campus, 157 80 Athens, Greece

<sup>4</sup> Department of Chemical Engineering, College of Engineering, King Saud University Riyadh, Saudi Arabia

Carbon nanotubes (CNT) have drawn attention due to their extraordinary electrical, mechanical and thermal properties, which make from CNT a very promising material in many applications. Also thermoplastic composites research is trying to exploit the exceptional properties of CNT for preparation of new materials [1]. However, when CNT are used as the nanofiller in thermoplastic matrices, problems appear with dispersion and agglomeration of CNT and compatibility with the polymeric matrix during the processing. One way to solve these problems is the surface modification of CNT with functional groups [2] or coating with conductive polymers [3].

In this work the dilution of a commercial polypropylene masterbatch containing 20 wt.% CNT (Hyperion, USA) by various types of polypropylene (PP) matrices was used for preparation of nanocomposites. Maleinated PP (PP-MA) as well as unmodified PP matrices with different melt flow indexes (MFI = 2, 8, 12 g/10 min.) were used. Since CNT act as nucleating agent, their presence influenced the crystalline morphology of the polymer and consequently the physical and mechanical properties of prepared composites. These properties are also influenced by the polymer/CNT interfaces, which render the dispersion of the filler in polymer matrix. Therefore crystallization kinetics, thermal, rheological, and mechanical properties of the composites as functions of PP-type and CNT content were studied. Phenomena of charge transport in composites below and above percolation threshold are reported.

PP-MA matrices show enhanced interaction with CNT, what is reflected as the strongest increase of the Young's modulus with increasing CNT content. The lowest conductivity percolation threshold of around 2 wt. % CNT was found when using PP-MA with MFI = 2. We observed a shift in crystallization and melting to higher temperatures by increasing the amount of CNT. The increase of crystallization rate was more pronounced by PP-MA matrix with MFI = 8. The quality of crystallites was the best in the nanocomposites prepared using PP-MA MFI = 2. In samples with unmodified PP matrices the effect of CNT on the melting behaviour is less pronounced.

*Acknowledgement.* The research was supported by German-Slovak bilateral project "Electrical conductive nanocomposites" (D/05/15215) and by project of the Scientific Grant Agency of the Ministry of Education of Slovakia and the Slovak Academy of Sciences (VEGA 2/7103/27).

## References

1. McIntosh D, Khabashesku VN, Barrera EV. *Chem Mater* **18** (2006) 4561.
2. Kyotani T, Nakazaki S, Xu WH, Tomita A. *Carbon* **39** (2001) 782.
3. Fan J., Wan M, Zhu D, Chang B, Pan Z, Xie S. *Synth Met* **102** (1999) 1266.

# Research and Development of Electrotechnical Applications of Nanocrystalline Materials

<sup>1</sup>Jozef Kuchta, <sup>1</sup>Marek Franko, <sup>1</sup>Miroslav Fulier, <sup>2</sup>Peter Švec, <sup>3</sup>Jan Bydžovský

<sup>1</sup> *Electrotechnical Research and Projecting Company, j.s.c;*  
*Trenčianska 19, SK-018 51 Nová Dubnica, Slovakia*  
*e-mail: [kuchta@evpu.sk](mailto:kuchta@evpu.sk), [fulier@evpu.sk](mailto:fulier@evpu.sk)*

<sup>2</sup> *Institute of Physics, Slovak Academy of Sciences, 845 11 Bratislava, Slovakia*

<sup>3</sup> *Faculty of Electrical Engineering and Information Technology, Slovak University of Technology, 812 19 Bratislava, Slovakia*

The paper presents series of 8 to 40kVA transformers based on nanocrystalline cores from material of the Vitroperm 500F and Fy.type. Power electronics is one of important application fields of nanocrystalline materials (NCM); most common exploitation of these materials in magnetic circuits can be seen from the typical scheme of the frequency converter for switching mode power supply, see Fig. 1. Transformers and choke coils are representative parts of magnetic circuits in the switching mode power supplies as shown by dashed lines in Fig.1.

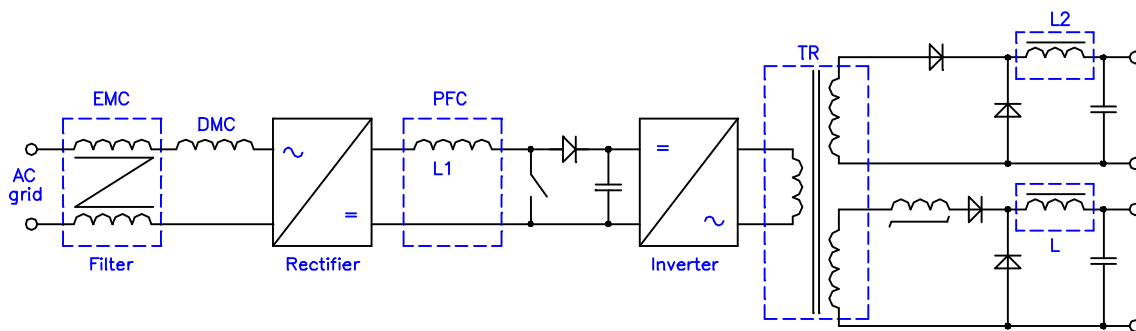


*Fig. 1: Principal scheme of frequency converter with represented magnetic circuits*

As magnetic circuits are essential functional parts of converters, their size, losses [W], weight and optimal design are of utmost importance. One of the most important features of these magnetic circuits is their operation in most cases with non-sinusoidal voltage and current and in frequency interval from 50 Hz to 20 (40) kHz.

Availability of various materials for appropriate frequency interval and their specific price (price for weight unit) will be presented.

R&D work was oriented on the development of transformers series based on nanocrystalline cores Vitroperm 500F produced by fy. Vaccumschmelze and by their equivalents prepared at the Institute of Physics SAS for these applications. The properties of both material types will be compared.



*Fig. 2: Representative samples of the developed transformer series*



*Fig. 3: Nanocrystalline core before (left) and after filling (right).*

### **Acknowledgement**

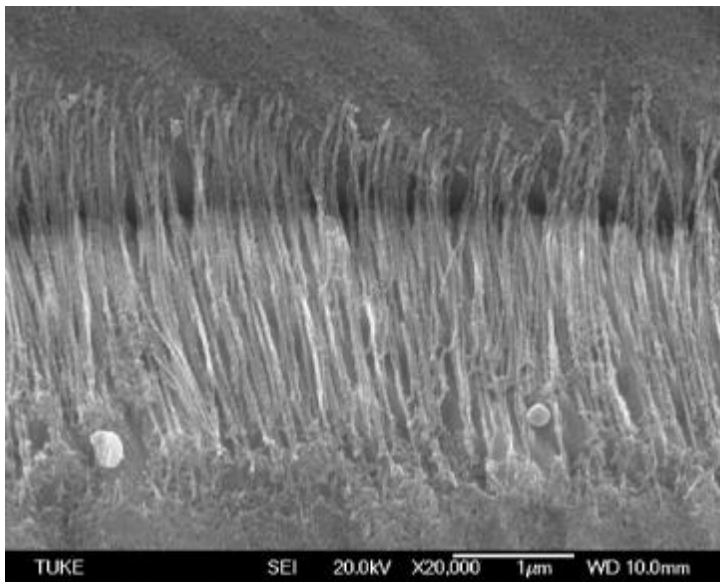
This work was supported by the Slovak Research and Development Agency under the contract No. APVT-99-017904.

## Preparation of nanorods Fe by precipitation from solid solution

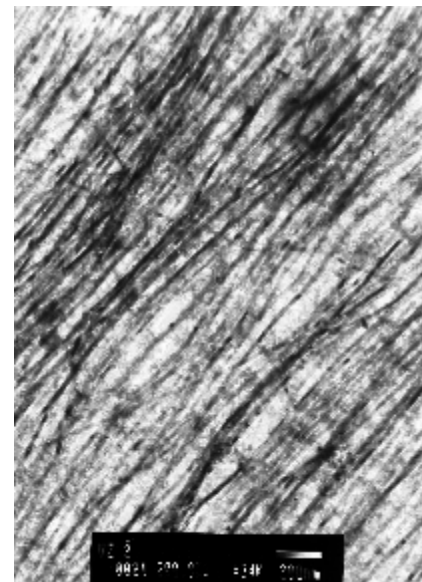
*S.Longauer, O. Milkovič, G.Janák*  
*Technical University of Košice*

Nanowires (*NW*) or nanorods (*NR*) of Fe have wide potential applications but most important one is probably in ultra high-density magnetic storage devices. Requirement is small diameter of *NR*, high aspect ratio to give anisotropic magnetic response and high density of perpendicular *NR*.

Variety of methods which fabricate such *NR* have been reported : infiltration of iron to carbon nanotubes [1], decomposition of ferrocene [2,3] electrochemical coating of nanoporous templates [4], decomposition of iron pentacarbonyl in magnetic field [5] or spontaneous decomposition of  $\text{La}_{1-x}\text{Sr}_x\text{FeO}_3$  with perovskite structure [6]. From our research results and references [7] is known that in CuFe alloys after some treatment the discontinuous precipitation of Fe *NRs* from Cu matrix appears. The *NRs* have dimensions, morphology and density very similar to *NRs* fabricated in mentioned methods. In submitted article there are results which show that extraction of Fe *NW* or *NR* from Cu matrix is possible and details of extraction process are in [8]. It is concluded that controlled discontinuous precipitation of Fe *NR* from solid solution can be competitive cheap method for preparation of self assembled *NR* for magnetic storage devices.



Discontinuous precipitation of Fe *NR*, SEM



Extracted Fe *NR* to carbon replica, TEM

### Referencies

- [1] P.M.Ajayan, S.Iijima, *Nature*, 1993, 361,333, [2] S.Hampel et al, *Carbon*, 2006, [3] F.Geng, H.ong, *Physica B*, 382, 2006, 300, [4] Cai-Ling Xu et all. *Materials Letters*, 60,2006, 2335, [5] G.H.Lee et al., *Scripta Mat.*49, 2003,1151, [6] L.Mohaddes –Ardabili et al., *Nature Materials*, 2004,3, 533, [7] S.Saji, S.Hori, G.Mima, *Trans.Jap.Inst.Met*, 1973, 14,82, [8] O.Milkovič- PhD thesis , TU Košice, 2007

## Effect of field annealing on magnetic anisotropy and coercivity in nanocrystalline Fe-Co-M-B-(Cu) (M=Zr, Mo) alloys

<sup>1</sup>Jozef Marcin, <sup>1</sup>Jana Turčanová, <sup>2</sup>Peter Švec and <sup>1</sup>Ivan Škorvánek

<sup>1</sup>*Institute of Experimental Physics, Slovak Academy of Sciences, Watsonova 47,  
040 01 Košice, Slovakia*

<sup>2</sup>*Institute of Physics, Slovak Academy of Sciences, Dúbravská cesta 9, 842 28 Bratislava, Slovakia*

The technological driving force behind this study is the optimization of the alloy composition and heat treatment process in order to obtain HITPERM-type nanocrystalline materials with improved soft magnetic properties. A special attention has been devoted to the study of the effects of annealing under presence of external magnetic field in order to produce controllable uniaxial anisotropy in the samples. We report on the effects of both longitudinal and transverse magnetic field applied during the heat treatment on the magnetic behavior of two alloys with the composition  $\text{Fe}_{44.5}\text{Co}_{44.5}\text{Zr}_7\text{B}_4$  and  $\text{Fe}_{38}\text{Co}_{38}\text{Mo}_8\text{B}_{15}\text{Cu}$ . Sheared loops with good field linearity were achieved for all investigated alloys after annealing in transverse magnetic field. The stronger response to the transverse field-annealing is observed for the alloy containing Zr. Here, the induced anisotropy values up to  $K_u \sim 1250 \text{ Jm}^{-3}$  can be reached. A heat treatment under the presence of longitudinal magnetic field results for the Mo-containing samples in squared hysteresis loops characterized by coercive field values in the range of 3 - 8  $\text{Am}^{-1}$ , which are lower than those reported for field annealed FeCoNbB-based alloys [1]. Such characteristics tailorable by field-annealing are of particular interest for various sensors and high frequency application devices.

[1] ŠKORVÁNEK I. - MARCIN J. - KRENICKÝ T. - KOVÁČ J. - ŠVEC P. – JANIČKOVIČ D.: Improved soft magnetic behaviour in field-annealed nanocrystalline Hitperm alloys, *Journal of Magnetism and Magnetic Materials* 304, (2006) 203-207.

## Effect of pressure on magnetic properties of $\text{TM}_3[\text{Cr}(\text{CN})_6]_2 \cdot n\text{H}_2\text{O}$ nanoparticles

A. Zentko<sup>1</sup>, M. Zentková<sup>1</sup>, Z. Arnold<sup>2</sup>, M. Cieslar<sup>3</sup>, J. Kamarád<sup>2</sup>, V. Kavečanský<sup>1</sup>, S. Mařaš<sup>1</sup>,  
M. Mihalik<sup>1</sup>, Z. Mitróová<sup>1</sup>, and V. Zeleňák<sup>4</sup>

<sup>1</sup>*Institute of Experimental Physics SAS, Watsonova 47, 040 01 Košice, Slovakia*

<sup>2</sup>*Institute of Physics of the AS CR, v.v.i., Na Slovance 2, 182 21 Prague 8, Czech Republic*

<sup>3</sup>*Charles University, Ke Karlovu 5, 121 16 Prague 2, Czech Republic*

<sup>4</sup>*P.J.Šafárik University, Moyzesova 11, 04154 Košice, Slovakia*

In the last few years, there has been considerable interest in preparation and investigation of magnetic nanoparticles (NAP) because of their potential applications in high density recording media, but also for the reasons as macroscopic tunneling and quantum computing. After discovery of single – molecule magnet behavior in  $\text{Mn}_{12}$ -acetate with highest spin ground state  $S = 51/2$  one of the important issue of magnetism is the study of objects with magnetic moments intermediate between this value and the value of metallic NAP with  $S \geq 1000$ . NAP based on Prussian blue analogues (PBA) prepared by reverse micelle technique with  $S < 1000$  are promising candidates.

NAP based on  $\text{Mn}_3[\text{Cr}(\text{CN})_6]_2$  and  $\text{Ni}_3[\text{Cr}(\text{CN})_6]_2$  Prussian blue analogues (PBA) were prepared by reverse micelle technique. The prepared particles were characterized by infrared spectroscopy (IRS), X-ray powder diffraction technique and electron transmission microscopy (TEM). Results of IRS confirmed PBA and presence of AOT surfactant. TEM images show nanoparticles with average diameter of about 3.5 nm covered by AOT in both cases. The characteristic X-ray peaks of PBA are more diffused and wither. The average size 4.5 nm of NAP determined from X-ray measurements corresponds with TEM results. Magnetization measurements  $M(H)$ ,  $M(T)$  in zero field cooling (ZFC) and field cooling (FC) regime and AC susceptibility measurements were performed by commercial SQUID magnetometer. The Curie temperature  $T_C$  is reduced from  $T_C = 56$  K for Ni-PBA to  $T_C = 21$  K for Ni- NAP system and from  $T_C = 65$  K for Mn-PBA to  $T_C = 38$  K for Mn- NAP system. In our present paper we focus on study of pressure effect (up to 1.2 GPa) on magnetic properties of Ni-NAP and Mn-NAP. Applied pressure leads to the remarkable increase of  $T_C$  for Mn-PBA ( $\Delta T_C/\Delta p = +13$  K/GPa) and to only slight decrease of  $T_C$  for Ni-PBA ( $\Delta T_C/\Delta p = - 3$  K/GPa).

## Surface morphology in amorphous Fe-Mo-Cu-B ribbon system contribution

<sup>1\*</sup>M. Paluga, <sup>1</sup>P. Švec, <sup>1</sup>D. Janičkovič, <sup>1</sup>P. Mrafko

<sup>1</sup>*Institute of Physics, Slovak Academy of Sciences, Bratislava, Slovakia*

Ribbons of  $(\text{Fe-Co})_{79}\text{Mo}_8\text{Cu}_1\text{B}_{12}$  with Co/Fe ratio of 0, 1/12, 1/9 and 1/3 were prepared in amorphous state in form of ribbons ~20 microns thick and 6mm wide by planar flow casting method. The as-quenched state of the samples was checked by X-ray and electron diffraction. Magnetoresistance and magnetoimpedance measurements were performed on as quenched samples. Sample surfaces were analyzed using confocal microscopy. The effect of variation of Co/Fe ratio and temperature of the master alloy melt was investigated with respect to the values of micro-roughness. Samples were also investigated for surface texture of eventual quenched-in crystalline phases by X-ray diffraction; the presence of texture was observed in certain cases, disappearing with increasing Co-content. The correlation between as-quenched structure, magnetic properties, micro-roughness parameters, sample composition and master alloy melting temperature is discussed.

## Kinetics of crystallization in the Fe<sub>79</sub>Mo<sub>8</sub>Cu<sub>1</sub>B<sub>12</sub> amorphous alloy by synchrotron radiation

<sup>1</sup>M. Pavúk, <sup>1,2</sup>M. Miglierini, <sup>1</sup>T. Kaňuch, <sup>3</sup>P. Švec, <sup>3</sup>D. Janičkovič, <sup>4</sup>G. Schumacher, <sup>5</sup>I. Zizak

<sup>1</sup>*Slovak University of Technology, Bratislava, Slovakia*

<sup>2</sup>*Nanomaterials Research Centre, Olomouc, Czech Republic*

<sup>3</sup>*Institute of Physics, SAS, Bratislava, Slovakia*

<sup>4</sup>*Hahn-Meitner-Institute, Berlin, Germany*

<sup>5</sup>*BESSY, Berlin, Germany*

*In situ* X-ray diffraction using synchrotron radiation and *ex situ* atomic force microscopy were used to investigate the nanocrystallization of as-quenched Fe<sub>79</sub>Mo<sub>8</sub>Cu<sub>1</sub>B<sub>12</sub> (at.%) metallic alloy. This material belongs to the family of the Fe-*M*-B-(Cu) alloys (*M*=Zr, Nb, Hf, ...), called also NANOPERM. Continuous thin (thickness 20-22 μm) glassy metal strip was produced in air by the planar flow casting method. The evolution of the relative volume fraction of crystalline and amorphous phase was obtained from the diffraction line profile analysis of a region around (110) collected in the high-temperature range up to 600 °C during continuous heat treatment. The alloy was found to be not completely amorphous. The analysis of measurements has shown that a small amount (~ 8%) of crystalline phase is situated near the side of the ribbon, which has been in contact with the rotating wheel during production of the ribbon. This phenomenon occurs at the side, which has been subjected to a (theoretically) much better cooling conditions and thus higher cooling rate and, therefore, at the opposite side as one might expect. In addition, crystallization starts earlier at this side of the investigated ribbon.

This work was financially supported by the grants VEGA 1/4011/07, 2/5096/27, MSM6198959218, APVT 20-008404, and EC grants under IA-SFS contract RII 3-CT-2004-506008.

## Formation of nanostructures using different routes

<sup>1\*</sup>Gabriela Popescu, <sup>1</sup>Liana Vladutiu, <sup>2</sup>Mariana Lucaci, <sup>3</sup>I.Badoi

<sup>1</sup>University „POLITEHNICA“ of Bucharest, Romania

<sup>2</sup>National R&D Institute ICPE-CA, Bucharest, Romania

<sup>3</sup>INTEC SA, Bucharest, Romania

### Abstract

Over the past decade nanomaterials have been a subject of huge interest. These materials are notable for their extremely useful properties: exceptionally strong, hard and ductile at high temperatures, resistance to wear, erosion and corrosion, and chemically very active, and processed by different methods. Among synthesis techniques used for process these materials are:

- ✓ sol-gel route,
- ✓ plasma route,
- ✓ thermal spray processing,
- ✓ hydrothermal processing,
- ✓ high-energy ball milling,
- ✓ electrodeposition,
- ✓ other chemical and physical techniques.

The paper aim of the paper is to present a comprehensive review of these techniques used for obtain nanoscale particles or powders with positive implications for many industries, such as chemical, paint, paper, glass, cosmetic, metal, computer, pharmaceutical and biomedical – just to name a few. A special attention will be given to processing of nanostructured materials and composites using chemical and solid state routes.

**Keywords:** nanoscale particles, nucleation and growth from solution, mechanical attrition, ball milling

## Carbon nanotubes added hexagonal WO<sub>3</sub> films for sensing applications

<sup>1,4\*</sup> *Katarína Sedláčková*, <sup>2</sup> *Radu Ionescu*, <sup>3</sup> *Csaba Balázs*

<sup>1</sup> *Thin Film Physics Laboratory, Research Institute for Technical Physics and Materials Science, HAS, Konkoly-Thege M. út. 29-33, 1121 Budapest, Hungary*

<sup>2</sup> *Universitat Rovira i Virgili, ETSE-DDEEA, Campus Sescelades, Av. Països Catalans 26, E-43007 Tarragona, Spain*

<sup>3</sup> *Ceramics and Composites Laboratory, Research Institute for Technical Physics and Materials Science, HAS, Konkoly-Thege M. út. 29-33, 1121 Budapest, Hungary*

<sup>4</sup> *Institute of Electrical Engineering, Dúbravská cesta 9, 84101 Bratislava, Slovakia*

A world-wide concern for environmental safety that demands monitoring the emission of hazardous gases into the atmosphere, combined with recent advances in wireless sensor networks is increasing the need of low-power gas sensors and low-cost.

Among metal oxides, between themselves the tungsten oxides are among the most used materials in electro-, photo- and gasochromic applications.

In this work, a soft chemical nanocrystalline processing route has been demonstrated for the preparation of hexagonal tungsten oxides by the acidic precipitation of Na<sub>2</sub>WO<sub>4</sub>·2H<sub>2</sub>O solution at temperatures as low as 120 °C and 330 °C.

The structural properties of films were investigated by TEM Philips CM-20. The sensing properties of films were measured to gaseous ammonia at various temperatures.

We founded the correlation between structure (Fig. 1) and gas sensing properties (Fig. 2) of WO<sub>3</sub> films. The average size of WO<sub>3</sub>·1/3 H<sub>2</sub>O crystallites is ~ 50 ÷ 100 nm. After the heat treatment of films, the average size of WO<sub>3</sub> crystallites decreased to ~ 30 ÷ 50 nm. The electron diffraction of the film confirmed the phase change from orthorhombic to hexagonal one. The gas measurements were performed by direct injection using a gas syringe, and the arrows in the graphics indicate the total amount of gas present in the measurement chamber after successive injections.

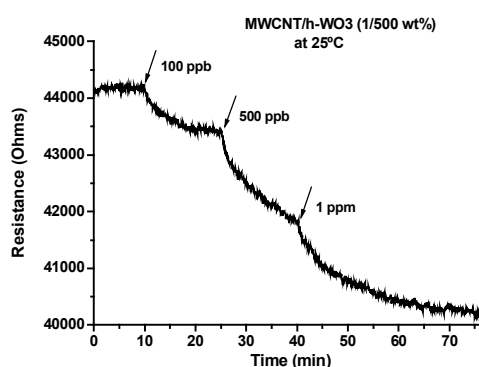
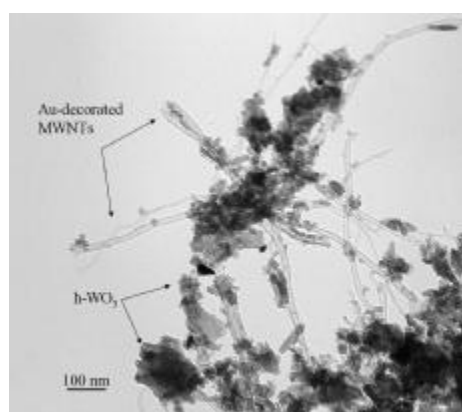


**Figure 1:** TEM image of the heat treatment film with h-WO<sub>3</sub> nanocrystallites with metal (Au) decorated MWCNTs.

**Figure 2:** Resistance change experience of h-WO<sub>3</sub> film with carbon nanotubes in NO<sub>2</sub>.

## Carbon-metal (Ni or Ti) nanocomposite thin films

<sup>1\*</sup>R.O. Grasin, <sup>1,3</sup>K. Sedláčková,  
<sup>2</sup>T. Ujvári, <sup>2</sup>I. Bertóti, <sup>1</sup>G. Radnóczy

<sup>1</sup>*Research Institute for Technical Physics and Materials Science, Hungarian Academy of Sciences, Konkoly-Thege M. út. 29-33, 1121 Budapest, Hungary*

<sup>2</sup>*Research Institute of Materials and Environmental Chemistry, Chemical Research Centre, P.O. Box 17, 1525 Budapest, Hungary*

<sup>3</sup>*Institute of Electrical Engineering, Dúbravská cesta 9, 84101 Bratislava, Slovakia*

Previous works revealed that C-Ni nanocomposite thin films have various structural and mechanical properties depending on preparation conditions [1]. Nanocomposite coatings composed of crystalline and amorphous nanophase mixtures have recently attracted increasing interest with respect to industrial applications as protective coatings [1, 2]. More generally, the use of carbon – metal composite films is aimed to ensure a good adhesion of the films to different substrates, to increase their hardness, modulus of elasticity and improve their wear properties [3].

A comparison between structure and mechanical properties of dc sputtered C-Ni and C-Ti nanocomposite thin films has been made in the growth temperature range of 25-800°C. C-Ni films undergo morphological and phase change at 400°C deposition temperature, while the C-Ti films possess the same phase state and morphological character in the whole range of deposition temperatures. Despite the structural differences the dependence of hardness (H) and elastic modulus (E) on the deposition temperature shows very similar behaviour. The same character of the hardness and modulus curves is mostly influenced by the structure and the morphology of the carbon matrix. The difference in absolute value between the H and E curves of C-Ni and C-Ti could be related to the C-metal bonds, chemical stability and mechanical properties of the corresponding carbide phase. The hardness and reduced elastic modulus of C-Ni and C-Ti nanocomposite films show similar behavior as a function of the deposition temperature in the 25-800°C range displaying a maximum in both properties at 200°C growth temperature.

The similarity of the hardness and elastic modulus as the function of the deposition temperature in C-Ni and C-Ti systems is mostly due to the properties of the carbon matrix. The difference in the absolute values in H and E could be related to the strength of C-Ni and C-Ti bonds. The more strong covalent bonds between C-Ti compared to C-Ni and the thermal stability of TiC compared to Ni<sub>3</sub>C above 400°C can also contribute.

The more steep decrease of the modulus curve in C-Ni compared to the C-Ti above 400°C deposition temperature must be in connection with the changes of the crystalline phase from Ni<sub>3</sub>C to fcc Ni and substantial graphitization of the C matrix in the C-Ni films.

[1] K. Sedláčková, P. Lobotka, I. Vávra, G. Radnóczy, Structural, electrical, and magnetic properties of carbon-nickel composite thin films; Carbon 43 (2005) 2192-2198

[2] Pei YT, Galvan D, De Hosson JThM, Cavaleiro A., Surface Coatings and Technology 2005; 198 (44-50)

[3] Laidani N, Calliari L, Speranza G, Micheli V., Galvaneto E., Surface & Coatings Technology 1998; 100-101:116-124

## Characterization of thin hard films using micro and nano analysis

<sup>1</sup>B. Škorić, <sup>1</sup>D. Kakaš, <sup>2</sup>G. Favaro and <sup>1</sup>A. Miletić

<sup>1</sup>University of Novi Sad, Serbia,

<sup>2</sup>CSM Instruments SA, Peseux, Switzerland

Thin hard coatings deposited by physical vapour deposition (PVD), e.g. titanium nitride (TiN) are frequently used to improve performance in many engineering applications

In this paper, we present the results of a study of TiN films which are deposited by a Physical Vapor Deposition and Ion Beam Assisted Deposition. In the present investigation the samples with duplex coating was studied, and subsequent ion implantation was provided with N<sup>5+</sup> ions. The ion implantation was applied to enhance the mechanical properties of surface. The most successful and widespread model for nanoindentation data analysis is one in which the unloading data are assumed to arise from a purely elastic contact. The form most often used is known as the Oliver and Pharr method.

This paper describes the successful use of the nanoindentation technique for determination of hardness and elastic modulus. In the nanoindentation technique, hardness and Young's modulus can be determined by the Oliver and Pharr method, where hardness (H) can be defined as:  $H = P_{\max}/A$ , where  $P_{\max}$  is maximum applied load, and A is contact area at maximum load. In nanoindentation, the Young's Modulus, E, can be obtained from:  $1/E_r = (1 - \nu^2)/E + (1 - \nu^2)/E_i$ , where  $\nu_i$  = Poisson ratio of the diamond indenter (0.07) and  $E_i$  = Young's modulus of the diamond indenter. Therefore, in recent years, a number of measurements have been made in which nanoindentation and AFM have been combined.

Indentation was performed with CSM Nanohardness Tester. The results are analyzed in terms of load-displacement curves, hardness, Young's modulus, unloading stiffness and elastic recovery. The nanohardness of coating measured by Berkovich indenter is about 42.4 GPa. The analysis of the indents was performed by Atomic Force Microscope. The stress determination follows the conventional  $\sin^2\psi$  method, using a X-ray diffractometer. The analyzed AE signal was obtained by a scratching test designed for adherence evaluation. AE permits an earlier detection, because the shear stress is a maximum at certain depth beneath the surface, where a subsurface crack starts. The critical load Lc2 corresponds to the load inducing the partial delamination of the coating.

Coating is often in tensile stress with greater microhardness. The film deposition process exerts a number of effects such as crystallographic orientation, morphology, topography, densification of the films. The evolution of the microstructure from porous and columnar grains to densel packed grains is accompanied by changes in mechanical and physical properties. A variety of analytic techniques were used for characterization, such as scratch test, calo test, SEM, AFM, XRD and EDAX. Therefore, by properly selecting the processing parameters, well-adherent TiN films with high hardness can be obtained on engineering steel substrates, and show a potential for engineering applications.

The experimental results indicated that the mechanical hardness is elevated by penetration of nitrogen, whereas the Young's modulus is significantly elevated.

The deposition process and the resulting coating properties depend strongly on the additional ion bombardment.

## The properties of affinity biosensors based on nanofabricated surfaces

<sup>1</sup>L. Svobodová, <sup>1</sup>M. Šnejdárková, <sup>2</sup>T. Hianik

<sup>1</sup> *Institute of Animal Biochemistry and Genetics, Slovak Academy of Sciences, Moyzesova 61,  
900 28 Ivanka pri Dunaji, Slovak Republic*

<sup>2</sup> *Department of Nuclear Physics and Biophysics, FMPI CU, Mlynská dolina F1,  
842 48 Bratislava, Slovak Republic*

The specific interaction between the protein immunoglobulin E (IgE) as the analyte and its 45-nt aptamer as immobilized receptor has been measured directly by quartz crystal microbalance (QCM). The mixture of a new class of macromolecule polymer – poly(amidoamine) (PAMAM) dendrimer and the 1-hexadecanethiol was used for the formation of surface on the gold-coated quartz crystal by self-assembly method. PAMAM dendrimers were modified with the neutravidin and immediately conjugated by the biotinylated-DNA aptamer. The detection of human IgE was monitored by measuring of the frequency changes shift. The obtained detection limit was 100 ng/ml of IgE. The complex IgE-aptamer was dissociated by applying 0.1 M glycine-HCl buffer, pH 2.3. The immobilized biotinylated-DNA aptamer can be recognized repeatedly by the specific IgE antibody. As a control for non-specific interactions we used bovine serum albumin (BSA). Interaction of BSA with a sensor surface was negligible.

# $\text{Y}_2\text{Ba}_4\text{CuRuO}_y$ nanoparticles in $\text{YBa}_2\text{Cu}_3\text{O}_{7-\delta}$ bulk superconductors

<sup>1</sup>Šefčíková M., <sup>1</sup>Šuster D., <sup>1</sup>Kavečanský V., <sup>1</sup>Diko P.

<sup>2</sup>Babu H., <sup>2</sup>Cardwell D.

<sup>1</sup>*Institute of Experimental Physics, Slovak Academy of Sciences, Košice, Slovakia*

<sup>2</sup>*IRC in Superconductivity, University of Cambridge, Cambridge, UK*

The synthesized  $\text{Y}_2\text{Ba}_4\text{CuRuO}_y$  (Ru2411) nanoparticles have been added to the  $\text{YBa}_2\text{Cu}_3\text{O}_{7-x}$  (Y123) matrix. The nanocomposite Y123/Ru2411 bulk superconductors were grown by TSMG (Top Seeded Melt Growth) process. The sample microstructure was analysed by scanning electron microscope (SEM). We found the Ru based nanosize particles trapped in the Y123 growing crystal (fig.1). These nanoparticles are homogenously distributed in the TSMG bulk. Qualitative composition of these particles was estimated by EDAX microanalysis (fig.2). This analysis showed that except Ru also Yb is present in the Ru2411 particles. Yb comes from the interlayer, which was placed between the Y123/Ru2411 sample and monocrystalline MgO substrate during TSMG process to protect Y123 crystal nucleation by the MgO substrate .

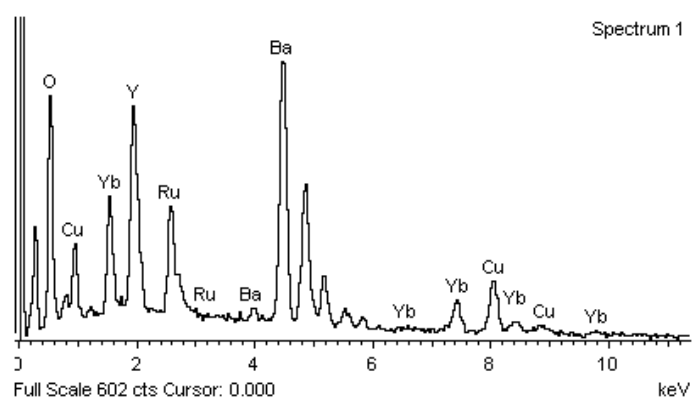
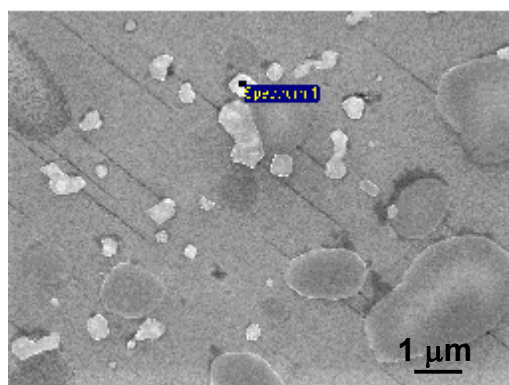


Fig.1 SEM micrograph. Bright Ru2411.

Fig.2 EDAX spectrum of Ru2411 particle.

This work has been supported by VEGA project No. 2/7052/27, APVV projects No. 51-061505 and LPP 0334-06, EU network NESPA, and by the Centrum of Excellence of Slovak Academy of Sciences NANOSMART.

# Fragmentation of Ag nanoparticles in aqueous ambient by nanosecond laser pulses

<sup>1</sup>Petr Šmejkal, <sup>2</sup>Jiří Pflieger, <sup>1</sup>Blanka Vlčková

<sup>1</sup>Department of Physical and Macromolecular Chemistry, Faculty of Science, Charles University in Prague, Hlavova 2030/8, Prague, Czech Republic

<sup>2</sup>Institute of Macromolecular Chemistry, ASCR, v.v.i., Heyrovský Sq. 2, Czech Republic

A novel method of metal nanoparticles preparation, a laser ablation of metal target in liquid ambient, was introduced by Henglein et al. in 1993 [1]. Subsequent experiments showed that morphology of silver nanoparticles prepared by laser ablation can be further modified by fragmentation caused by subsequent laser pulses [2]. Recently, the laser ablation is considered to be a well established method for preparation of chemically pure silver nanoparticles in liquid ambient suitable for variety of applications, for example as a functional substrate for Surface enhanced Raman spectroscopy and/or for applications requiring monodisperse sols, such as nanoparticle assembling [3] etc. However, although several ablation/fragmentation based methods have been refined to allow preparation of silver nanoparticles well suited for desired applications [3] they are still based on trial/error experiments and the mechanism of laser ablation/fragmentation remains not fully explained.

In this contribution, we focused our attention on the impact of nanosecond laser pulses on silver nanoparticles in the Ag hydrosol stabilized by adsorbed citrate ions. We simultaneously recorded the transmitted light intensity from incident laser irradiation during fragmentation with individual pulses of various energies. In addition to that, the surface plasmon extinction (SPE) spectra were recorded in-situ, immediately after the laser pulse interaction with the Ag nanoparticle hydrosol. The experiments showed that the pulse energies above 50 mJ results in less stable hydrosols - nanoparticles tend to aggregate as seen

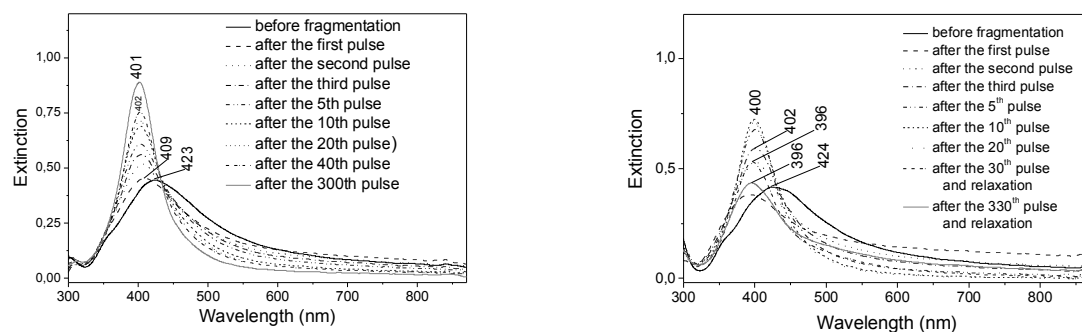


**Fig. 1:** Pulse by pulse evolution of SPE spectra in the course of laser fragmentation at energy 37 mJ/pulse (left) and at energy 93 mJ/pulse (right).

from the increase of extinction in the red spectral region (Fig. 1 right). For the efficient preparation of hydrosols with fragmented non-aggregated nanoparticles, the energies between 15-50 mJ are the most suitable, providing stable hydrosols with narrow nanoparticle size distribution (Fig. 1 left).

**Acknowledgment:** Financial support by the 203/07/0717 grant awarded by the Grant Agency of the Czech Republic is gratefully acknowledged.

[1] A. Fojtik, A. Henglein, Ber. Buns.-Gesellschaft. Phys. Chem. Chem. Phys., **97**, 252 (1993)

[2] M. Procházka, P. Mojžeš, J. Štěpánek, B. Vlčková, P.Y. Turpin, Anal. Chem., **69**, 5103 (1997)

[3] P. Šmejkal, B. Vlčková, J. Pflieger, I. Šloufová, M. Šlouf, Spectrochim. Acta, A **59**, 2321 (2003); A. Taleb, C. Petit, M.P. Pileni, Chem. Mater., **9**, 950 (1997)

## Indentation Tests of CNT+ZrO<sub>2</sub> Composite

<sup>1</sup>J. Špaková, <sup>2</sup>A. Duszová, <sup>1</sup>L. Hegedusová, <sup>1</sup>J. Dusza

<sup>1</sup>*Institute of Materials Research, Slovak Academy of Sciences, Watsonova 47, 04353 Košice, Slovak Republic*

<sup>2</sup>*Technical University of Košice, Faculty of Metallurgy, Letná 9, 042 00 Košice, Slovak Republic*

During the last few years new ceramic - carbon nanotube/fibre composites have been developed with two aims; to improve the mechanical properties of the ceramic materials by reinforcing with carbon nanotubes/fibres (CNT/F) and to develop functionalized ceramics with improved magnetic and electrical properties. It seems that CNT/Fs in the form of single-wall (SWCNT) or multi-wall (MWCNT) should be an ideal reinforcing element for composites due to their light weight, high aspect ratio and exceptional high strength. Additionally CNTs exhibit high electrical conductivity and therefore can change the character of ceramics from insulating to electrically conductive.

The aim of the present contribution is to study the influence of CNFs addition on the microstructure and properties of ZrO<sub>2</sub>/carbon nanofibre composite.

## Formation of metastable phases in Ni-rich Fe-Ni-Nb-B rapidly quenched system

<sup>1</sup>\*P. Švec, <sup>1</sup>D. Muller, <sup>2</sup>J. Turčanová, <sup>1</sup>D. Janičkovič, <sup>2</sup>I. Škorvánek, <sup>1</sup>P. Švec Sr.

<sup>1</sup>*Institute of Physics SAS, Bratislava, Slovakia*

<sup>2</sup>*Institute of Experimental Physics SAS, Kosice, Slovakia*

*\*fyzipsvc@savba.sk*

Transformations from amorphous state in alloys obtained by rapid quenching of the melt are investigated on the case of  $(\text{Fe-Ni})_{93-x}\text{Nb}_7\text{B}_x$  with varying Ni to Fe ratio and for different contents of B. Focus is placed on systems with Ni/Fe = 1, 2, and 3 and B content  $x = 12, 15, 17$  and 20. Formation of nanocrystalline bcc-Fe(Ni) phase is observed for lower metalloid contents and for lower ratio of Ni to Fe, followed by formation of larger grains of  $(\text{Fe-Ni})_{23}\text{B}_6$ . Higher content of Ni or B leads to a change of mechanism where the large unit-cell  $(\text{Fe-Ni})_{23}\text{B}_6$  structure of the type  $\text{Cr}_{23}\text{C}_6$  is formed in a rapid single-stage transformation. The emergence of the phases during (nano)crystallization is investigated with respect to the presence of large atoms of Nb and to the changes of local order induced by large variations of Fe/Ni. The mechanism of formation of the  $\text{Cr}_{23}\text{C}_6$  type structures from locally ordered metal-rich and metalloid-rich clusters by slight atomic rearrangements is discussed. A deviation from the usual two-stage pattern leading to a rapid single-stage crystallization with direct formation of stable phases, incidentally present also in the structure of the precursor master alloys, is analyzed.

## Quantum Processes of Self-Assembly, Photosynthesis and Molecular Computing in Artificial Minimal Living Cells

Arvydas Tamulis and Vykintas Tamulis

Vilnius University Institute of Theoretical Physics and Astronomy, A. Gostauto 12, Vilnius, Lithuania,  
e-mail: tamulis@itpa.lt

We used quantum mechanical (QM) electron correlation interactions density functional theory (DFT) methods (*i.e.* high precision quantum mechanical simulations) to investigate various self-assembled photoactive bioorganic systems of artificial minimal living cells [1-6]. The cell systems studied are based on peptide nucleic acid (PNA) and consisted of up to 360 atoms (not including the associated water or methanol solvent shells) and are up to 3.0-4.2 nm in diameter. The electron correlations interactions originating the hydrogen bonds and Van der Waals weak chemical bonds that increase due to the addition of a polar solvent (water or methanol) molecules, and fatty acid (FA) and precursor fatty acid (pFA) molecules play a critical role in the QM interaction based self-assembly of the photosynthetic center and functioning of the photosynthetic processes of the artificial minimal living cells. The distances between the separated sensitizer, precursor fatty acid, and water or methanol molecules are comparable to Van der Waals and hydrogen bonding radii. As a result these nonlinear quantum interactions compress the overall system resulting in a smaller gap between the HOMO and LUMO electron energy levels and photoexcited electron tunneling occurs from the sensitizer (either a 1,4-bis(N,N-dimethylamino) naphthalene or a  $[\text{Ru}(\text{bpy})_2(4,4'\text{-Me-2-2'-bpy})]^{2+}$ ) to pFA molecules (notation used: Me = methyl; bpy = bipyridine).

The electron tunneling and associated light absorption of most intense transitions as calculated by the time dependent density functional theory (TD DFT) method differs from spectroscopic experiments by only 0.3 or 0.2 nm, which is within the value of experiment errors [6]. This agreement implies that the quantum mechanically self-assembled structures of minimal living cells very closely approximate the realistic ones.

Quantum mechanical electron correlation experiments of self-assembly of above described artificial minimal living cells show that these cells are complex systems because only entire ensemble of PNA, and sensitizer, and pFA, and FA and water molecules is stable and perform quantum photosynthetic processes. Removing the small part of nucleobase, FA and water molecules leads to the structural changes in comparison with realistic structures and difference in comparison with the spectroscopic values of photoexcited electron tunneling from sensitizer (1,4-bis(N,N-dimethylamino)naphthalene to pFA molecules. QM electron correlation experiments of self-assembly of artificial minimal living cells removing the main part of nucleobase, and FA and water molecules leads to the degradation of these cells [3-5]. We can state what the inclusion of ever more water, and fatty acid, and pFA molecules, and waste pieces of the pFA molecules and nucleobase molecules in the different artificial minimal living cells results in a shift of the absorption spectrum to the red for the artificial protocell photosynthetic centre, leading to an ever closer approach to the real experimental value and indicates the measure of

the complexity of this quantum complex system, *i.e.* a minimal protocell. It is important to say that only QM electron correlation TD-DFT experiments with minimal living cells gives results exactly comparable with spectroscopic results and all other more simplified QM methods such as local gradient DFT or *ab initio* Hartree-Fock gives structures and spectra far from the experimentally measured. The corresponding of experimental absorption spectra peaks and our QM calculated confirm that our chosen method of designing single electron nano photocells might be useful not only for artificial living organisms but also for wide implementation in the nano photodevices, and molecular computers. Our goals are by using quantum mechanical experiments to predict the possibility of biochemical experimental synthesis of molecular electronics and spintronics logical elements information based artificial living organisms or nanobiorobots for nanomedicine and cleaning of nuclear, chemical and microbial pollutions.

We are creating molecular electronics logic gates regulating the photosynthesis, growing and dividing of artificial living cells and nanobiorobots [7-13]. Implementation of quantum information bits based on spatially localized electron spins in stable molecular radicals was investigated by unrestricted time dependent functional theory methods [8-10]. The g-tensor shift calculations of neutral radical molecules was performed for beta-diketone and syringate. beta-diketone neutral radical moiety with an attached hydrocarbon chain. Beta-diketone is suitable for construction of quantum computing processing devices because the qubit is relatively stable due to the small magnitude of g-tensor shift component that is aligned with the external magnetic field, *i.e.* the direction of hydrocarbon chain which provide the self-assembled monolayer an attachment of the molecule to a substrate [12]. TD DFT simulations of the artificial minimal living cells with implemented molecular electronics and spintronics gates done using self-assembled neutral radical molecules beta-diketone and syringate show that it is possible to construct more general ControlNOT and NAND logic functions suitable for the production of the nanobiorobots. Designed of variety of the molecular spintronics devices will regulate photosynthesis and growth of artificial minimal living cells in the conditions of external magnetic fields, while also providing a perspective of the requirements for success in the synthesis of new forms of artificial living organisms.

[1] Jelena Tamuliene, Arvydas Tamulis, "Quantum Mechanical Investigations of Self-Assembled System Consisting of Peptide Nucleic Acid, Sensitizer, and Lipid Precursor Molecules", *Lithuanian Journal of Physics*, vol 45, No 3, p.p. 167-174, 2005.

[2] A. Tamulis, V. Tamulis A. Graja, "Quantum mechanical modeling of self-assembly and photoinduced electron transfer in PNA based artificial living organism", *Journal of Nanoscience and Nanotechnology*, 6, 965-973 (2006).

[3] Arvydas Tamulis and Vykintas Tamulis, "Quantum Self-Assembly and Photoinduced Electron Tunneling in Photosynthetic System of Minimal Living Cell", *Viva Origino*, vol. 35, p.p. 66-72, 2007.

[4] Arvydas Tamulis and Vykintas Tamulis, "Quantum Self-Assembly and Photoinduced Electron Tunneling in Photosynthetic Systems of Artificial Minimal Living Cells", *Origins of Life and Evolution of Biospheres*, vol. 37, 473-476, 2007.

[5] A. Tamulis, V. Tamulis, H. Ziock, S. Rasmussen, "Influence of Water and Fatty Acid Molecules

on Quantum Photoinduced Electron Tunnelling in Photosynthetic Systems of PNA Based Self-Assembled Protocells”, in “*Multi-scale Simulation Methods for Nanomaterials*”, eds. R. Ross and S. Mohanty, John Wiley & Sons, Inc., New Jersey, 2007, in press.

[6] S. Rasmussen, J. Bailey, J. Boncella, L. Chen, G. Collins, S. Colgate, M. DeClue, H. Fellermann, G. Goranovic, Y. Jiang, C. Knutson, P.-A. Monnard, F. Moufouk, P. Nielsen, A. Sen, A. Shreve, A. Tamulis, B. Travis, P. Weronksi, W. Woodruff, J. Zhang, X. Zhou, and H. Ziock, “Assembly of a minimal protocell”, in MIT Press book, “*Protocells: Bridging nonliving and living matter*”, eds S. Rasmussen, M. Bedau, L. Chen, D. Krakauer, D. Deamer, N. Packard, and P. Stadler, 2007, in press.

[7] Arvydas Tamulis, Jelena Tamuliene, Vykintas Tamulis, Aiste Ziriakoviene, “Quantum Mechanical Design of Molecular Computers Elements Suitable for Self-Assembling to Quantum Computing Living Systems”, *Solid State Phenomena*, Scitec Publications, Switzerland, Vols. 97-98, p.p. 175-180, 2004.

[8] A. Tamulis, V. I. Tsifrinovich, S. Tretiak, G. P. Berman, D. L. Allara, “Neutral Radical Molecules Ordered in Self-Assembled Monolayer Systems for Quantum Information Processing”, *Chem. Phys. Lett.*, **436**, p.p. 144 - 149 (2007).

[9] J. Tamuliene, A. Tamulis, J. Kulys, “Electronic Structure of Dodecyl Syringate Radical Suitable for ESR Molecular Quantum Computers”, *Nonlinear Analysis: Modeling and Control*, Vol. 9, No 2, p.p. 185-196 (2004).

[10] A. Tamulis, V. Tamulis, “Variety of Self-Replicating Complex Living System Based on Quantum Information”, book of abstracts of conference “*Chemiogenesis 2005*”, Venice, Italy, Sept. 28 – Oct. 01, 2005, page 18.

[11] Jelena Tamuliene, Arvydas Tamulis, Aiste Ziriakoviene, Andrzej Graja, „Quantum Chemical Design of Two Logical Functions Molecular Device“, *Lithuanian Journal of Physics*, vol. **46**, p.p. 163-167 (2006).

[12] Z. Rinkevicius, Arvydas Tamulis, Jelena Tamuliene. “Beta-Diketo Structure for Quantum Information Processing”, *Lithuanian Journal of Physics*, vol. **46**, p.p. 413-416 (2006).

[13] Arvydas Tamulis and Vykintas Tamulis, “Quantum Mechanical Design of Molecular Electronics OR Gate for Regulation of Minimal Cell Functions”, *Journal of Computational and Theoretical Nanoscience*, vol. 4, No. 6, 2007.

## Preparation of semi – 1D transition metal oxide structures

T. Tätte, M. Paalo, R. Talviste, J. Shulga, K. Saal, A. Lõhmus and I. Kink

*Institute of Physics, Univ. of Tartu, & Estonian Nanotechnology Competence Center,  
142 Riia St, 51014 Tartu, Estonia.*

e-mail: [tanelt@fi.tartu.ee](mailto:tanelt@fi.tartu.ee)

Recently many new technologies have been suggested for designing silica based optical devices in nanoscale [1]. However, there are insuperable drawbacks in realizing optics based on silica (glass and quartz) because of their low refractive indexes. To overcome that high refractive index materials like transition metal oxides must be used instead of silica. But these oxides decompose at elevated temperatures rather than transform to spinnable melts. Thus, fibers drawing and shape molding of these materials is not possible. In order to shape transition metal oxides to low-dimensional fibers and needles we have recently proposed a new approach that utilizes alkoxide based concentrates as precursors [2,3]. Moreover, we have shown that these precursors can be effectively used for grafting defined shape microscopic oxide lines to different flat substrates [4]. We have successfully applied our method in preparing conductive and optically transparent tips of Sb doped SnO<sub>2</sub> for simultaneous STM–photon imaging, which enabled 1-2 nm lateral and atomic vertical resolution in STM regime [5]. In this work we generalize the conceptual background of preparation of transition metal oxides, and take an insight to critical aspects in particular practical applications.

### References:

- [1] D. Gates, X. Qiaobing, S. Michael, R. Declan, W C. Grant, G. M. Whitesides, *Chemical Reviews* 2005, 105(4), 1171-1196.
- [2] T. Tätte, T. Avarmaa, R. Lõhmus, U. Mäeorg, M.-E. Pistol, R. Raid, I. Sildos, A. Lõhmus, *Materials Science & Engineering, C* 2002 19 (1-2) 101-104.
- [3] T. Tätte, M. Paalo, V. Kisand, V. Reedo, A. Kartushinsky, K. Saal, U. Mäeorg, A. Lõhmus, I. Kink, *Nanotechnology* 2007, 18, 531-535.
- [4] V. Jacobsen, T. Tätte, R. Branscheid, U. Mäeorg, K. Saal, I. Kink, A. Lõhmus, M. Kreiter, *Ultramicroscopy* 2005, 104(1), 39-45.
- [5] V. Kisand, J. Shulga, T. Tätte, U. Visk, M. Natali, G. Mistura, M. Paalo, M. Lobjakas, I. Kink, *Materials Science & Engineering B* 2007 137(1-3) 162-165.

# Synthesis and superparamagnetic properties of FePt-nanoparticles

<sup>1\*</sup>T. Traußnig, <sup>2</sup>S. Landgraf, <sup>3</sup>I. Letofsky-Papst, <sup>3</sup>G. Kothleitner, <sup>4</sup>K. Rumpf, <sup>4</sup>P. Granitzer, <sup>1</sup>U. Brossmann, <sup>4</sup>H. Krenn and <sup>1</sup>R. Würschum

<sup>1</sup>Institut für Materialphysik, Technische Universität Graz, Petersgasse 16, A-8010 Graz, Austria

<sup>2</sup>Institut für Physikalische und Theoretische Chemie, Technische Universität Graz, Technikerstraße 4, A-8010 Graz, Austria

<sup>3</sup>Institut für Elektronenmikroskopie und Feinstrukturforchung, Technische Universität Graz, Steyrergasse 17/III, A-8010 Graz, Austria

<sup>4</sup>Institut für Physik, Karl-Franzens-Universität Graz, Universitätsplatz 5, A-8010 Graz, Austria

FePt-nanoparticles are prospective candidates for future data storage media. In the present project monodisperse FePt-particles are synthesized via chemical route by thermal decomposition of iron pentacarbonyl and reduction of platinum acetylacetonate in a polyol process. The spherical particles with a small diameter of 3.4 nm and a narrow size distribution (Fig. 1) are coated by oleic acid and oleylamin by means of which a fixed interparticle distance can be obtained. The coated particles are dispersed in hexane under Ar-atmosphere for further processing. Subsequent annealing gives rise to the formation of intermetallic phases with high anisotropy. From zero-field cooling (ZFC) and field-cooling (FC) measurements in a SQUID-magnetometer a superparamagnetic blocking temperature of 23 K is deduced for unannealed fcc-type nanoparticles (Fig. 2). Exchanging of the surfactants opens up the way to tailor the interparticle distance. Measurements aiming at studying the effect of dipole-dipole interactions in dependence on the interparticle distance are in progress.

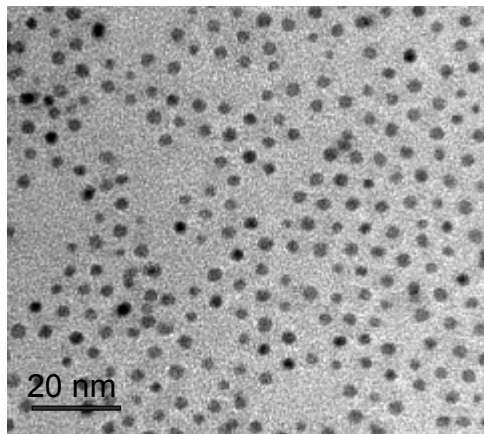


Fig. 1:  
TEM-picture of as-synthesized FePt-particles

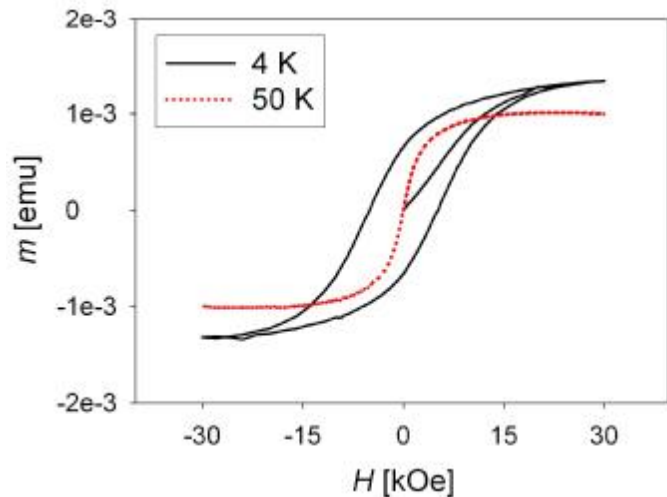


Fig. 2:  
Magnetization behaviour above and below blocking temperature  
( $m$ : magnetic moment;  $H$ : magnetic field)

*Acknowledgement: Financial support by NAWI Graz is appreciated*

## Structure and magnetic properties of FeNiNbB nanocrystalline alloys

J. Turčanová<sup>1</sup>, J. Marcin<sup>1</sup>, J. Kováč<sup>1</sup>, D. Janičkovič<sup>2</sup>, P. Švec<sup>2</sup> and I. Škorvánek<sup>1</sup>

<sup>1</sup> *Institute of Experimental Physics, Slovak Academy of Sciences, SK-043 53 Košice, Slovakia*

<sup>2</sup> *Institute of Physics, Slovak Academy of Sciences, SK-842 53 Bratislava, Slovakia*

Nanocrystalline soft magnetic ribbons, with a composition of  $(\text{Fe}_{1-x}\text{Ni}_x)_{81}\text{Nb}_7\text{B}_{12}$  (where  $x = 0, 0.16, 0.25, 0.33$  and  $0.5$ ), were prepared by melt spinning and subsequent crystallization. The presence of ultrafine grains ranging in size from 5 to 15 nm was evidenced by TEM. The temperature dependencies of magnetization of as-quenched alloys revealed that value of the Curie temperature of amorphous phase,  $T_c(\text{am})$ , increases with addition of Ni from 362 K (for  $x=0$ ) to 565 K (for  $x=0.5$ ). The results of DSC calorimetry showed a continuous decrease of the onset crystallization temperature with an increase of Ni content from  $T_{x1} = 774$  K (for  $x=0$ ) to  $T_{x1} = 704$  K (for  $x=0.5$ ). The Ni-free sample and the sample with Ni content  $x=0.14$  exhibit after annealing the behavior that is more or less anticipated for the NANOPERM-type samples. On the other hand, rather surprising  $M(T)$  behavior caused by the partial BCC-FCC phase transformation in the nanocrystalline grains was observed for the alloys with higher Ni content. Here, the magnetization in temperature range above  $T_c(\text{am})$  decreases with increasing content of nanocrystalline grains. The addition of Ni has a beneficial effect on the magnetic softness of the optimally heat treated nanocrystalline samples. The best magnetic properties coincided with the development of a nanocrystalline phase just above the primary crystallization temperature. The appearance of the secondary crystallization products caused deterioration of good magnetic properties. The magnetic measurements at high temperatures revealed a marked magnetic hardening when temperature approaches the Curie temperature of amorphous residual phase. This hardening was less significant for the samples containing higher amount of Ni.

## PROCESSING OF SOME HYDROGEN STORAGE METALLIC MATERIALS

<sup>1</sup>Mariana Lucaci, <sup>1</sup>Violeta Tsakiris, <sup>2</sup>Alexandru Biris, <sup>3</sup>Radu Liviu Orban,  
<sup>4</sup>Gabriela Popescu, <sup>4</sup>Liana Maria Vladutiu

<sup>1</sup>INCDIE ICPE-CA, Bucharest, Romania

<sup>2</sup> INCDTIM Cluj Napoca, Romania

<sup>3</sup> Technical University of Cluj Napoca, Romania

<sup>4</sup> University of "POLITEHNICA" of Bucharest, Romania

### Abstract

Mg<sub>76</sub>Ti<sub>12</sub>Fe<sub>12-x</sub>Ni<sub>x</sub> (x =4, 8) alloys were prepared by mechanical alloying and the hydrogen storage properties were investigated systematically. In the Mg<sub>76</sub>Ti<sub>12</sub>Fe<sub>12</sub> and Mg<sub>76</sub>Ti<sub>12</sub>Ni<sub>12</sub> alloys, the main binary alloy phases are Fe<sub>2</sub>Ti and Mg<sub>2</sub>Ni respectively. There are same binary alloy phase structures included Fe<sub>2</sub>Ti, Mg<sub>2</sub>Ni and NiTi in the Mg<sub>76</sub>Ti<sub>12</sub>Fe<sub>8</sub>Ni<sub>4</sub> and Mg<sub>76</sub>Ti<sub>12</sub>Fe<sub>4</sub>Ni<sub>8</sub>alloys.

For the Mg<sub>76</sub>Ti<sub>12</sub>Fe<sub>12-x</sub>Ni<sub>x</sub> (x=8), alloy mechanical alloyed for 20 hrs, the maximum hydrogen storage capacity is of 1.5 % wt, from which only 1 %wt is reversible in the pressure domain of 60-0.1 bar. This is happening due to form in the system of at least two hydrogen absorption phases which work in this domain and the pressure plateau for a phase is much below 0.1 bar pressure.

Fe and Ni coexistence is favorable to improve hydrogen storage properties.

**Keywords:** hydrogen-absorbing materials; metal hydrides; nanostructured materials; mechanical alloying; intermetallics

## Magnetostriction measurements of (Fe-Co)-Mo-Cu-B alloys with varying atomic Fe/Co ratio

<sup>1\*</sup>G. Vlasák, <sup>2</sup>C. F. Conde, <sup>1</sup>D. Janičkovič, <sup>1</sup>P. Švec

<sup>1</sup> *Institute of Physics, Slovak Academy of Sciences, Bratislava, Slovakia*

<sup>2</sup> *Dept. of Physics of Condensed Matter, University of Sevilla, Apto. 1065, Sevilla, Spain*

Amorphous rapidly quenched ribbons of  $(\text{Fe-Co})_{79}\text{Mo}_8\text{Cu}_1\text{B}_{12}$  with the ratio  $\text{Co/Fe} = 0, 1/12, 1/9, 1/6, 1/4, 1/3, 1/2$  and 1 were prepared by planar flow casting. The dependence of Curie temperature  $T_C$  on Co/Fe ratio was determined by magnetic thermogravimetry as well as from temperature dependencies of sample dilatation, measured using a special dilatometer designed for these materials [1]. Due to the presence of the invar effect it was possible to measure the spontaneous volume magnetostriction in the temperature interval between 300 K and  $T_C$ . Using special disc shaped samples field dependencies of magnetostriction in parallel and perpendicular directions of applied magnetic field were obtained by direct measurement method [2]. Subsequently, saturation magnetostriction and volume magnetostriction as well as forced magnetostriction were computed. Saturation magnetostriction increases with increasing Co/Fe ratio from 0 up to 14 ppm, depending both on the Co/Fe ratio and on the shift of  $T_C$  with composition. The alloy with ratio  $\text{Co/Fe}=0$  exhibits  $T_C$  in the vicinity of room temperature, thus field dependencies of magnetostriction, corresponding to the dependencies of a paramagnetic system (with saturation magnetostriction equal zero), are practically linear functions of applied field and approach saturation only for high field values.

[1] G. Vlasak, P. Svec, J. Electrical Engineering 55 (2004) 81.

[2] G. Vlasak, J. Mag. Magn. Mater. 215-216 (2000) 476.

## Magnetic relaxations and memory effect in nickel –chromium cyanide nanoparticles

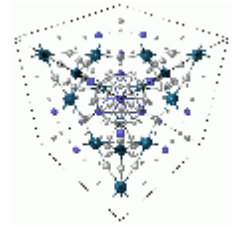
M. Zentková<sup>1</sup>, A. Zentko<sup>1</sup>, M. Mihalik<sup>1</sup>, S. Maťaš<sup>1</sup>, Z. Mitróová<sup>1</sup>, Z. Jagličič<sup>2</sup> and V. Zelenák<sup>3</sup>

<sup>1</sup>*Institute of Experimental Physics SAS, Watsonova 47, 040 01 Košice, Slovakia*

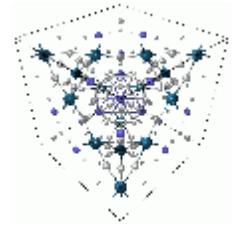
<sup>2</sup>*Institute of Mathematics, Physics and Mechanics, Jadranska 19, 1000 Ljubljana, Slovenia*

<sup>3</sup>*Institute of Chemistry, P. J. Šafárik University, Faculty of Science, Moyzesova 11, 040 01 Košice*

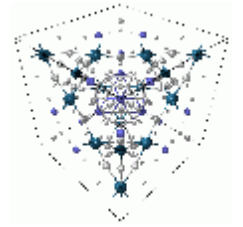
We present our results of magnetization measurements on the Ni-Cr cyanide nanoparticle system, which belongs to the group of Prussian blue analogues. Transition 3d metal Prussian blue analogues form a large cubic system  $A_x[B(CN)_6]_y \cdot nH_2O$ , where metal ion A occupies all the summits and all the centers of the faces and the  $[B(CN)_6]$  groups are located at the octahedral sites. One possible structure displays a  $A:B=3:2$ , with one third of  $[B^{3+}(CN)_6]$  vacancies filled by water molecules. The B coordination sphere is left unchanged but the mean coordination sphere of A becomes  $A(NC)_4(H_2O)_2$ . The mean number of B neighbors around A is now four and the crystal structure is fcc. Magnetic nanoparticles of Prussian blue analogs have been prepared by reverse micelle technique using p-nitrobenzylpyridine as a peripheral ligand to separate the particles from inverted micelle medium and then to disperse the capped particles in organic solvents. The prepared samples have been characterized by means of X-ray diffraction and TGA analysis. The magnetic measurements have been performed on SQUID magnetometer in the temperature range from 4.2 to 300 K. In the contribution we will compare magnetic properties in paramagnetic region and spin glass like features (such as frequency dependence of AC susceptibility, the hysteresis between zero field cooled and field cooled magnetization, the time dependence of magnetization both after the sample has been field and zero field cooled) for polycrystalline and nanocrystalline powders of  $Ni_3[Cr(CN)_6]_2 \cdot 12H_2O$ . We report on the memory effect observed in  $Ni_3[Cr(CN)_6]_2 \cdot 12H_2O$  magnetic nanoparticles.



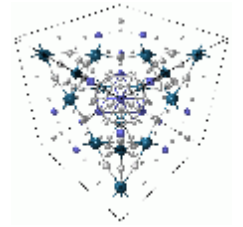
**NOTES**



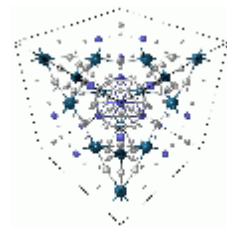
**NOTES**



**NOTES**



**NOTES**



**NOTES**

# NANOVED 2007

4 th International Conference on Nanosciences and Nanotechnologies

Program and Abstracts

Editros:

Franišek Simančík

Peter Švec

Ivo Vávra

Slovak Academy of Sciences

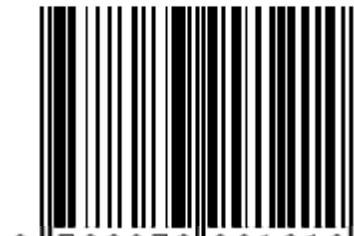
Bratislava

Published by Tribun EU,

Brno 2007

Vydal: Tribun EU

ISBN 978-80-7399-121-0



9 788073 991210 >